



Appendix 7

Mine design additional information
– *3D numerical modelling*



Appendix 7.1

Pillar design analysis using La Model - Hume Coal Project (K.A. Heasley 2018)

Keith A. Heasley, Ph.D., P.E.
Mining Engineering Consulting
DUNS#: 8019636333
2988 Compressor Station Rd.
Bruceton Mills, WV 26525
keith.heasley@mail.wvu.edu
(304) 379-3004
June 28, 2018

c/o Russell Frith
Principal Geotechnical Engineer
Mine Advice Pty Ltd.
A.B.N. 15 152 928 222
7 / 17 Babilla Close
Beresfield, NSW, 2322
russellfrith@mineadvice.com.au
W: 02 4088 0600

Subject: Submittal of the report on the numerical modelling study of the Hume Coal mine using the LaModel program.

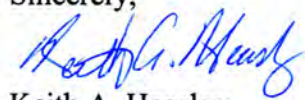
Russell:

I have completed my LaModel analysis of the highwall mining type pillar design at the proposed Hume Coal mine. This analysis included: 1) an evaluation of a suitable coal model to use in LaModel, 2) a parametric study of the overburden elastic modulus and lamination thickness, 3) a series of 2-D and 3-D models to investigate the pillar system stability and associated subsidence as a function of geometry and overburden conditions, and 4) a couple of worst-case scenarios with failed pillars.

After developing the appropriate overburden and coal properties, the 2-D and 3-D models showed that the subcritical width and length of the web pillar panel caused all of the web pillar safety factors to be higher than the corresponding tributary area loading results from ARMPS-HWM. Also, the single failed web pillar model demonstrated that safety factors of the adjacent pillars decrease, but in all of the models the adjacent pillars do not fail. Also, the surface subsidence in these failed single web pillar models is seen to only increase by about 1 mm. In the failed web pillar section models, the adjacent barrier and chain pillars are seen to remain stable.

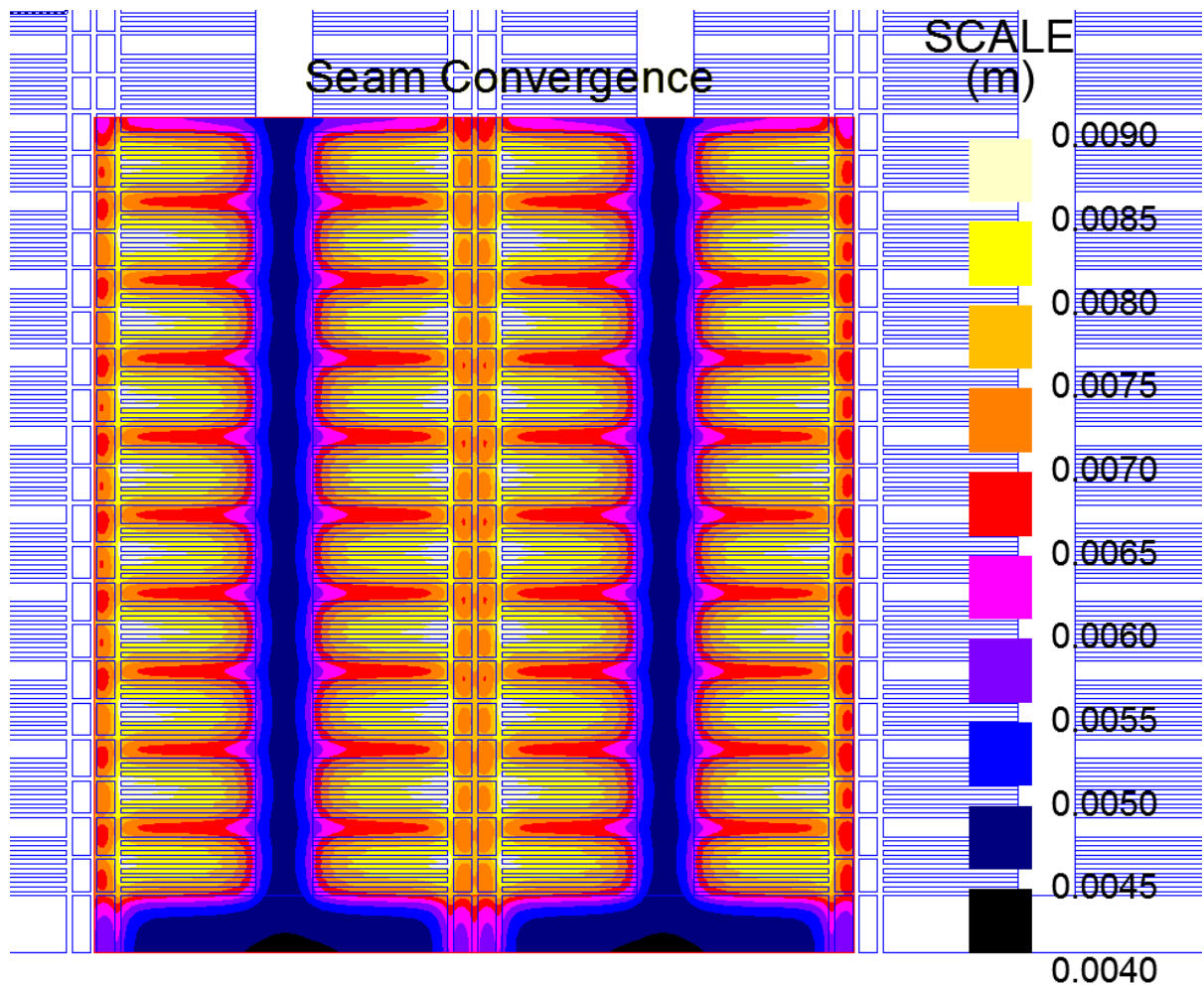
If I can be of any further assistance, or you have any questions, please do not hesitate to contact me.

Sincerely,


Keith A. Heasley

Pillar Design Analysis Using LaModel

For
Hume Coal and MineAdvice



Keith A. Heasley
Ph.D., P.E.
29 May, 2018

Executive Summary

Hume Coal Pty Ltd (Hume Coal) is currently seeking government approval for a new underground coal mine which utilizes a mine design based on the application of coal pillars of similar dimensions to those used in highwall mining (HWM). Following a peer review of Hume Coal's subsidence assessment by the NSW Department of Planning, Home Coal's geo-technical consultant, Mine Advice, requested that 3-D numerical modelling be undertaken of the new mine design.

The required numerical modelling study was split into five distinct stages as a result of the design approach, namely:

- Stage 1:** Confirm of the use of the Mark-Bieniawski (M-B) pillar strength formula and the LaModel "coal wizard" to define the pillar properties.
- Stage 2:** Conduct exercises to investigate a suitable lamination thickness based on the LaModel "lamination thickness wizard" and back analysis of Berrima Colliery.
- Stage 3:** Develop a series of 2-D models to investigate overall system stability in the 2-D section as a function of varying overburden conditions.
- Stage 4:** Develop a series of broader-scale 3-D models that include the length of the web pillars, chain pillars, and also adjacent barrier pillars, to examine system stability in 3-D, again as a function of varying overburden conditions.
- Stage 5:** Analyze a couple of scenarios involving the removal of certain web pillars to simulate their complete failure in order to understand the response of the surrounding pillars and their residual stability factors.

The result of the Stage 1 analysis was that the Mark-Bieniawski pillar strength formula was chosen to be used in subsequent models because: 1) the difference in output between the M-B coal material and the competing model was insignificant in the elastic range, 2) the M-B coal material is easier to use since it is tightly integrated into LaModel, and 3) the M-B coal model has been verified with very large databases. From the Stage 2 analysis of rock mass stiffness and lamination thickness, the laboratory test result ranges of elastic modulus (E) of 8.2, 16.5 and 23.2 GPa (low, average and high) were selected to be used for subsequent models. Also, based on the results from the lamination thickness wizard and the back-analysis of Berrima Colliery, conservative values for the overburden rock mass lamination thickness of 20 and 40 m were chosen to be used in subsequent models.

In both the results from the 2-D models in Stage 3 and the 3-D models in Stage 4, the subcritical width and length of the web pillar panel causes all of the web pillar safety factors to be higher than the corresponding tributary area loading results. Essentially, some of the tributary area overburden weight from above web pillars is carried by the intra-panel and inter-panel barriers, and to a lesser extent by the chain pillars, in the LaModel analysis. The amount of load transferred to the adjacent barrier pillars was seen to be directly related to the stiffness of the overburden.

The results from the single failed web pillar model in Stage 5 shows that safety factors of the adjacent pillars decrease, but in all of the models those adjacent pillars do not fail. Also, the surface subsidence in these failed single web pillar models is seen to only increase by about 1 mm. In the failed web pillar section models of Stage 5, the adjacent barrier and chain pillars are seen to remain stable. Also, with the entire section failed, there was only a localised increase in surface subsidence of between 16 and 24 mm.

Table of Contents

	Page
Executive Summary	i
List of Figures	iii
List of Tables	iv
Background	1
Scope of Work	2
The LaModel Program	4
Introduction	4
Origins	4
LaModel Basic Formulation	5
LaModel Enhancements and Upgrades	7
LaModel Pedigree	9
Modeller Experience	10
LaModel Calibration	11
<u>Rock Mass Stiffness:</u>	12
<u>Coal/Pillar Strength:</u>	13
<u>Gob Stiffness/Loading:</u>	18
Hume Mine Models	18
Stage 1 – Investigation of Coal Models	18
Stage 2 – Investigation of Rock Mass Lamination Thickness	19
Stage 3 – 2-D Models	20
Stage 4 – 3-D Models	21
Stage 5 – Worst-Case Scenarios, Failed Web Pillar & Failed Section	24
References	24
Appendix A – Author’s Curriculum Vitae	A-1

List of Figures

	Page
1 Generic Pillar Layouts at Various Depths.....	3
2 Laminated Overburden Schematic.....	6
3 In-Seam Material Models in LaModel	7
4 Schematic of Pillar Load and LaModel Element Mapping.....	15
5 Stress-Strain Curve for Hume 5.5 m Wide Web Pillar.....	17
6 Seam Convergence: 120 m Deep, 40 m Laminations, 16.5 GPa Modulus .	23

List of Tables

	Page
1 Critical Panel Design Dimensions at Three Depths.....	2
2 Grid Sizes for Two-Dimensional Models	21
3 2-D Model Results.....	21
4 3-D Model Results.....	22

Background

Hume Coal Pty Ltd (Hume Coal) is currently seeking government approval for a new underground coal mine which utilizes a mine design based on the application of coal pillars of similar dimensions to those used in highwall mining (HWM).

Mine Advice Pty Ltd (Mine Advice) requested that 3-D numerical modelling be undertaken following a peer review of the Hume Coal subsidence assessment by the NSW Department of Planning's mining expert consultants, Professor Ismet Canbulat and Emeritus Professor Jim Galvin.

Different generic pillar layouts at different depths were provided by Hume Coal (see Figure 1 and Table 1) with the following design logic:

- (a) The mine layout consists of several different pillar types – web pillars, intra-panel barriers, chain pillars, inter-panel barriers (providing separation between adjacent panels), barriers between mains and panels, and mains development pillars (see Figure 1). The interaction between web pillars, intra-panel barriers, chain pillars and inter-panel barriers is the focus of the numerical modelling.
- (b) The primary design method used for determining the final mine layout following the completion of mining was ARMPHS-HWM, it being selected due to the supporting case-history database being generally consistent with the mining geometries of the Hume Project.
- (c) The key 2-D design condition in terms of overall pillar system stability, is the section through a panel of web-pillars and intra-panel barrier pillars as analyzed by ARMPHS-HWM. In the 2-D case, these pillars and drives are of infinite length.
- (d) ARMPHS-HWM was applied to the 2-D section in what is considered to be a conservative manner in that:
 - Plunges or drives have been limited to no more than 120 m as compared to more typical HWM drive lengths in the range 300 m to 500 m.
 - The distance between intra-panel barriers has been set at no more than 60 m as part of attempting to ensure sub-critical overburden behavior between such barriers. At the lowest cover depth of 80 m, this results in a panel width-to-depth (W/H) ratio of 0.71, this being the maximum value between intra-panel barriers anywhere within the mine layout. The maximum cover depth is on the order of 160 m with an associated W/H of 0.325. It should be noted that the maximum 60 m width between barrier pillars is not actually achieved in most of the cases, due to the fact that adding an additional web pillar & drive would bring the width to >60m.
 - Pillar dimensions have been determined based on applying both a minimum pillar width-to-height ratio (w/h) and a Stability Factor (SF) criteria, the design selected being the widest pillar outcome. These final design dimensions for three depths are presented in Table 1.
 - No stabilising benefit has been applied relating to the lack of an open cut highwall at the outby end of the unsupported drives, this being an obvious de-stabilising plane of weakness that exists in all surface HWM cases, but will be absent in the underground environment. The de-stabilising influence of a highwall also usually exists in the area of a

HW mine with the highest panel width to depth ratio, potentially further contributing to its adverse influence on pillar stability outcomes.

- (e) Due to the drive lengths being limited to 120 m and the typical cover depth ranging from 80 m to 160 m, it was recognised, particularly for the deeper cover areas, that areas of web pillars would have a tendency to be shielded from full overburden load by the inter-panel barrier pillars and chain pillars due to the W/H decreasing below 1.

Table 1. Critical Panel Design Dimensions at Three Depths.

Depth (m)	Number of Entries	Entry Width (m)	Desired Rib Pillar Width (m)	Desired Barrier Width (m)
80	8	4.0	3.5	14.0
120	7	4.0	4.1	16.8
160	6	4.0	5.5	20.9

Scope of Work

The required numerical modelling study was split into five distinct stages as a result of the design approach, namely:

- Stage 1:** Confirm of the use of the Mark-Bieniawski pillar strength formula and the LaModel “coal wizard” to define the pillar properties.
- Stage 2:** Conduct exercises to investigate a suitable lamination thickness based on the LaModel “lamination thickness wizard” and back analysis of Berrima Colliery
- Stage 3:** Develop a series of 2-D models to investigate overall system stability in the 2-D section as a function of varying overburden conditions.
- Stage 4:** Develop a series of broader-scale 3-D models that include the length of the web pillars, chain pillars, and also adjacent barrier pillars, to examine system stability in 3-D, again as a function of varying overburden conditions.
- Stage 5:** Analyze a couple of scenarios involving the removal of certain web pillars to simulate their complete failure in order to understand the response of the surrounding pillars and their residual stability factors.

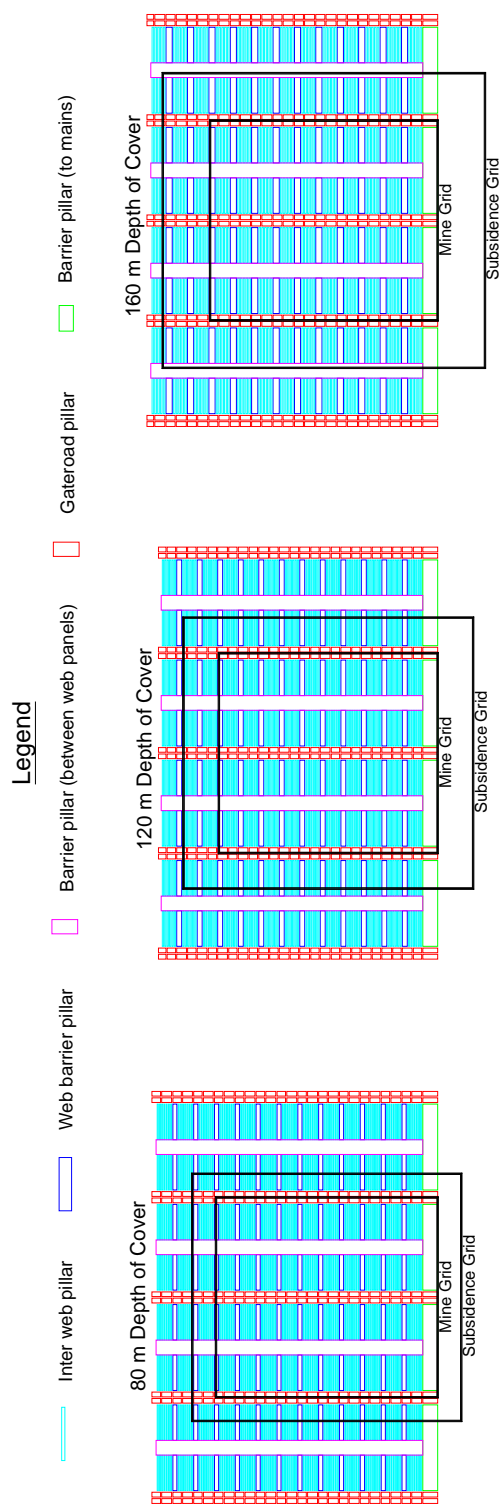


Figure 1. Generic Pillar Layouts at Various Depths.

The LaModel Program

Introduction

If one wishes to perform mechanical analysis of the geologic structure of a mining operation, there are several broad mathematical techniques available. For instance, one may choose finite-element, boundary-element, discrete-element, finite-difference techniques and/or hybrid combinations of the above techniques. In general, these mathematical techniques each have specific strengths and weaknesses when applied to a specific geologic environment, mining geometry, mining scale and material behavior. Naturally, in each practical application, the mathematical technique best suited to the prevailing conditions should be applied.

To analyze the displacements and stresses associated with the extraction of large tabular deposits such as coal, potash and other thin vein-type deposits, the displacement-discontinuity (DD) version of the boundary-element (BE) technique is frequently the method of choice. In the displacement-discontinuity approach, the mining horizon/seam is treated mathematically as a discontinuity in the displacement of the surrounding media. (The strata above the seam moves down toward the seam, and the strata below the seam moves up toward the seam; thus the seam is a discontinuity in the displacement field where the strata movement changes from downward to upward at the seam location, hence the name "Displacement-Discontinuity.") With the DD method, only the planar area of the seam is discretized in order to obtain the solution, and only the vertical strata movements are analyzed in detail. Often, this limited analysis is sufficient, since in many applications, only the vertical distributions of stress and convergence on the seam horizon are of interest. Also, by limiting the detailed analysis to only the vertical seam movements, the DD method provides exceptional computational savings over other techniques which discretize the entire body (such as finite-element, discrete-element or finite-difference). It is a direct result of this computational efficiency that enables the DD method to quickly solve problems involving very large areas of tabular excavations. In the U.S., the quick solution times and minimal parameter input have resulted in the LaModel program becoming the primary coal mine analysis tool for situations more complex than those covered by the simple empirical calculations of programs such as ALPS and ARMPS (see "Pedigree" section below).

Origins

In the early 1960's, mining researchers (Salamon, 1962; Berry, 1960) had found that the available homogeneous, elastic, overburden models were not able to reasonably predict surface subsidence for the British coal mines. Therefore, the researchers were exploring the use of non-homogeneous models for effectively calculating, or predicting surface subsidence at these mines. One non-homogeneous elastic model, a laminated overburden model, was derived by Dr. Salamon in his Ph.D. dissertation (Salamon, 1962). This laminated overburden model was much more flexible than the previous homogeneous, isotropic, elastic overburden model and provided realistic calculations of surface subsidence. At this point in history, without modern computers, all of these mathematical overburden models were implemented as analytical equations for calculating the desired results.

With the advent of the early computers in the late 60's, many of the mathematical overburden models were quickly converted into numerical codes for calculating the displacements and stresses at the seam level. In South Africa, under the auspices of Salamon, the MINSIM program was developed (Plewman *et al.*, 1969). This program implemented a homogeneous, isotropic, elastic overburden model into what was called a "seam element" method. This seam element method allowed the in-seam material (for thin, tabular seams) to be modelled with

some sophistication, while the overburden was simply treated as one homogeneous, isotropic, elastic material. This mathematical simplification of the overburden model allowed relatively large areas of a mine to be simulated in a very reasonable amount of time.

During the same time period, researchers in the United States (Crouch, 1976) were developing very similar types of homogeneous, elastic, overburden programs with what they called the "displacement-discontinuity" method, which was essentially identical to the seam-element method. One of these programs, called MULSIM (Sinha, 1979), was ported to the "new" personnel computers (Beckett and Madrid, 1988) and then widely used in the U.S. mining industry over the next decade (Kripakov *et al.*, 1988, Zipf and Heasley, 1990, Zipf, 1992, Zelanko and Heasley, 1995).

These early models with the MULSIM program and its homogeneous elastic overburden were successfully used to model the stresses in large areas of single and multiple-seam coal mines and to help in designing adequate pillar sizes (Zelanko and Heasley, 1995). However, very early on, it was observed that the calculated seam displacements (and particularly the calculated surface subsidence) with the homogeneous, isotropic, elastic overburden model were much less than typically observed. To solve this problem with the stiff overburden and limited displacements, Salamon's laminated overburden model was implemented into a full-featured displacement-discontinuity program. This was the genesis of the present LaModel program (Heasley and Salamon, 1996, Heasley, 1998).

LaModel Basic Formulation

Conceptually, the overburden in the laminated model consists of a horizontal stack of thin plates with cohesionless, frictionless interfaces (see Figure 2). All of the plates have the same elastic modulus (E), Poisson's ratio (ν), and thickness (t), what is called "homogeneous stratifications" (a simplification that was necessary in order to perform the mathematical derivation). This homogeneous stratification formulation does not require the detailed specification of the properties for each individual layer and yet it still provides the desired suppleness of the laminated overburden model (as compared to a homogeneous, isotropic, elastic model).

From this conceptual model, the fundamental second-order, partial differential equation which mathematically represents the laminated overburden model can be derived (Heasley, 1998):

$$\frac{\partial^2 s}{\partial x^2} + \frac{\partial^2 s}{\partial y^2} = \frac{4\sqrt{3(1-\nu^2)}}{E t} \sigma_i \quad (1)$$

where:

s = the seam convergence

x, y = horizontal coordinates/directions

σ_i = the induced stresses applied to the seam (overburden, multiple-seam, material, etc.)

This equation mathematically defines the exact relationship between the curvature (second derivative of the convergence, s) of the roof and floor of the seam, the mechanical properties (E , ν and t) of the overburden and the stresses (σ_i) applied to the seam.

Ground Surface

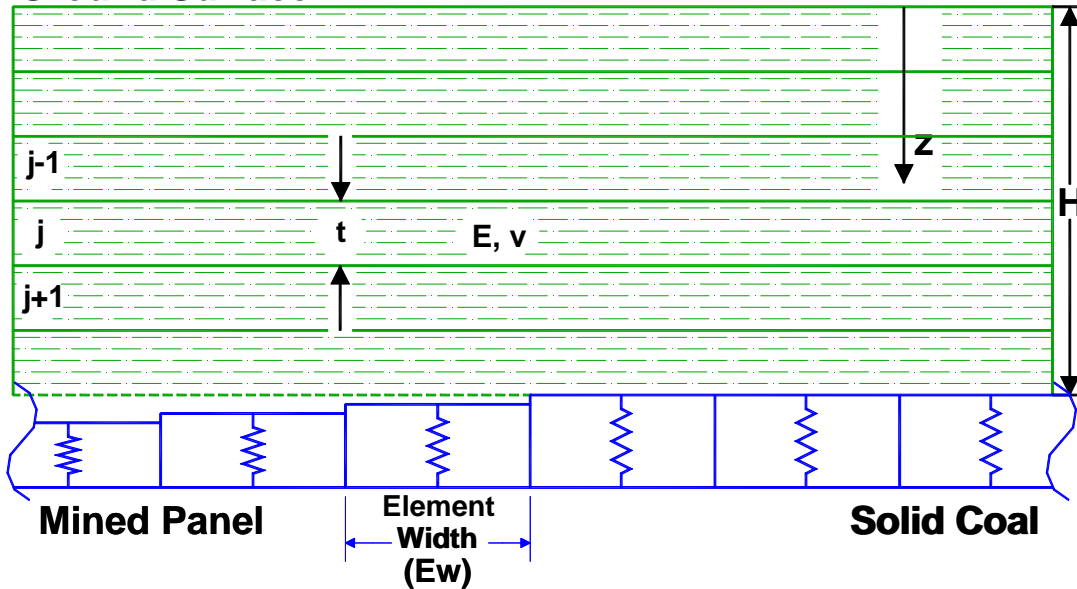


Figure 2. Laminated Overburden Schematic.

The structure of this fundamental equation produces several significant behavioral outcomes of the laminated overburden model:

- 1) First, it can be seen in equation 1 that the bending of the roof (and floor) are inversely proportional to the linear product of the rock mass elastic modulus (E) and the rock mass lamination thickness (t). Thus, increasing either E or t by a given percentage will have the same effect, which is to proportionally decrease the bending ability (increase the stiffness) of the overburden by that percentage. Increasing both E and t by a given multiplier will increase the roof stiffness by the square of that multiplier, and increasing either E or t by a given multiplier and dividing the other parameter by the same multiplier will have no effect on the roof stiffness.
- 2) Second, the rock mass Poisson's Ratio is buried in the term:

$$\sqrt{3(1-v^2)} \quad (2)$$

This formulation causes changes in the Poisson's Ratio to have very limited practical impact. Consider that a reasonable Poisson's Ratio might vary from 0.20 to 0.40. With these limits on the Poisson's Ratio, the factor in equation 2 varies from 1.70 to 1.59. Thus doubling the Poisson's Ratio from 0.20 to 0.40 only affects the rock mass stiffness by 6.5%. Thus, in practical situations, the user does not need to be overly concerned with a precise value for the Poisson's Ratio.

In addition to the laminated formulation of the rock mass, LaModel provides 6 different material models to use for defining the stress-strain response of the in-seam elements (see Figure 3):

- A. Linear Elastic for Coal, defined by the Elastic modulus (E)
- B. Strain-Softening for Coal: defined by Peak stress (σ_p) Peak strain (ε_p), Residual stress (σ_r) and Residual strain (ε_r)
- C. Elastic-Plastic for Coal: defined by Peak stress (σ_p), Peak strain (ε_p), and Plastic modulus (E_p)
- D. Bi-Linear Hardening for Gob (Goaf): defined by Offset stress (σ_o), Offset strain (ε_o), and Hardening modulus (E_h)
- E. Strain-Hardening for Gob: defined by Initial modulus (E_i), Final modulus (E_f) and Ultimate stress (σ_u)
- F. Linear Elastic for Gob: defined by the Elastic modulus (E). (Note, that all of the gob material models include a “Gob Height Factor” to compensate for the difference between the gob thickness and the extraction thickness.)

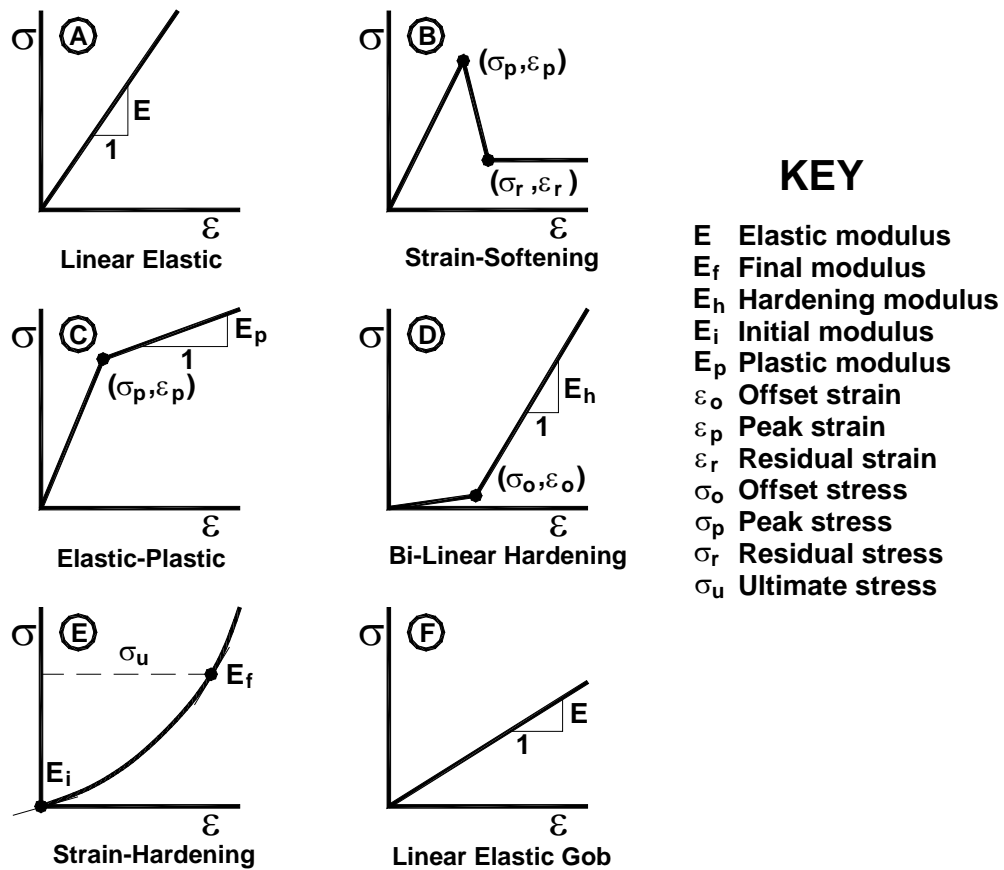


Figure 3. In-Seam Material Models in LaModel

LaModel Enhancements and Upgrades

LaModel was originally developed in 1993 as a research program for Dr. Heasley's Ph.D. dissertation, which was completed in 1998 (Heasley, 1998). LaModel was first presented in the literature in 1996 (Heasley and Salamon, 1996), and LaModel 1.0 was distributed to the public in 1997 (Heasley, 1997). The initial version of LaModel could calculate: seam convergence, total vertical stress, overburden stress, multiple-seam stress and subsidence for single and

multiple seams with complex geometries and variable topography. Version 1.0 was limited to a 250 x 250 grid and 26 different in-seam materials.

In addition to the basic mathematical formulation presented above that was available in the original version, the LaModel program has continually been upgraded and enhanced over the last 20 years, as the need arose. The present program (Version 4.0) is written in Microsoft Visual C++ and runs in the Windows operating system. This version can analyze a 2000 x 2000 grid with 6 different material models and 52 different individual in-seam materials.

The original LaModel 1.0 program required an ASCII text file for input that was manually created by the user in a tedious rigid format, including manually inputting the material codes for each grid element. One did not have to create many of these manual input files before the user starting searching for a better way to input the required data. Therefore, it was not long before a preprocessing program, LamPre 2.1, with forms-based parameter input and spreadsheet-type grid input was created (Heasley and Agioutantis, 2001). Also, in the same time frame, many users were searching for realistic/accurate input parameters for the in-seam material properties. So, a “Coal Wizard” (which helped generate Mark-Bieniawski pillar strengths) and a “Gob Wizard” (which helped determine gob properties from expected abutment angle gob loading) were also implemented in LamPre 2.1. All of the material wizards in LaModel are essentially based on the results of the extensive case history databases used for the ALPS and ARMPS programs (Heasley and Agioutantis, 2001). Simultaneously with developing LamPre, a post-processing program, LamPlt 2.1, which plotted colored-square plots and cross-sections of the LaModel output, was created.

As previously stated, the original LaModel in 1997 had the capability for a seam grid that was 250 by 250 (or 62,500) elements. As computers became more powerful and users desired larger grid sizes, the grid was expanded to 400 by 400 (160,000) elements with LaModel 2.1 (Heasley and Agioutantis, 2001), 1000 by 1000 (1,000,000) elements in 2004 (Wang and Heasley, 2005), and ultimately to 2000 by 2000 (4,000,000) elements in LaModel 3.0. With the expansion in grid size and the corresponding number of grid elements, there came a distinct need to automate the grid generation process. The automatic grid generation for both the mine and overburden grids was originally accomplished indirectly in AutoCAD using AutoCAD Automation commands in 2003 (Heasley *et al.*, 2003) and then more directly and efficiently from within AutoCAD using an AutoCAD Runtime eXtension (ARX) program (Wang and Heasley, 2005). The AutoCAD commands for LaModel can take an AutoCAD map of the pillar plan and overburden, and automatically convert these into the appropriate seam and overburden grids. This addition of automatic gridding of the seam and overburden grids for LaModel from a mine map and overburden contours in AutoCAD has been a significant time saver, particularly with the larger mine models. As part of the AutoCAD integration, LamPlt was upgraded with the capability of creating a Drawing Exchange File (DXF) of the colored-square plots. The DXF files of the LaModel output can be downloaded into AutoCAD and overlain on the mine map for enhanced analysis and graphical display (Heasley, 2008b).

Through the years, as a particular need was determined, either through personal experience or through the request of other users, or as LaModel was applied to unique problems not originally envisioned, various other calculations were added into the LaModel program suite including:

- 1) Pillar safety factor calculations (Hardy and Heasley, 2006)
- 2) Intra-seam subsidence and strain calculations (Hardy and Heasley, 2006)
- 3) A fault model (Heasley, 2008a)

- 4) Energy and energy release calculation (Sears and Heasley, 2009)
- 5) Roof bending stress calculation
- 6) A strain-softening coal property wizard (Li and Heasley, 2014)
- 7) A local mine stiffness calculation (Li and Heasley, 2015)
- 8) A material property wizard for optimizing subsidence calculations (Yang and Heasley, 2016)

Also, the laminated overburden model and LaModel have been incorporated into other programs. In order to make a simple, quick version of LaModel, a complete 2-D laminated overburden program called LaM2D was created (Akinkugbe and Heasley, 2004). This program was never really accepted by a large number of users, but the underlying programming was eventually incorporated into the Analysis of Multiple-Seam Systems (AMSS) program by NIOSH to provide the multiple-seam stress impact. The AMSS program is presently used by many ground control practitioners and is essentially mandated by MSHA for the analysis of multiple-seam mines in the U.S. (Stricklin, 2013). In another software development project, in which the objective was to improve mine design by combining numerical stress analysis with geologic modeling, the LaModel program was combined with AutoCAD and SurvCADD to create a "Stability Mapping" program (Wang and Heasley, 2005). This stability mapping system has been very successfully applied by a number of ground control professionals (Stewart et al., 2006), and its use should increase as improved pillar designs are required in increasingly more geologically challenging conditions.

In the most recent extension of the LaModel program, a computer code (ARMPS-LAM) was developed to effectively implement the laminated overburden model into the ARMPS program (Zhang et al., 2014). This program takes the basic ARMPS geometric input for defining the mining plan and loading condition and then automatically develops, runs, and interprets a full LaModel analysis of the mining geometry to output the stability factor on the Active Mining Zone (AMZ), all without further user input. Using ARMPS-LAM, the ARMPS 2010 database of 645 case histories was analyzed. In a logistic regression of this database analysis, the ARMPS-LAM program was seen to be slightly more accurate than ARMPS 2010 by accurately predicting success or failure of the case histories 71% of the time versus 63% accuracy for the original ARMPS (Zhang et al., 2014).

LaModel pedigree

As previously mentioned, the LaModel program was first distributed to the public in 1997 (Heasley, 1997). From this initial introduction, the program has continued to see increased use and acceptance in the mining industry. A recent analysis of papers published at the International Conference on Ground Control in Mining has found that over 50 papers in the last 20 years have used LaModel in their research (Newman, 2014).

One reason for LaModels ready acceptance is that it fills an essential niche in the pillar design spectrum between the simple empirical programs, such as ALPS, ARMPS and AMSS, and the extremely involved, time-consuming 3-D continuum modeling programs, such as finite-element or finite-difference codes. If the analysis problem is too complex, or non-typical, for the simple empirical programs, then LaModel is often the next step for mine engineers, consultants and researchers to solve the problem. Besides its relative simplicity, a number of other factors have undoubtedly contributed to its ready acceptance in the mining industry:

- 1) The program has always been free.
- 2) Considerable effort (in the form of the lamination thickness, coal and gob wizards) has been expended on helping the user to quickly and easily develop realistic material properties based on generally accepted in-seam and rock mass behavior.
- 3) The automatic mine and overburden grid generation through AutoCAD greatly ease the user's burden in model development
- 4) The continual enhancements have allowed LaModel to stay relevant to the industry's contemporary challenges.

LaModel has also been the primary analysis program to use when the accuracy and acceptance of the results were critical. LaModel was used by MSHA in the extensive back-analysis of the highly publicized 2007 Crandall Canyon Mine collapse with 9 associated fatalities (Heasley, 2008a). As a result of this work, MSHA funded the development of the Lamination Thickness and Gob Wizards in LamPre. The program was again used by MSHA to investigate the influence of overburden and multiple-seam stress on the occurrence of floor bleeders (cracks releasing methane), that may have been a contributing factor to the highly publicized 2010 Upper Big Branch Mine explosion and 29 associated fatalities (MSHA, 2011; Heasley, 2014). Most recently, LaModel was the primary analysis tool used by the mine and MSHA to investigate the Brody Mine rib burst with 2 associated fatalities (MSHA, 2014). In addition to widespread use in the United States, LaModel is also used by a number of consultants in both Australia and South Africa.

Recently MSHA specifically mentioned/recommended the use of the LaModel program for the analysis of complex or non-typical roof control plans (Stricklin and Triebisch, 2012; Stricklin, 2013). While the use of NIOSH pillar analysis programs such as ALPS, ARMPS or AMSS are still recommended for basic designs, roof control plans of complex and/or non-typical underground mining situations are to be supplemented with a LaModel analysis. These complex scenarios are defined as either room-and-pillar retreat mining greater than 1000 feet, bump or bounce prone mines or coal seams, or other criteria considered unusual by the District Manager (Stricklin, 2013).

Modeller Experience

As you have no doubt determined from reading the previous history and formulation of LaModel, the author of this report, Dr. Keith A. Heasley, was the developer and is the primary proponent of the LaModel program (Heasley, 1998; Hardy and Heasley, 2006; Heasley, 2011; Heasley 2014). Until very recently, every line of code in LaModel and LamPlt was written by Dr. Heasley. The LaModel program, research on it, and its application and enhancement have been the primary research focus of Dr. Heasley throughout his 30-year research career at the U.S. Bureau of Mines, NIOSH and West Virginia University. The vast majority of the LaModel research and all of the enhancements and upgrades to the program have been performed by Dr. Heasley or by graduate students under his direction.

But Dr. Heasley's experience with LaModel is certainly not just academic. He has continually worked with practicing engineers at the mines and the regulatory agencies to help develop LaModel into a realistic, effective modeling tool. In fact, many of the enhancements to LaModel were the direct result of striving to analyze/solve difficult ground control problems at operating mines. Further, during his career Dr. Heasley has performed numerous practical consulting projects that have resulted in successful operating mine designs (see Appendix A). Several of the consulting projects on which he was the principal author were very high-profile and very thoroughly reviewed:

- 1) Back analysis of the 2007 Crandall Canyon Mine collapse (MSHA 2008; Heasley, 2008a).
- 2) Investigation on the floor bleeders at the 2010 Upper Big Branch Mine explosion (MSHA 2011; Heasley, 2014).
- 3) Back analysis of the 2014 Brody Mine fatal rib burst (MSHA, 2014).

Basically, there is no one with better knowledge of the LaModel program or more extensive experience in developing practical mine designs using the LaModel program than the author.

LaModel Calibration

Since the geologic environment is so complex, any numerical model of geology must be a simplification of the true complex geo-mechanics. However, to be effective, a numerical mining model does not have to accurately simulate every nuance of the geo-mechanics, but just has to reasonably simulate the most significant geo-mechanical behaviors of the given problem. Since the mechanical simulation in any numerical model is only an approximation of the true mechanics of the geologic situation, the input parameters to the model naturally need to be calibrated in order to have a suitable level of confidence in the model results. For optimum calibration results, the best available information, either: measured, observed or empirical should be used. The laminated overburden model and in-seam material models in LaModel are certainly simplified approximations of the true geo-mechanical behavior; and therefore, the LaModel input parameters need to be calibrated to reality, and like any geo-mechanical model, the realism of a LaModel analysis depends almost entirely on the accuracy/realism of the calibrated input parameters (Heasley 2008b; Heasley 2012).

After many years of experience with the LaModel program, it is clear that in many situations the overburden model in LaModel is not as flexible as the true overburden, especially in caving situations where vertical joints are assumed to be activated. The laminated overburden model in LaModel is inherently more flexible than a homogeneous elastic overburden as used in previous displacement-discontinuity codes, and it is more flexible than a stratified elastic model without bedding plane slip as used in many continuum programs. However, using reasonable values of input parameters, the LaModel program still does not produce the level of seam convergence and/or surface subsidence as measured in the field. It is believed that this displacement limitation in the model may primarily be due to the lack of any consideration for vertical joint movement in the program. The laminated model concentrates on simulating bedding plane slip in the overburden, but it does not consider any overburden movement due to vertical/sub-vertical joint slip, thereby potentially limiting the amount of vertical calculated displacements. In the context of the modelling undertaken for Hume Coal, where remnant pillar design is required to maintain overburden movements to very low levels for reasons of minimising environmental impacts and certainly does not involve overburden caving, the LaModel formulation of simply bending strata is judged to be a reasonable/realistic assumption, since the minimal vertical movements would not be expected to destress vertical joints and so allow significantly vertical shear slip to occur.

Knowing the inherent limitations of the LaModel formulation, the user should plan to calibrate the input parameters in order to obtain realistic outputs. In LaModel, the primary parameters that need to be calibrated are:

- 1) The rock mass stiffness,
- 2) The coal/pillar strength,
- 3) The gob stiffness

Fortunately, a lot of previous effort has been invested into assisting the LaModel user in determining the most realistic/accurate values to use for these primary parameters. Specifically, the pre-processor program, LamPre, implements a Lamination Thickness Wizard for optimizing rock mass stiffness, a Coal Wizard for implementing realistic pillar strengths and a Gob Wizard for implementing realistic gob loading. All of these wizards allow the user to easily incorporate the best contemporary knowledge of coal mining mechanics into optimizing parameter values for a given mining situation. Further, each of the parameter wizards allows the user to easily implement average, empirically-verified behavior, or to customize the given parameter to their unique mining situation based on simple observations or measurements. The specific methodology and algorithms used to implement the LaModel parameter wizards are discussed in the following sections.

Rock Mass Stiffness: The stiffness of the rock mass in LaModel is primarily determined by two parameters, the lamination elastic modulus and lamination thickness. Increasing the modulus or increasing the lamination thickness will increase the stiffness of the overburden (see “LaModel Basic Formulation” and Equation 1 above). With a stiffer overburden: 1) the lateral extent of the abutment stresses will increase, 2) the barrier pillars will carry a higher percentage of the overburden load, 3) the convergence over the gob areas will decrease and 4) the multiple seam stress concentrations will be smoothed over a larger area. When calibrating for realistic stress output, it is recommended that the rock mass stiffness should be calibrated to produce a realistic extent of abutment zone at the edge of the critical gob areas, since this is one of the easiest observations to obtain and has been measured on numerous occasions. Since changes in either the elastic modulus or lamination thickness cause a similar response in the model, it is most efficient to keep one parameter constant and only adjust the other. When calibrating the rock mass stiffness, it has been found to be most efficient/practical to initially select a reasonable lamination elastic modulus (with a thickness weighted average or approximate value) and then solely adjust the lamination thickness to adjust the rock mass stiffness for the model calibration.

In calibrating the lamination thickness for a model based on the extent of the abutment zone, it would be best to use specific field measurements of the abutment zone from the mine in question. However, typically these types of field measurements are not available for a specific mine. In this case, visual observations of the extent of the abutment zone underground due to changes in rib conditions can often be used. Most operations personnel in a mine have a fairly good idea of how far the stress effects on the ribs can be seen from an advancing face or adjacent gob.

Without any site-specific field measurements or observations, average historical field measurements can be used. In particular, historical field measurements used in determining the abutment loading in ALPS and ARMPs would indicate that, on average, the extent of the abutment zone (D) at depth (H) (with both terms expressed in units of ft) for a large extraction panel should be (Mark and Chase, 1997; Mark, 1992):

$$D = 9.3\sqrt{H} \quad (3)$$

or that 90% of the abutment load should be within:

$$D = 5\sqrt{H} \quad (4)$$

Once the desired extent of the abutment zone (D) at a given site is determined, an equation derived from the fundamental laminated overburden model (Heasley 2008b; Heasley *et al.*, 2010; Heasley, 2012) can be used to determine the lamination thickness (t) required to match that desired abutment extent based on the abutment zone distance (D) and the value of some of the other site parameters:

$$t = \frac{2E_s \sqrt{12(1-v^2)}}{E \times M} \times \left(\frac{D-d}{\ln(1-L_g)} \right)^2 \quad (5)$$

Where:

- E = The elastic modulus of the overburden
- v = The Poisson's Ratio of the overburden
- E_s = The elastic modulus of the seam
- M = The seam thickness
- d = The extent of the coal yielding at the edge of the gob
- L_g = The fraction of gob load within distance D

Equation 5 is implemented in the Lamination Thickness Wizard of LamPre and provides an optimum lamination thickness to use for matching the desired empirical abutment stress extent; however, it should be remembered that the value for the abutment extent as given in Equations 4 and 5 was determined from relatively wide longwall gobs and may not be most appropriate for narrow gobs or non-caving situations (such as the Hume Coal proposal). Further, the lamination thickness determined with Equation 5, may not be best for accurately calculating displacement and/or subsidence values. When using Equation 5, the user is fairly accurately matching the "global" stress transfer measured in the field with the global stress transfer in the model. In many practical mining situations, the more "local" stress transfer between adjacent pillars or between adjacent multiple seams is probably determined by the more local flexing of the thinner strata laminations in the immediate roof or interburden. To optimally match these more local effects or to compromise between matching global and local stress transfer, a thinner lamination thickness than determined by Equation 5 may be appropriate.

Coal/Pillar Strength: In conjunction with an accurate load distribution, a realistic strength of the in-seam coal is critical to determining pillar stability. However, determining a realistic/accurate coal strength is not a simple matter and the issue of pillar strength has been a research topic for many years. In a study by Mark and Barton (1997), they looked at more than 4000 UCS tests from 60 different coal seams and tried to apply a seam-specific coal strength to the ARMPS database to improve the statistical fit. However, the statistical analysis found no correlation between the ARMPS stability factor of failed pillars and coal strength. They found that pillar design using ARMPS was more reliable when a uniform coal strength of 6.2 MPa (900 psi) was used. To explain this outcome, they observed that initially, it was very difficult to get a representative sample of coal for laboratory testing; and then, it was difficult to accurately scale the lab strength to accurate in situ strength.

In practice, the most commonly accepted coal pillar strength formulas were determined by back-analysis of field case histories with either failed, or failed and stable pillars (Mark, 1999; Galvin, 2010; Mark, 2010). In particular, the empirically-derived Mark-Bieniawski (M-B) coal pillar strength formula has been verified against numerous case histories and has become the default standard in the U.S. coal industry. The M-B pillar strength formula is used in the NIOSH ALPS and ARMPS programs, which have been widely accepted for a number of reasons:

- 1) They are very easy to use with just minimal geometric input
- 2) They are supported by statistical analysis and calibration to very large databases (> 100 for ALPS and > 645 for ARMPs) of case histories (Mark, 1992; Mark and Chase, 1997)
- 3) They are readily accepted and preferred/recommended by U.S. regulatory agencies (Stricklin, 2013)

Therefore, in order to stay compatible with ALPS and ARMPs, and to stay compatible with their large empirical databases, the LaModel Coal Wizard generates coal properties that match the Mark-Bieniawski pillar strength formula and the ALPS and ARMPs default 900 psi (6.2 MPa) coal strength.

The Mark-Bieniawski pillar strength formula and the default 900 psi (6.2 MPa) coal strength, have primarily been validated based on back-analysis of U.S. case histories. However, the entire wide geographic and geologic distribution of coal seams in the U.S. was used in the back-analysis of the database; and therefore, it would be expected that most international coal seams would fall within the geologic bounds of the database. Further, there is no reason to believe that the research (mentioned above) by Mark and Barton (1997), which showed that pillar design using ARMPs was more reliable when a uniform coal strength of 6.2 MPa (900 psi) was used, would not also be broadly applicable. Galvin (2016) also noted the similarity of underlying coal strength between Australia and South Africa.

To understand how the M-B pillar strength formula is implemented into LaModel through the coal wizard, it is best to start from the derivation of the M-B formula. In the original derivation of the Mark-Bieniawski coal pillar strength formula (Mark and Chase, 1997), and in the more formal derivation later (Johnson *et al.*, 2014), it was determined that the Bieniawski square pillar strength formula implies a linear stress gradient on the pillar at the point of failure (see Figure 4):

$$\sigma_p(x) = S_i \left(0.64 + 2.16 \left(\frac{x}{h} \right) \right) \quad (6)$$

Where:

$\sigma_p(x)$ = Peak Coal Stress

x = Distance into Pillar

S_i = Insitu Coal Strength

h = Pillar Height

This stress gradient was then applied to a rectangular pillar to generate the Mark-Bieniawski (M-B) rectangular pillar strength formula (Mark and Chase, 1997):

$$S_p = S_i \left[0.64 + 0.54 \left(\frac{w}{h} \right) - 0.18 \left(\frac{w^2}{lh} \right) \right] \quad (7)$$

Where:

S_p = Pillar Strength

S_i = Insitu Coal Strength

w = Pillar Width

l = Pillar Length

h = Pillar Height

Pillar Load Bearing Capacity

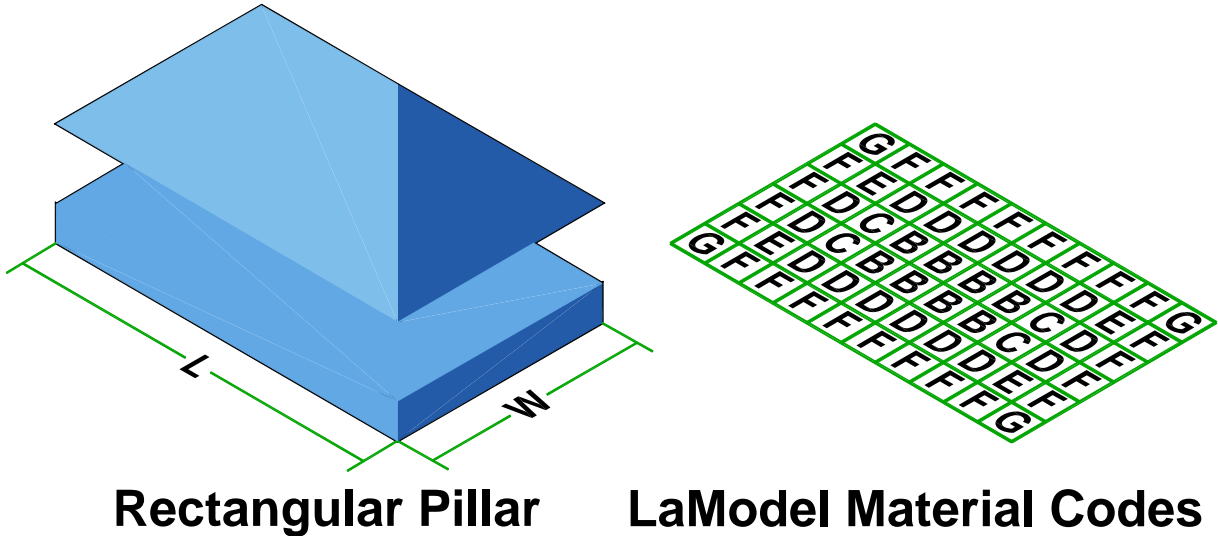


Figure 4. Schematic of Pillar Load and LaModel Element Mapping.

To implement the M-B pillar strength formula into LaModel using square elements, the elements in the pillar are organized into rings, or zones, of elements circumferentially around the pillar (see Figure 4). Each zone, known as a “yield zone,” is composed of 2 material letter codes, one for a “side” element and one for a “corner” element. The average peak stress on a side element is simply determined as the peak strength at the center of the side element, since the stress gradient is linear across the side elements:

$$\sigma_{p-s}(\bar{x}) = S_i \left(0.64 + 2.16 \left(\frac{\bar{x}}{h} \right) \right) \quad (8)$$

Where:

$\sigma_{p-s}(\bar{x})$ = Average Peak Coal Stress for Side Element

\bar{x} = Distance into Pillar at Center of Element

S_i = Insitu Coal Strength

h = Pillar Height

For the corner element, the stress profile across the top of the element is a bit more complex than for a side element. The stress profile above a corner element resembles one quarter of a pyramid. This corner element geometry results in the average stress across the corner element being equal to the stress 1/6 of an element short of the center of the corner element (Johnson *et al.*, 2014):

$$\sigma_{p-c}(\bar{x}) = S_i \left(0.64 + 2.16 \left(\frac{\bar{x} - \frac{w_e}{6}}{h} \right) \right) \quad (9)$$

Where:

$\sigma_{p-c}(\bar{x})$	= Average Peak Coal Stress for Corner Element
\bar{x}	= Distance into Pillar at Center of Element
S_i	= Insitu Coal Strength
h	= Pillar Height
w_e	= Element Width

Equations 8 and 9 are implemented into the LamPre Coal Wizard and allow the user to quickly and easily generate M-B yield zones and associated elements to produce a M-B pillar strength. Further, the materials codes generated in the coal wizard are then designed to be automatically applied as yield zones to the pillars in the grid editor. Thus LaModel users, through the combination of the coal wizard and the automatic yield zone application in the grid editor can quickly and easily generate pillar with the generally accepted M-B pillar strength. For the element strain values, the user inputs a desired elastic modulus and the respective peak strains are determined from the given elastic modulus and the peak stress.

In order to exactly match the M-B pillar strength formula at the pillar peak strength, the coal element's average peak stress as given by Equations 8 and 9 are implemented into an elastic, perfectly-plastic element model (model C in Figure 3). Therefore, as the elements fail, typically from the outside of the pillar inward, they maintain their peak stress through any post-failure strain. Using this elastic, perfectly-plastic failure response, when the pillar yields sufficiently that the inner most elements reach their peak stress (and associated peak strain) at the point of peak pillar strength (see Figure 5), all of the outer elements in the pillar will be at their peak stress; and therefore the pillar stress profile will exactly match that shown in Figure 4, and peak pillar strength will be exactly equal to the M-B pillar strength, as implemented through Equations 8 and 9.

To determine the complete pillar stress-strain curve in LaModel (for calculating pillar safety factors) the individual stress-strain curves for each element in the pillar are essentially summed, or integrated together to produce a cumulative stress-strain curve for the entire pillar, similar to that shown in Figure 5 for a 5.5 m wide rib pillar at Hume. From this cumulative pillar stress-strain curve, the program can determine an average peak pillar stress and associated average peak strain. Then based on the actual calculated pillar stress and strain, the pillar safety factor can be determined.

(In this document, I use the term, pillar “safety factor,” in the classic mechanical engineering sense, where the calculated strength of a pillar is divided by the calculated load on the pillar to get the safety factor. LaModel is a mechanics-based program where all of the output loads and displacements are mechanically balanced against the input loading, and material strengths and stiffness. I reserve the term, “stability factor,” for the calculation used in ALPS and ARMPS, where the recommended stability factor is always an average safety factor, calculated a certain way over a particular area, and then compared to a database to develop a recommended value. The ALPS and ARMPS calculations do not follow strict mechanics to distribute loads and do not consider displacements in the calculation. When I am calculating the ratio of strength to load for a particular pillar, I call that a safety factor. When I average the pillar safety factors over a particular area similar to the ARMPS calculation in order to compare the average safety factor output with the ARMPS database, then I would call the result a Stability Factor.)

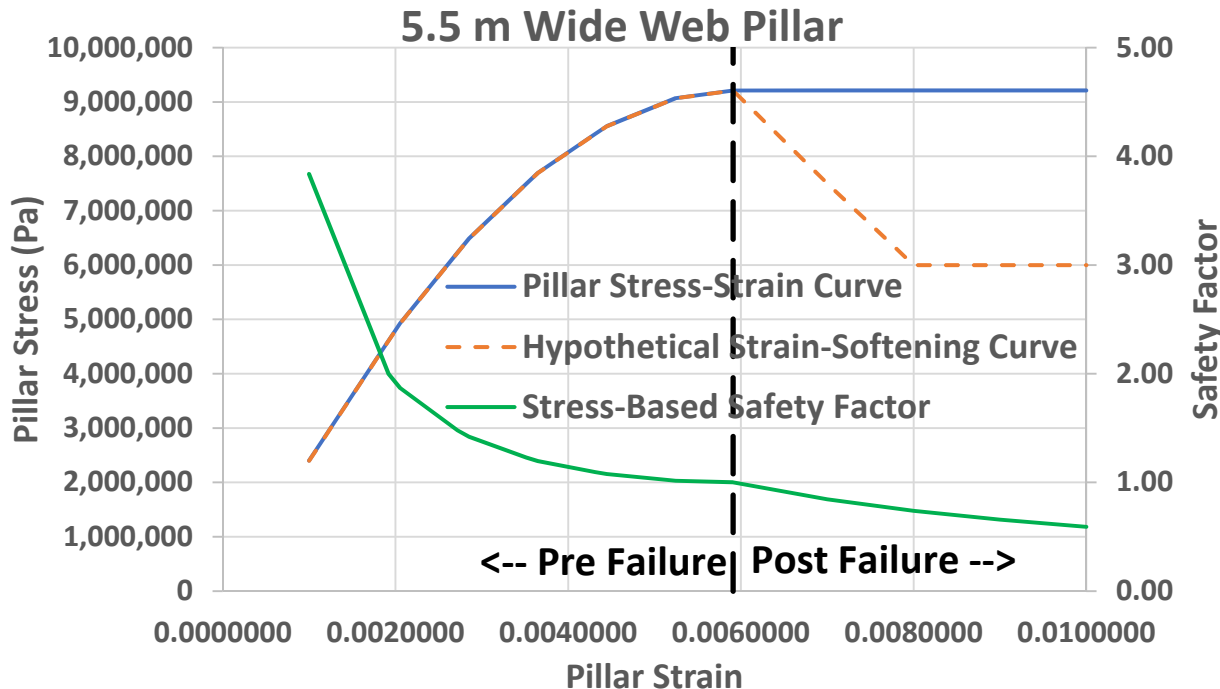


Figure 5. Stress-Strain Curve for Hume 5.5 m Wide Web Pillar.

Using the elastic, perfectly-plastic element in the coal wizard, also means that the pillar will maintain its peak strength throughout the post-failure range (see Figure 5). For thinner pillars that may be strain-softening after failure and for wider pillars that may be strain-hardening after failure, the elastic, perfectly-plastic behavior would be accurate through the elastic range up to the point of peak strength, but would then deviate from the expected strain-softening or strain-hardening behavior in the post-failure range (see Figure 5). Therefore, the elastic, perfectly-plastic pillar strength approach as used in these models is only accurate when used to model pillars with safety factors greater than 1. However, as long as the pillars in a model are below the peak strength, which means the pillars are within the elastic range and have safety factors > 1.0 (and are in the pre-failure range in Figure 5), the response of an elastic-plastic model is essentially identical to the response of a strain-softening or strain-hardening model.

In the Hume Mine models, the web pillars have w/h ratios of: 1.00, 1.17 and 1.57 for the 80, 120 and 160 m deep pillar plans, respectively. These web pillars would almost certainly be strain-softening after failure (Das, 1987), but in all of the Hume models, including those with pillars removed, the web pillars are in the pre-failure, elastic range with safety factors > 1. In the Hume Mine models, the intra-panel barrier pillars have w/h ratios of: 4.00, 4.80 and 5.97 for the 80, 120 and 160 m deep pillar plans, respectively. With these w/h ratios, the intra-panel pillars would be expected to behave elastic-plastic after failure (Das, 1987); and therefore, the elastic-plastic pillar behavior is probably very appropriate.

Gob Stiffness>Loading: In a LaModel analysis with gob areas, the interaction between the overburden stiffness and gob stiffness determines how the overburden load above the gob is distributed between the gob and the adjacent pillars. With the overburden stiffness initially calibrated to match a desired extent of the abutment stress (or by some other method), the gob stiffness then becomes the parameter that functionally determines the overburden load distribution. Therefore, the calibrated gob stiffness determines how much load is distributed to

the abutment loading; and therefore, it is critical for accurately calculating the pillar stresses and safety factors.

In LamPre, the gob wizard is designed to provide the user with a gob stiffness that matches a desired abutment angle. In the gob wizard, the default abutment angle is 21° which matches the value used in ALPS and ARMPS (Mark, 1992; Mark and Chase, 1997). Using the gob wizard, the gob stiffness is then calibrated by adjusting the gob modulus until a calculated two-dimensional gob loading matches the empirical gob load (Heasley et al., 2010) as determined by the chosen abutment angle.

For the Hume Mine and associated models, there are no gob areas and no gob material; therefore, calibration of the gob is not applicable. The brief description of the gob calibration is simply included here for completeness in describing the calibration of LaModel.

Hume Mine Models

Stage 1 - Investigation of Coal Models

In this initial stage of the modeling analysis at Hume Coal, two different coal models were compared in order to determine which one might be best for the subsequent modeling. The first coal model was developed by Dr. Russell Frith (RF) to incorporate an elastic stage, a plastic stage and then a post-failure stage that could vary from strain-softening to strain-hardening based on the width-to-height ratio (w/h) of the pillar. The parameters for this RF coal model were developed from laboratory, field and analytical analysis of coal specimens and pillars. The second coal model was the Mark-Bieniawski model as implemented into LaModel, and explained above.

To compare the two different coal models, a simple 2-D LaModel grid was developed to simulate a panel of web pillars with 7 entries, 4 m wide entries, 4 m wide web pillars and 18 m wide barrier pillars. For the model, 0.5 m elements were used on a grid that was 140 elements wide by 10 elements high. The depth in the model was set at 120 m and the rock mass was simulated with 5 m thick layers with an elastic modulus 16.5 GPa. Using this mine grid and rock mass properties, the two different coal materials with identical elastic moduli, but different peak strengths were implemented into the model and the solutions were obtained.

Essentially, the model results were almost identical. The RF coal pillars resulted in an average web pillar SF of 1.323, and the M-B coal pillars resulted in an average web pillar SF of 1.331. The difference between the models in this practical application for Hume is barely evident in the third significant digit. Essentially, with a SF of 1.3, both coal models are still operating well in the elastic range, and with an identical elastic modulus, the two coal models are behaving identically before failure. The slight difference between the two coal models only comes from slight differences in their implementation. Both models mostly stay elastic with the same modulus, but the M-B model allows a small yield zone at the edge of the pillar (a little softer), whereas the RF model does not yield at the edge in the given model.

The outcome of this brief comparison was that the Mark-Bieniawski pillar strength formula was chosen to be used in subsequent models because:

- 1) The difference in output between the M-B coal material and the RF coal material is insignificant.

- 2) The M-B coal material is simpler and easier to use because it is presently implemented into the coal wizard, automatic yield zone generation, and safety factor calculations in LaModel.
- 3) The M-B coal model has been verified and calibrated with the very large databases associated with ALPS and ARMPS.

Stage 2 - Investigation of Rock Mass Lamination Thickness

The next parameters to be investigated with some preliminary analysis were the rock mass elastic modulus and the rock mass lamination thickness. The overburden above the proposed Hume Project mine workings is dominated by the Hawkesbury Sandstone, varying in thickness between 80 m and 120 m within the project area. Given the cover depth range of 80 m to 160 m, it is assumed that the overall overburden stiffness is mostly dictated by the Hawkesbury Sandstone. Laboratory testing of 15 Hawkesbury Sandstone (HSS) core samples from the Hume Project (noting that not all samples from the HSS were sandstone – only 92% were sandstone) returned elastic modulus (E) values ranging from 8.2 GPa to 23.2 GPa with a mean value of 16.5 GPa. In subsequent models, all three values for E of 8.2, 16.5 and 23.2 GPa (low, average and high) were selected to be used as part of the modeling study in order to cover the range of potential overburden modulus values.

For investigating appropriate rock mass lamination thicknesses to use in the modeling, a couple of scoping studies were performed. First, the lamination thickness wizard was run on the various depths (80, 120 and 160 m) and rock mass modulus values for the Hume Panels. The wizard suggested a range of values for the given range of depths and rock mass moduli based on default abutment zone assumptions, since no site-specific observational data of abutment extent was available from the proposed Hume Mine. In particular, a low lamination thickness of 22.8 m was determined for the shallow cover (80 m) and stiff overburden (23.2 GPa), and a high lamination of 120.9 m was determined for the deeper cover (160 m) and softer overburden (8.2 GPa).

Next, a number of very simply back-analysis models were run to simulate the Berrima Mine. The Berrima mine has very similar geology to Hume, and at Berrima they were extracting 120 m wide panels at a depth of 160 m with an extraction height of 2.3 m and an overall extraction ratio of 85%. At Berrima, the subsidence over the panels was measured to stay below 10 mm. The Berrima Mine back-analysis models were defined with the given dimensions and then the rock mass lamination thickness was calibrated to match a subsidence of 10 mm, in conjunction with the three rock mass elastic moduli. The back-analyses resulted in:

- 1) a lamination thickness of 285 m with the rock modulus of 8.2 GPa.
- 2) a lamination thickness of 185 m with the rock modulus of 16.5 GPa
- 3) a lamination thickness of 155 m with the rock modulus of 22.3 GPa

a range in lamination thickness of 155 to 285 m.

Based on the results of the two simple scoping studies and considering a desire to keep the lamination thickness conservatively low (to err on the side or putting additional load on the rib pillars), the rock mass laminations thicknesses of 20 and 40 m were chosen to use in subsequent models.

Stage 3 – 2-D Models

With a reasonable coal model and a range of conservative rock mass stiffness parameters developed in the first two design stages, the next step was to develop a series of 2-D models to investigate overall system behavior and stability in the 2-D section within the range of the parameters selected for sensitivity analysis.

In order to best fit the desired entry and web pillar widths (see Table 1 and Table 2) of the panel designs at the three chosen depths, a 0.5 m wide element was strategically chosen to exactly fit the 3.5 m and 5.5 m wide web pillars, while also being very close to matching the 4.1 m wide web pillar (see Table 2). Also, the 4 m wide entry was fit exactly. LaModel has a requirement that the grid size be divisible by 10, and for expediency, it was desired to only model one panel of rib pillars, so the size of the intra-panel barrier pillar was varied in the 2-D models to fit a grid that was 140 elements wide (see Table 2).

Table 2. Grid Sizes for Two-Dimensional Models

Depth (m)	Element Size (m)	Number of Entries	Entry Width (m)	Entry Elements	Desired Rib Pillar Width (m)	Rib Pillar Elements	Modeled Rib Pillar Width (m)	Desired Barrier Width (m)	Barrier Elements	Modeled Barrier Width (m)	Total Elements
80	0.5	8	4.0	8	3.5	7	3.5	14.0	27	13.5	140
120	0.5	7	4.0	8	4.1	8	4.0	16.8	36	18	140
160	0.5	6	4.0	8	5.5	11	5.5	20.9	37	18.5	140

Using the overburden and coal properties, and grid dimensions as detailed above, the 2-D models were developed and run. With 3 depths, 3 potential rock mass modulus values and 2 potential rock mass laminations thicknesses, the total number of potential 2-D models is 18. However, only a strategic set of 13 of these potential different models was run. The primary convergence, stress and safety factor output from these models, along with the comparable ARMPS safety factors, is presented in Table 3. For each 2-D model, the average web pillar safety factor from the given number (7 at 80 m deep, 6 at 120 m deep and 5 at 160 m deep) of web pillars in each model was calculated. Also, to illustrate how the loading on the web pillars varies across the panel, the individual safety factors from the web pillar at the center of the panel (which would have the highest overburden load and lowest SF) and the “outer” web pillar adjacent to the intra-panel barrier pillar (which would have the lowest overburden load and highest SF) were extracted from the model outputs and are presented in Table 3. The safety factor of the intra-panel barrier pillar is also presented in Table 3.

In the 2-D model results in Table 3, it can be seen that the subcritical width of the panel causes all of the LaModel web pillar safety factors to be higher than the corresponding ARMPS-HWM results (calculated with tributary area loading). Essentially, some of the tributary area overburden weight that is assumed in ARMPS-HWM is actually carried by the adjacent intra-panel barriers in the LaModel analysis. The amount of load carried by the adjacent barrier pillars is seen to increase (as represented by a higher web pillar safety factor and lower barrier pillar safety factor) as the overburden gets stiffer with increased elastic modulus and/or lamination thickness. (Please note that the barrier pillar safety factors calculated in ARMPS-HWM do not include any overburden support from the web pillars, while the LaModel analysis elastically distributes the overburden load according to the relative stiffness of the pillars and overburden.) Also in the model results, the multiplicative nature of E and t is evident, with the results for models containing E of 8.2 GPa and t of 40 m being almost identical to models containing E of 16.5 GPa and t of 20 m (for the same depth).

Table 3. 2-D Model Results

Depth (m)	Lamination Thickness (m)	Rock Mass Elastic Modulus (Gpa)	Average Web Pillar Safety Factor	Center Web Pillar			Outer Web Pillar			Barrier Pillar		
				Convergenc e (m)	Stress (Pa)	Safet y Facto r	Convergenc e (m)	Stress (Pa)	Safet y Facto r	Convergenc e (m)	Stress (Pa)	Safet y Facto r
80	ARMPS-HWM			1.680			1.680			1.680		2.550
80	20	8.2	1.798	0.006251	4,286,457	1.726	0.005635	3,864,000	1.914	0.004446	3,048,882	5.695
80	20	16.5	1.843	0.006098	4,181,486	1.769	0.005519	3,784,757	1.954	0.004712	3,230,893	5.374
80	20	23.2	1.864	0.006006	4,118,614	1.796	0.005487	3,762,286	1.966	0.004839	3,317,986	5.233
80	40	8.2	1.842	0.006100	4,182,571	1.768	0.005520	3,785,243	1.954	0.004709	3,229,314	5.377
80	40	16.5	1.885	0.005910	4,052,429	1.825	0.005466	3,747,957	1.973	0.004961	3,401,607	5.105
80	40	23.2	1.903	0.005822	3,992,043	1.853	0.005455	3,740,514	1.977	0.005065	3,473,400	4.999
120	ARMPS-HWM			1.280			1.280			1.280		2.260
120	20	8.2										
120	20	16.5	1.408	0.008769	5,733,700	1.362	0.007940	5,309,263	1.470	0.006527	4,475,594	4.737
120	20	23.2										
120	40	8.2	1.408	0.008772	5,735,525	1.361	0.007942	5,310,313	1.470	0.006524	4,473,556	4.739
120	40	16.5	1.450	0.008350	5,523,213	1.414	0.007742	5,211,175	1.498	0.006847	4,693,183	4.518
120	40	23.2	1.468	0.008165	5,429,625	1.438	0.007673	5,176,771	1.508	0.006981	4,783,587	4.432
160	ARMPS-HWM			1.310			1.310			1.310		1.660
160	20	8.2										
160	20	16.5	1.414	0.010572	6,734,364	1.379	0.009855	6,407,609	1.450	0.008378	5,670,056	3.739
160	20	23.2										
160	40	8.2										
160	40	16.5	1.446	0.010148	6,560,609	1.416	0.009626	6,291,282	1.476	0.008689	5,883,828	3.603
160	40	23.2	1.460	0.009970	6,485,700	1.432	0.009548	6,249,536	1.486	0.008822	5,974,344	3.549

Stage 4 – 3-D Models

With very encouraging results from the 2-D models, a similar series of full 3-D models that incorporate the length of the web pillars, along with the chain pillars and the adjacent inter-panel barrier pillars (see Figure 1) were developed to examine the pillar system behavior and stability in three dimensions. These 3-D models used the same parameter input values of depth, rock mass modulus, lamination thickness and coal model as used in the 2-D analysis (see Tables 3 and 4).

The 3-D LaModel simulation of the Hume Mine pillar plan encompassed a fairly large area of the mine (see the “Mine Grid” area in Figure 1), essentially two full panels, chain pillar entries to chain pillar entries, 675 m in width and about 750 m in length. This extended grid size helps keeps any edge effects from the boundary conditions from affecting the area of interest around the middle web pillar panels. Also, the mine grids were sized to end in the larger chain and intra-panel barrier pillars to help minimize edge effects. Again, as in all of the models, a 0.5 m element size was used to best fit the given entry and pillar dimensions (see Table 1) resulting in mine grids that were 1350 elements wide by 1500 elements high. These 3-D mine grids were automatically generated from a digital version (AutoCAD map) of the Hume Mine. Note, when a mine grid is automatically digitized with a repeating pillar size (4.1 m for instance) that does not exactly fit the element size (0.5), then you will see in the resulting element grid that every so often (in this case every fifth pillar) a pillar will be generated with an additional element to get the element grid to correctly match the mine coordinates. On the boundary of the mine grid, the boundary condition was set to “Symmetric” for all four sides.

For the subsidence calculation, a subsidence grid was developed on the surface. This subsidence grid was larger than the mine grid on all four sides by an amount equal to the depth (essentially assuming a very conservative 45° angle from the extent of the modelled workings) and used a 5 m element size. This resulted in subsidence grids of (see Figure 1):

- 1) 835 X 910 m (167 X 182 elements) for the 80 m deep model.
- 2) 915 X 980 m (183 X 196 elements) for the 120 m deep model.
- 3) 995 X 1090 m (199 X 218 elements) for the 160 m deep model.

Since the model is relatively shallow, the surface effect calculation was implemented to provide the most accurate subsidence.

The primary output from the 3-D models, along with the comparable ARMPS-HWM safety factors, is presented in Table 4. For each 3-D model, the safety factors from the center web pillar, the off-center web pillar (the pillar adjacent to the center web pillar) and the outer web pillar (adjacent to the barrier) were extracted from the model outputs. Since the safety factor varies along the length of the narrow web pillar, for each of these average pillars, an Average, Outby, Middle, and Inby safety factor were calculated (see Table 4). The Outby and Inby safety factors were calculated 10 elements from the respective ends of the pillar to minimize end effects. Also, the safety factor of the intra-panel barrier pillar and chain pillar as well as the maximum surface subsidence were extracted from the models and presented in Table 4.

Table 4. 3-D Model Results

				Center Web Pillar - SF				Off-Center Web Pillar - SF				Outer Web Pillar - SF				Barrier Pillar	Gate Pillar	
Depth (m)	Lamination Thickness (m)	Rock Mass Elastic Modulus (Gpa)	Analysis Type	Average	Outby	Middle	Inby	Average	Outby	Middle	Inby	Average	Outby	Middle	Inby	Safety Factor	Safety Factor	Maximum Subsidence
80			ARMPS	1.68	1.68	1.68	1.68	1.68	1.68	1.68	1.68	1.68	1.68	1.68	1.68	2.68		
80	20	8.2	LaModel	1.73	1.62	1.71	2.05	1.74	1.62	1.72	2.06	1.91	1.75	1.90	2.21	5.58	5.10	0.00280
80	20	8.2	Failed Pillar					1.40	1.38	1.36	1.73	1.80	1.68	1.78	2.13	5.50	4.92	0.00365
80	20	8.2	Failed Section													2.94	3.30	0.02353
80	20	16.5	LaModel	1.79	1.72	1.75	2.17					1.97	1.84	1.93	2.33	5.33	5.00	0.00268
80	40	23.2	LaModel	1.92	1.86	1.86	2.33					2.04	1.94	1.98	2.44	5.09	4.84	0.00246
120			ARMPS	1.31	1.31	1.31	1.31	1.31	1.31	1.31	1.31	1.31	1.31	1.31	1.31	2.03		
120	20	16.5	LaModel	1.38	1.31	1.36	1.61	1.41	1.33	1.39	1.63	1.48	1.39	1.47	1.70	4.40	3.24	0.00357
120	40	16.5	LaModel	1.45	1.38	1.42	1.69	1.47	1.40	1.44	1.71	1.52	1.44	1.50	1.77	4.26	3.21	0.00334
120	40	23.2	LaModel	1.47	1.41	1.45	1.73	1.49	1.42	1.47	1.75	1.54	1.46	1.51	1.79	4.21	3.20	0.00328
160			ARMPS	1.31	1.31	1.31	1.31	1.31	1.31	1.31	1.31	1.31	1.31	1.31	1.31	2.00		
160	20	16.5	LaModel	1.39	1.29	1.38	1.58	1.40	1.29	1.39	1.59	1.46	1.33	1.45	1.65	4.25	2.59	0.00426
160	20	16.5	Failed Pillar					1.16	1.14	1.14	1.37	1.31	1.23	1.29	1.52	4.09	2.45	0.00511
160	20	16.5	Failed Section													2.72	1.86	0.01642
160	40	23.2	LaModel	1.46	1.38	1.44	1.67					1.52	1.40	1.50	1.71	4.07	2.59	0.00369

In Table 4 and Figure 6, the three-dimensional effects of the sub-critical length of the web pillars along with the sub-critical width of the panels can be seen. Not only do the web pillar safety factors increase as the web pillar gets closer to the intra-panel barrier, but it can also be seen that the web pillar safety factors increase as the location in the web pillar approaches the inter-panel barriers. In Figure 6, it can be seen that the panel convergence is limited on all four sides by the barrier and chain pillars. Essentially, some of the tributary area overburden weight that is assumed in ARMPS-HWM is also carried by the inter-panel barriers and (to a lesser extent) by the chain pillars in the LaModel analysis. Similar to the 2-D analysis, the amount of load carried by the adjacent barrier pillars is seen to increase (as represented by a higher web pillar safety factor and lower barrier pillar safety factor) as the overburden gets stiffer with increased elastic modulus and/or lamination thickness.

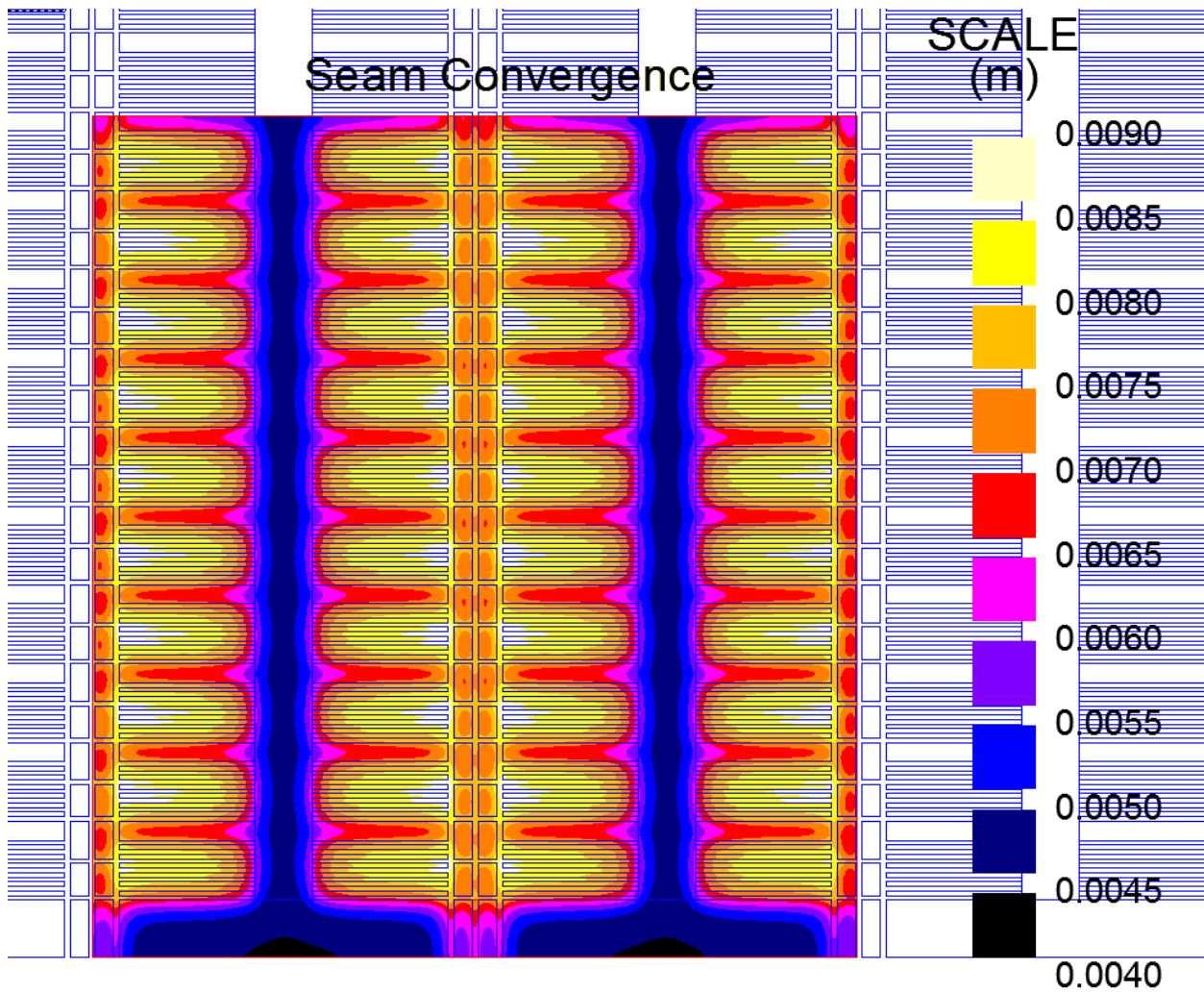


Figure 6. Seam Convergence: 120 m deep, 40 m Laminations, 16.5 GPa Modulus.

One aspect of the 3-D analysis that was not necessarily expected, is the slight reduction of the safety factor on the outby end of the web pillars below the average ARMPS-HWM value, near the chain pillars for some of the least stiff rock mass parameter combinations. For these least stiff rock mass models, the safety factor is slightly less (< 2-5%) than in the perfectly 2-D ARMPS-HWM analysis, although it is not an equivalent comparison since the ARMPS-HWM stability factors are assumed to be averages for entire pillars, which are being compared to the length-wise safety factors which are available from the outputs of the 3D model. In the 3-D model, there are two effects which are contributing to this model outcome. First, not only does the outby end of the rib pillar have to support its share of the overburden above it, it also has to help support half of the overburden weight from the adjacent panel entry. Also, as the pillars are modeled in LaModel, the outby end of the web pillar has a reduced load carrying ability due to the free face and associated yield zone on the end of the web pillar. Further, as the stiffer rock mass parameters are used, as suggested by the observation-based lamination thickness wizard and Berrima back-analysis, the pillar safety factors at the outby end of the web pillars, are again above the ARMPS-HWM values.

Stage 5 – Worst-Case Scenarios, Failed Web Pillar and Failed Section

In a couple of additional models for the 80 m deep design and the 160 m deep 3-D models, the center web pillar of a panel was removed and all web pillars in a panel were removed. In both cases, no gob or support was used to replace the removed pillars. These models were intended to simulate the pillar safety factor and/or subsidence response to a very conservative model of single failed web pillar or to failure of the entire section of web pillars.

The results from the failed web pillar and failed section models are also given in Table 4, and an analysis of these results provides some critical insight into the mine response to potential pillar failure. In the failed single web pillar simulations, the safety factors of the adjacent pillars are seen to decrease, but in both models (80 and 160 m deep) the adjacent barrier and chain pillars do not approach a failed condition. Also, the surface subsidence in these failed pillar models is seen to only increase by about 1 mm. In the failed web pillar section models, all support from the web pillars was removed in the panel, yet the adjacent barrier and chain pillars remain stable. Also, with an entire web pillar section failed, there was an increase in local surface subsidence of between 16 and 24 mm.

References

- Akinkugbe O and K A Heasley, 2004, The new two-dimensional LaModel program, in Proceedings: 23rd International Conference on Ground Control in Mining, West Virginia University, Morgantown, WV, p. 146–153.
- Beckett L A and R. S. Madrid, 1988, MULSIM/NL – A structural analysis computer program for mine design, USBM IC 9168, U.S. Department of the Interior, U.S. Bureau of Mines, Washington, DC, 302 p.
- Berry, D S, 1960, An elastic treatment of ground movement due to mining - part I. isotropic ground, Journal of Mechanics and Physics of Solids, vol. 8, p. 280-292.
- Crouch, S L, 1976, Analysis of stresses and displacements around underground excavations: an application of the displacement-discontinuity method, Geomechanics Report, University of Minnesota, Minneapolis, MN, 267 p.
- Das, M N, 1986, Influence of width/height ratio on post failure behavior of coal, International Journal of Mining and Geological Engineering, vol. 4, p. 79-87.
- Galvin, J M, 2016, Ground engineering - principles and practices for underground coal mining, Springer, New York, NY.
- Galvin, J M, 2010, The UNSW pillar design methodology and considerations for using this and other empirical pillar system design approaches, in Proceedings: 3rd International Workshop on Coal Pillar Mechanics and Design, Department of Health and Human Services, Centers for Disease Control and Prevention, National Institute for Occupational Safety and Health, Washington, DC, p. 19–29.
- Hardy, R and K A Heasley, 2006, Enhancements to the LaModel stress analysis program, Preprint 06-067, Society of Mining Engineers Annual Meeting, St. Louis, Missouri, Mar. 26-29, 2006, 7 p.
- Heasley, K A and M D G Salamon, 1996, A new laminated displacement-discontinuity program: fundamental behavior, in Proceedings: 15th International Conference on Ground Control in Mining, West Virginia University, Morgantown, WV, p. 111-126.
- Heasley, K A, 1997, A new laminated overburden model for coal mine design, in Proceedings: New Technology for Ground Control in Retreat Mining, NIOSH IC 9446, Department of Health and Human Services, Centers for Disease Control and Prevention, National Institute for Occupational Safety and Health, Washington, DC, p. 60-73.

- Heasley, K A, 1998, Numerical modeling of coal mines with a laminated displacement-discontinuity code, PhD thesis, Colorado School of Mines, Golden, CO, 187 p.
- Heasley, K A and Z Agioutantis, 2001, LAMODEL - a boundary element program for coal mine design, in Proceedings: 10th International Conference on Computer Methods and Advances in Geomechanics, University of Arizona, Tucson, AZ, p. 1679-1682.
- Heasley, K A, Z Agioutantis and Q Wang, 2003, Automatic grid generation allows faster analysis of coal mines, Transactions of the Society for Mining Metallurgy, and Exploration, Inc., Denver, CO, Vol. 314, p. 75-80.
- Heasley K A, 2008a, Back analysis of the Crandall Canyon Mine using the LaModel program, appendix in: Underground Coal Mine – Fatal Underground Coal Burst Accidents August 6 and 16, 2007, DOL-MSHA RI, U.S. Department of Labor, Mine Safety and Health Administration, Arlington, VA, 46 p.
- Heasley, K A, 2008b, Some thoughts on calibrating LaModel, in Proceedings: 27th International Conference on Ground Control in Mining, West Virginia University, Morgantown, WV, p. 7–13.
- Heasley, K A, M M Sears, I B Tulu, C H Calderon-Arteaga and L W Jimison, II, 2010, Calibrating the LaModel program for deep cover pillar retreat coal mining, in Proceedings: 3rd International Workshop on Coal Pillar Mechanics and Design, Department of Health and Human Services, Centers for Disease Control and Prevention, National Institute for Occupational Safety and Health, Washington, DC, p. 47–57.
- Heasley, K A, 2011, A retrospective on LaModel (or Dr. Heasley's wild wide), in Proceedings: 30th International Conference on Ground Control in Mining, West Virginia University, Morgantown, WV, p. 21-29.
- Heasley, K A, 2012, Calibrating the LaModel program for site specific conditions, in Proceedings: 31st International Conference on Ground Control in Mining, West Virginia University, Morgantown, WV, p. 48-55.
- Heasley, K A, 2014, LaModel – a program for coalmine modelling,” in Proceedings: AusRock 2014: Third Australasian Ground Control in Mining Conference, Sydney, Australia, 6 p.
- Johnson, J C, J K Whyatt and M C Loken, 2014, A generalized method for calculating pillar cell capacities for boundary element modeling of coal, Preprint 14-162, Society of Mining Engineers Annual Meeting, Salt Lake City, Utah, Feb. 23-26, 2014, 15 p.
- Kripakov, N P, L A Beckett, D A Donato and J S Durr, 1988, Computer-assisted mine design procedure for longwall mining, USBM RI 9172, U.S. Department of the Interior, U.S. Bureau of Mines, Washington, DC, 38 p.
- Li, K and K A Heasley, 2014, Using field measurements to quantify the post-failure behavior of coal, in Proceedings: 48th U.S. Symposium on Rock Mechanics, Minneapolis, MN, Paper 14-7133, 7 p.
- Li, K and K A Heasley, 2015, Calculating the potential for coal pillar bumps using a local mine stiffness criterion, in Proceedings: 49th U.S. Symposium on Rock Mechanics, San Francisco, CA, Paper 15-241, 8 p.
- Mark, C, 1992, Analysis of longwall pillar stability (ALPS); an update, in Proceedings: Workshop on Coal Pillar Mechanics and Design, USBM IC 9315, U.S. Department of the Interior, U.S. Bureau of Mines, Washington, DC, p. 238-249.
- Mark, C and T M Barton, 1997, Pillar design and coal strength, in Proceedings: New Technology for Ground Control in Retreat Mining, NIOSH IC 9446, U.S. Department of Health and Human Services, National Institute for Safety and Health, Washington, DC, p. 49-59.
- Mark, C and F E Chase, 1997, Analysis of retreat mining pillar stability (ARMPS), in Proceedings: New Technology for Ground Control in Retreat Mining, NIOSH IC 9446, U.S.

- Department of Health and Human Services, National Institute for Safety and Health, Washington, DC, p. 17-34.
- Mark, C, 1999, Empirical methods for coal pillar design, in Proceedings: 2nd International Workshop on Coal Pillar Mechanics and Design, NIOSH IC 9448, U.S. Department of Health and Human Services, National Institute for Safety and Health, Washington, DC, p. 145-154.
- Mark, C, 2010, Pillar design for deep cover retreat mining: ARMPS Version 6 (2010), in Proceedings: 3rd International Workshop on Coal Pillar Mechanics and Design, Department of Health and Human Services, Centers for Disease Control and Prevention, National Institute for Occupational Safety and Health, Washington, DC, p. 106–122.
- MSHA, 2008, Fatal underground coal burst accidents August 6 and 16, 2007, Crandall Canyon Mine, DOL-MSHA, RI, U.S. Department of Labor, Mine Safety and Health Administration, Arlington, VA, 472 p.
- MSHA, 2011, Fatal underground mine explosion, April 5th, 2010, Upper Big Branch Mine, DOL-MSHA RI, U.S. Department of Labor, Mine Safety and Health Administration, Arlington, VA, 971 p.
- MSHA, 2014, Underground coal mine fatal rib burst accident, May 12, 2014, Brody Mining LLC, DOL-MSHA RI, U.S. Department of Labor, Mine Safety and Health Administration, Arlington, VA, 29 p.
- Newman, C R , 2014, The online LaModel user's and training manual, development and testing, M.S. Thesis, West Virginia University, Morgantown, WV, 133 p.
- Pauza, A., 2018, Personal Communication.
- Plewman, R P, F H Deist and W D Ortlepp, 1969, The development and application of a digital computer method for the solution of strata control problems, Journal of the South African Institute of Mining and Metallurgy, vol. 70 (9), p. 33-44.
- Salamon, M D G, 1962, The influence of strata movement and control on mining development and design, PhD thesis, University of Durham, 334 p.
- Sears, M M and K A Heasley, 2009, An application of energy release rate, in Proceedings: 28th International Conference on Ground Control in Mining, West Virginia University, Morgantown, WV, p. 10–16.
- Sinha, K P, 1979, Displacement-discontinuity technique for analyzing stresses and displacement due to mining in seam deposits, PhD thesis, University of Minnesota, Minneapolis, MN, 311 p.
- Stewart, C L, R E Stone and K A Heasley, 2006, Mine stability mapping, in Proceedings: 25th International Conference on Ground Control in Mining, West Virginia University, Morgantown, WV, p. 277-283.
- Stricklin, K G and G Triebisch, 2012, Report on coal pillar recovery under deep cover, PIB No. P12-10, U.S. Department of Labor, Mine Safety and Health Administration, Arlington, VA, 5 p.
- Stricklin, K G, 2013, roof control plan approval and review procedures, Handbook Number PH13-V-4, U.S. Department of Labor, Mine Safety and Health Administration, Arlington, VA, 81 p.
- Wang Q. and K A Heasley, 2005, Stability mapping system, in Proceedings: 24th International Conference on Ground Control in Mining, West Virginia University, Morgantown, WV, p. 243–249.
- Yang, J and K A Heasley, 2016, Calibrating LaModel for subsidence, in Proceedings: 35th International Conference on Ground Control in Mining, West Virginia University, Morgantown, WV, p. 104-112.
- Zelanko, J C and K A Heasley, 1995, Evolution of conventional gate entry design for longwall bump control: two southern Appalachian case studies, in Proceedings: U.S. Bureau of Mines Technology Transfer Seminar, USBM Spec. Pub. 01-95, U.S. Department of the

- Interior, U.S. Bureau of Mines, Washington, DC, p. 167-180.
- Zhang, P, K A Heasley and Z G Agioutantis, 2014, A comparison Between ARMPS and the new ARMPS-LAM programs, in Proceedings: 33rd International Conference on Ground Control in Mining, West Virginia University, Morgantown, WV, p. 170-174.
- Zipf, R K and K A Heasley, 1990, Decreasing coal bump risk through optimal cut sequencing with a non-linear boundary element program, in Proceedings: 31st U.S. Symposium on Rock Mechanics, Balkema, Netherlands, p. 947–954.
- Zipf, R K, 1992, MULSIM/NL theoretical and programmer's manual, USBM IC 9321, U.S. Department of the Interior, U.S. Bureau of Mines, Washington, DC, 62 p.

Appendix A

Author's Curriculum Vitae

DR. KEITH A. HEASLEY

Professor Emeritus – Dept. of Mining Engineering
West Virginia University
PO Box 6070;
359H Mineral Resources Building
Morgantown, WV 26506-6070
(304) 293-3842
keith.heasley@mail.wvu.edu

Heasley, Keith A.,
DBA: Mining Engineering Consulting
2988 Compressor Station Road
Bruceton Mills, WV 26525
(304) 379-3004
DUNS: 801963633
CELL: 304-216-9136

EDUCATION:

Ph.D., 1998, Mining and Earth Syst. Eng. (Minor-Computer Science), Colorado School of Mines,
Thesis: "Numerical Modeling of Coal Mines with a Laminated Displacement-Discontinuity Code"
M.S., 1988, Mining Engineering, The Pennsylvania State University,
Thesis: "Computer Modeling of Subsidence and Subsidence-Control Methods."
B.S., 1981, Mining Engineering, The Pennsylvania State University.

CAREER EXPERIENCE:

Professor Emeritus, Mining Engineering, WVU, Morgantown, WV, May, 2018 to present.
Charles T. Holland Professor, Mining Engineering WVU, August, 2012 to May, 2018
VP and Sec. of the Board, Alpha Foundation for the Improvement of Mining Safety and Health (a \$50M endowment), May, 2012 to present.
Professor, Mining Engineering - WVU, Morgantown, WV, May, 2007 to present.
Associate Professor, Mining Engineering - WVU, Morgantown, WV, Aug., 2001 to May, 2007.
Supervisory Mining Engineer - National Institute for Occupational Safety and Health (NIOSH), Pittsburgh Research Laboratory, Oct., 1997 to Aug, 2001.
Mining Engineer - U.S. Bureau of Mines, Pittsburgh Research Center, Aug., 1986 to Oct., 1997.
Project Engineer - Consolidation Coal Company, Cadiz, Ohio, Jun., 1981 to Aug., 1983.

HONORS AND AWARDS:

Pittsburgh Section of SME, Distinguished Service Award, 2016
Coal & Energy Division of SME, Distinguished Service Award, 2014
Old Timers Club Faculty Award, 2011 National Award
Society for Mining, Metall. & Exploration (SME), Syd S. Peng Ground Control in Mining Award, 2011
PA Coal Mining Inst. of America (PCMIA), Stephen McCann Educational Excellence Award, 2006
Pittsburgh Section of the SME of the AIME, Young Engineer's Award, 1990
The Pennsylvania State University, Top Graduating Senior in Min. Eng. (Old-Timers Award), 1981

PROFESSIONAL MEMBERSHIPS:

Registered Professional Engineer, Mining Engineering: PA, since 1996; WV, since 2010.
Member- Society for Mining, Metallurgy & Exploration (SME) of the AIME since 1978.
Instructor for the SME annual Professional Engineer (PE) Review Course, (2002-present); Pgh Sect. Board Member (1998-2004; 2007-2013); Eavenson Award Committee (2008-2011); Chair, Coal and Energy (C&E) Division (2006); Chair-Elect, C&E Division (2005); Program Coordinator, C&E Division (2003); Rock Mechanics Award Committee (2002-2005); Stefanko Award Committee (2001-2003); Woomer Award Committee (1997-2001);
Member- American Rock Mechanics Association (ARMA), since 1994.
Board Member (2003-2009); Board Secretary (2004-2006)

CONSULTING PROJECTS:

LaModel Analysis of Novel Mine Plan, Hume Coal – Mine Advice Pty Ltd, 2018
Subsidence Analysis of Abandoned Mines, Sunoco Pipeline – Tetra Tech, Inc., 2018
Roof Fall and Roof Support Analysis, Mine #32 – Prime Coal, LLC, 2017
LaModel Training – Alliance Coal, 2015
Analysis of an Innovative Longwall Mine Design – King, & Wood Mallesons, 2015
Back Analysis of Multiple Fatality Coal Bump – Jackson Kelly, PLLC, 2014
Stability Analysis of Cam Mining #28 Mine – DSi Underground, 2013
Multiple-Seam Model of Sentinel Mine – International Coal Group (ICG), 2013
Multiple-Seam Stability Analysis – AK Coal Resources, 2013
Subsidence Analysis of Rock Springs, WY – Tetra Tech, Inc., 2013
Multiple-Seam Model of Sentinel Mine – International Coal Group (ICG), 2012
Stability Impacts of Proposed Refuse Impoundment – Coal River Energy, 2011
LaModel Analysis of Geometry Changes to Reduce Floor Bending Stress - Patriot Coal Company, 2010
LaModel Analysis of Floor Bleeders at the Upper Big Branch Mine – MSHA, 2010
Multiple-Seam Model of Sentinel Mine – International Coal Group (ICG), 2010
LaModel Analysis of Delayed Subsidence Potential – Zapata, Inc., Blackhawk Division, 2010
Tackett v. Coal River Mining, LLC – Shuman, McCuskey & Slicer, 2010
Marathon Petroleum Co, v. Kiewit Construction Company - Kiewit, 2009
LaModel Training in Denver – MSHA, 2009
Stress and Deform. Analysis of Rect. and Arched Slopes – Appalachian Mining & Engineering, 2008
LaModel Analysis of Longwall Panels LW18-25 and LW25 at West Elk Mine – Arch Coal Co., 2008
Back Analysis of the Crandall Canyon Mine Using the LaModel Program – MSHA, 2008
LaModel Analysis of 23 Left – Harris #1 Mine – Peabody Energy, 2007
Subsidence Investigation for Charleroi Propane Terminal – Dominion Gas, 2007
Mark Castle v. Newtown Energy, Inc. - Shuman, McCuskey & Slicer, 2007
LaModel Analysis of the Northern Mining District – Bowie Resources, 2007
Mine Examination Services – Agapito Associates, 2007
LaModel Analysis of the 1-B Mining District – Bowie Resources, 2006
Stability Mapping Training – Bowie Resources, 2005

FUNDED RESEARCH PROJECTS:

Risk Guidelines for Mineral Extraction near Impoundments	COE,	10/12-12/12,	\$ 4,583
Modeling Roof Bolt Loading and Performance II,	NIOSH,	01/12-10/12,	\$ 24,279
Enhancing GC Safety through the LaModel Program,	NIOSH,	10/11-10/16,	\$1,079,547
Development of a Seismic System for Locating Trapped Miners,	NIOSH,	10/11-01/13,	\$ 110,511
Modeling Roof Bolt Loading and Performance,	NIOSH,	07/11-06/12,	\$ 43,611
Calibrating the LaModel Program for Deep Cover Pillar Retreat,	NIOSH,	04/08-12/10,	\$ 398,885
Advanced Rock Mechanics Analysis for HTHP Conditions,	DOE,	01/10-12/10,	\$ 70,000
Modeling Rock and Drill Cutter Behavior under HTHP Conditions,	DOE,	06/06-11/09,	\$ 441,273
Mine Stiffness Calculation for the LaModel Program,	CERB,	07/09-06/11,	\$ 60,000
Energy Release Rate Calculations for LaModel,	NIOSH,	03/08-02/09,	\$ 24,000
Incorporating the Roof Fall Risk Index (RFRI) into StabMap,	NIOSH,	07/06-11/07,	\$ 23,200
Development a Seismic Location System for Trapped Coal Miners,	CERB,	07/06-06/08,	\$ 35,500
Integration of the AMSS Computer program with LaModel,	NIOSH,	07/06-09/06,	\$ 10,000
Integrated Stability Mapping System for Mines, (StabMap),	NIOSH,	09/02-05/06,	\$ 255,500
Development of 2-D, Multi-Seam Stress Program (Lam2D),	CERB,	07/02-06/03,	\$ 33,500

TEACHING:

Over the last five years, I was responsible for teaching 15 courses (43 credits), and my Student Evaluation of Instruction (SEI) scores averaged 4.31/5.00 on a student-weighted basis for these courses. Further, over the last 5 years (10 possible awards), the WVU Mining Engineering senior design projects, which I teach, have won: 6 – 1st place, 2 – 2nd place and 2 - 3rd place awards.

GRADUATE STUDENTS SUPERVISED:

During the last 5 years, I graduated 5 Ph.D. students and 3 M.S. students. Over my 17-year career at West Virginia University, I have personally advised 9 M.S. and 7 Ph.D. students to graduation.

Student Name	Thesis Topic/Title	Degree and Date
Mehdi Rajaee	Implementing new Multiple-Seam Algorithms into the LaModel Program	Ph.D. Dec. 2017
Aanand Nandula	An Area-Based Calculation of the Analysis of Roof Bolt Systems (ARBS)	M.S. Aug. 2017
Kaifang Li	Implementing the Local Mine Stiffness Calculation in LaModel	Ph.D. Dec. 2016
Robert Krog	Critical Analysis of Longwall Ventilation Systems and Removal of Methane	Ph.D. Dec. 2016
Jian (Jack) Yang	Calibrating LaModel for Subsidence	M.S. Aug. 2016
Chris Newman	The Online LaModel User's & Training Manual: Development and Testing	M.S. Aug. 2015
Peng (Peter) Zhang	Implementing the Laminated Overburden Model Into ARMPS	Ph.D. May 2014
Morgan Sears	Calibrating the LaModel Program for Shallow Cover Multiple-Seam Mines	Ph.D. Dec. 2013
Ihsan Berk Tulu	New Abutment Angle Concept for Underground Coal Mining	Ph.D. Aug. 2012
Adeniyi Adebisi	Calculating the Surface Seismic Signal from a Trapped Miner	M.S. May 2012
Morgan Sears	Implementing Energy Release Rate Calculations Into the LaModel Program	M.S. Dec. 2009
Ihsan Berk Tulu	Modeling PDC Cutter Rock Interaction	M.S. Aug. 2009
Mickey Mitchell	Refuge Chambers	M.S. Aug. 2007
Matthew Petrovich	Stability Mapping with CMRR	M.S. Dec. 2006
Quanxi Wang	Hazard Index Mapping	Ph.D. Aug. 2005
Olayemi Akinkugbe	A Simple Two-Dimensional Boundary Element Program for Estimating Multiple Seam Interaction	M.S. Oct. 2004

TECHNOLOGY TRANSFER:

Instructor for the SME Review Course for the Professional Registration Examination of Mining/Mineral Engineers, (2002 – present).

Instructor for the “LaModel 4.0 Workshop” Training workshops (8 hours) presented to the coal mining industry, Beckley, WV, Evansville, IN, Morgantown, WV, and Grand Junction, CO, 2016.

Instructor for the “Pillar Design for Room and Pillar Mining Using ARMPS, AMSS and LaModel” 8 hr. workshops: Grand Junction, Pikeville, Norton, Harlan, Charleston, and Mullens, 2010.

Instructor for the “Multiple-Seam Analysis with LaModel” 8 hr. workshops: Morgantown, Charleston, Twin Falls, Norton, Pikeville, and Grand Junction, 2007-2008.

PUBLICATIONS:

In the last 5 years, I have been principal author (or second author with a student) on 12 technical papers at peer-reviewed conferences. Also, I have been on the executive organizing committees for the International Conference on Ground Control in Mining (since 2001). Some of the highlights of my recent publications are listed below:

- Krog, R. B. and K. A. Heasley, 2017, "Longwall Emissions During Falling Atmospheric Pressures and the Sample Frequency Required to Detect Them." Proceedings of the 16th North American Mine Ventilation Symposium, June 17-22, Colorado School of Mines, Golden, CO.
- Yang, Jian and Keith A. Heasley, "Calibrating LaModel for Subsidence," Proceedings of the 35th International Conference on Ground Control in Mining, Morgantown, WV, July 26-28, 2016, p. 104-112.
- Newman, Christopher, Zach Agioutantis and Keith Heasley, "Introducing the New Windows ARMPS-LAM Program," Proceedings of the 35th International Conference on Ground Control in Mining, Morgantown, WV, July 26-28, 2016, p. 98-103.
- Newman, Christopher R. and Keith A. Heasley, "Development of An Online User's and Training Manual for LaModel," Proceedings of the 34th International Conference on Ground Control in Mining, Morgantown, WV, July 28-30, 2015, p. 209-216.
- Li, Kaifang and Keith A. Heasley, "Calculating the Potential for Coal Pillar Bumps Using a Local Mine Stiffness Criterion," Proceedings of the 49th U.S. Symposium on Rock Mechanics, San Francisco, CA, June 28-July 1, 2015, Paper 15-241, 8 p.
- Heasley, Keith A., "LaModel – A Program for Coalmine Modelling," Proceedings of AusRock 2014: Third Australasian Ground Control in Mining Conference, Sydney, Australia, Nov. 5-6, 2014, 6 p.
- Zhang, Peng, Keith A. Heasley and Zacharias G. Agioutantis, "A Comparison Between ARMPS and the New ARMPS-LAM Programs," Proceedings of the 33rd International Conference on Ground Control in Mining, Morgantown, WV, July 29-31, 2014, p. 170-174.
- Li, Kaifang and Keith A. Heasley, "Using Field Measurements to Quantify the Post-Failure Behavior of Coal," Proceedings of the 48th U.S. Symposium on Rock Mechanics, Minneapolis, MN, June 1-4, 2014, Paper 14-7133, 7 p.
- Sears, Morgan and Keith A. Heasley, "Calibrating the LaModel Program for Shallow Cover Multiple-Seam Mines," Proceedings of the 32nd International Conference on Ground Control in Mining, Morgantown, WV, July 30-August 1, 2013, p. 99-106.
- Zhang, Peng and Keith A. Heasley, "Initial Results from Implementing a Laminated Overburden Model into ARMPS," Proceedings of the 32nd International Conference on Ground Control in Mining, Morgantown, WV, July 30-August 1, 2013, p. 239-247.
- Tulu, Ihsan B. and Keith A. Heasley, "Investigating Abutment Loading," Proceedings of the 31st International Conference on Ground Control in Mining, Morgantown, WV, July 31-August 2, 2012, p. 1-10.
- Heasley, Keith A., "Calibrating the LaModel Program for Site Specific Conditions," Proceedings of the 31st International Conference on Ground Control in Mining, Morgantown, WV, July 31-August 2, 2012, p. 1-8.

Appendix 7.2

Hume Coal Project - Interpretation of the numerical modelling study of the proposed Hume Project EIS mine layout (MineAdvice 2018)

HUME COAL PTY LTD

**Interpretation of the Numerical Modelling Study of the
Proposed Hume Project EIS Mine Layout**

JUNE 2018

REPORT: HUME22/1

REPORT TO :

Alex Pauza
Manager, Mine Planning
Hume Project
Hume Coal Pty Ltd

REPORT ON :

Interpretation of Numerical Modelling Study of the Proposed
Hume Project EIS Mine Layout

REPORT NO :

HUME22/1

REFERENCE :

Your Instructions to Proceed

PREPARED BY :

Russell Frith

REVIEWED BY :

Guy Reed and client's representative

DATE :

16th June 2018



.....
Russell Frith
Senior Principal Geotechnical Engineer

Disclaimer

This technical report has been prepared based on: (a) instructions by the Client as to the required scope of work; (b) technical and other supporting information supplied to Mine Advice by the Client; and (c) the use of relevant technical concepts and methods as determined by Mine Advice in their role as a consulting and professional engineering service provider. The Client warrants that all of the information it provides to Mine Advice is complete and accurate, and that it has fully disclosed to Mine Advice any and all relevant matters which may reasonably affect the conclusions that are reached in this report.

Every reasonable effort has been made to ensure that this document is correct at the time of publication, and a draft copy has been provided to the Client for full review before provision of a signed final copy upon which the Client may choose to act. To the fullest extent permitted by law, Mine Advice hereby disclaim any and all liability in respect of: (a) any claim for loss or damage touching or concerning this report, including but not limited to any claim for loss of use, loss of opportunity, loss of production, loss of interest, loss of earnings, loss of profit, holding or financial costs, costs associated with business interruption or any other direct, indirect or consequential loss allegedly suffered; and (b) any claim for loss or damage touching or concerning the acts, omissions or defaults of other contractors or consultants engaged by the Client. In the event of a breach by Mine Advice of a statutory warranty which cannot be contractually excluded, Mine Advice's liability to the Client for such breach shall be limited to the total fee paid to the client for the preparation of this report.

The report is a confidential document between Mine Advice and the Client (the parties) which may contain (for example) intellectual property owned by Mine Advice and/or confidential information/data owned by the Client. Both parties agree to maintain the confidentiality of the report to the fullest possible extent, albeit recognising the possible need for limited disclosure to regulatory authorities or third-party peer reviewers, and/or as required under a legal process. It is agreed that any such limited disclosure does not constitute publishing of the report into the public domain such that any recipients have no rights to use or refer to the contents outside of the specific purpose for which the report was made available. Any content of the report that is owned by one party can only be placed into the public domain by agreement with the other party. Unauthorised publishing of the report or part thereof that directly affects the business of the other party will be considered to be negligent behaviour and may allow the aggrieved party to seek damages from the other party.

It is also expressly noted that Mine Advice are not licensed to utilise, and do not utilise, the geotechnical design methodologies commonly referred to as ALTS, ADRS or ADFRS as part of their consulting activities, including that reported herein. Any reference made to or use of technical publications or research reports that include descriptions or details of these various design methodologies should not be construed as constituting the use of said design methodologies. Furthermore, any comments made about individual aspects of the published information and research pertaining to these design methodologies should not be taken as a comment (whether positive, negative or neutral) about the design methodologies. Mine Advice do not provide any such comment on such matters.

TABLE OF CONTENTS

1.0	INTRODUCTION	1
2.0	SUMMARY OF INITIAL LAYOUT DESIGN LOGIC.....	4
3.0	INTERPRETATION OF NUMERICAL MODELLING OUTCOMES	10
3.1	Description of the Chosen Numerical Modelling Package.....	10
3.1.1	Absence of Vertical Joints and Horizontal Stress in the Overburden.....	11
3.1.2	The Significance of Pillar Load Distributions within LaModel	12
3.2	Assessment Logic in Terms of the Modelling Process	14
3.3	Calibration with Measured Surface Subsidence at the Adjacent Berrima Colliery	15
3.4	2D LaModel Results Compared to ARMPS-HWM Designs.....	18
3.5	3D Model Results	21
3.5.1	80 m Cover Depth.....	22
3.5.2	160 m Cover Depth.....	25
3.6	Scenario Analysis	28
3.6.1	80 m Cover Depth.....	28
3.6.2	160 m Cover Depth.....	31
4.0	DISPLACEMENT-BASED STABILITY CRITERIA.....	33
4.1	A Conceptual Cause and Effect Model for Overburden Stability/Instability	33
4.2	Measurement Data that Supports the Basis of the Conceptual Overburden Model	36
4.3	Comments in Relation to the EIS Mine Layout at Hume	46
5.0	WEATHERING OF THE HAWKESBURY SANDSTONE (HBSS).....	47
6.0	OVERALL SUMMARY.....	50
7.0	REFERENCES	51
	APPENDIX A	53
	APPENDIX B	54

1.0 INTRODUCTION

This report contains the outcomes from two separate, but nonetheless interconnected pieces of work related to the development application for a new underground mine in the NSW Southern Highlands by Hume Coal Pty Ltd (Hume Coal), that proposes to utilise a mining method and associated mine layout that limits the potential impacts of mining-induced surface and sub-surface subsidence to acceptably low levels.

The key layout design attribute that is directly linked to subsidence impact control is that of coal pillar stability. Therefore, coal pillar design for long-term stability was the primary focus of the proposed EIS mine layout, and therefore has been a significant focus of both the two independent expert reviews conducted on behalf of DP&E (Galvin & Associates 2017 and Canbulat 2017), as well as the numerical modelling study that has subsequently been carried out by Dr Keith Heasley of the University of West Virginia in the United States on behalf of Hume Coal.

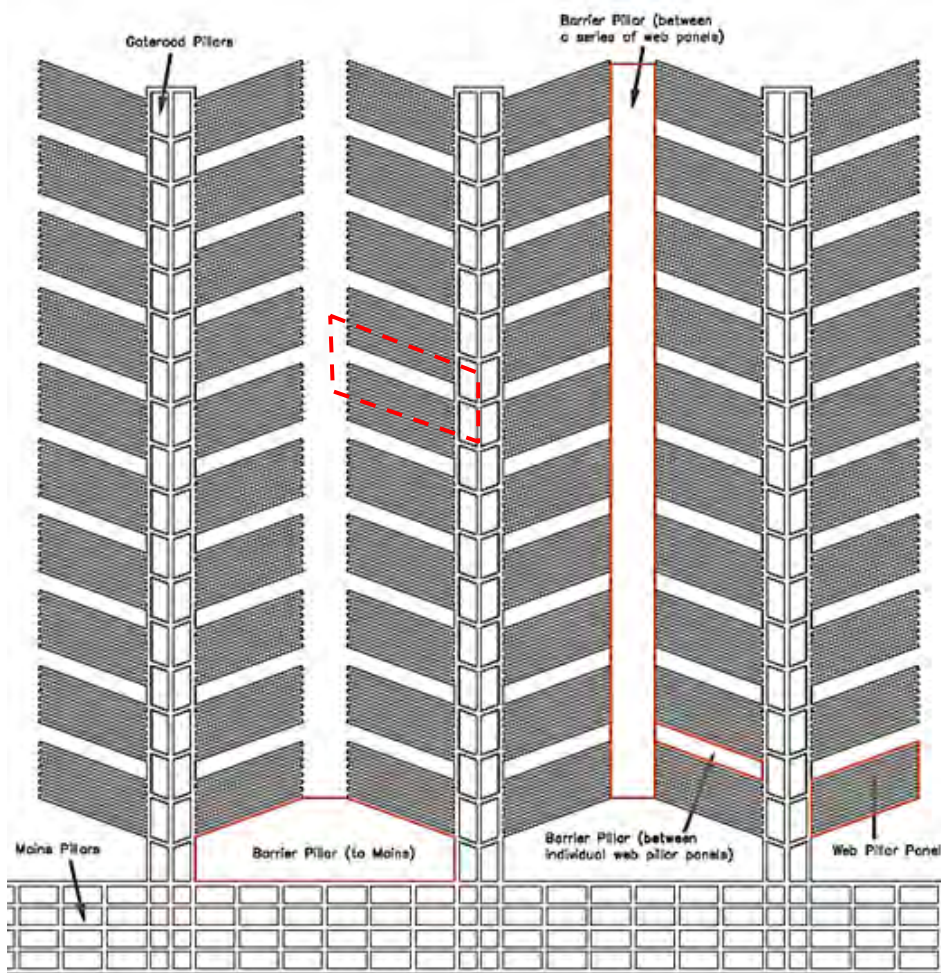


FIGURE 1. Basic Mining Layout including Different Coal Pillar Types (Mine Advice 2016a)

The proposed mining method and associated mine layout has a number of similar coal pillar geometries to highwall mining (HWM) layouts that are commonly used from either open cut highwall coal seam exposures or hillside seam outcrops, the generic proposed EIS mine layout being shown in Figure 1. This figure also identifies the various coal pillar types that are to be left in place.

A more detailed description of the derivation of the proposed mine layout is contained in **Mine Advice 2016a**. The following summary statements are reproduced below for convenience.

The three key environmental considerations are (i) the need to keep surface subsidence movements and impacts to an “imperceptible” level, (ii) the need to minimise the hydrogeological impact on the groundwater system, and (iii) the need to emplace all CHPP rejects back into the underground mine.

These environmental impact requirements resulted in the following being necessary outcomes as a result of the proposed mining:

- (a) *No en masse overburden caving either during or following mining.*
- (b) *Overburden fracturing to be either prevented or at worst maintained at insignificant levels.*
- (c) *No tensile opening of pre-existing jointing within the overburden.*
- (d) *Roadway roof instability to be minimised.*
- (e) *Any low permeability material that may be present between the coal seam and groundwater system should be left in place wherever possible.*
- (f) *Remnant mine workings must suitable for CHPP reject emplacement.*
- (g) *The mine layout must be sub-divided into discrete mining panels.*

*The remnant coal pillars to be left following the completion of mining have been developed to function as a system rather than as individual pillars, five fundamental coal pillar types being used (**Figure 1**):*

- *web pillars between drives.*
- *intra-panel barriers between a web pillar panel of narrow drives.*
- *inter-panel barriers which are either solid barriers between adjacent mining panels or the “chain” pillars used in the three heading development panels.*
- *barriers between the outbye ends of production panels and the main headings.*
- *the main headings pillars.*

It is noted that there are actually six pillar types shown in **Figure 1**, with the chain pillars and inter-panel barriers being classified as a single pillar type given that they are located at opposite ends of web pillars and intra-panel barriers. The behaviour of chain pillars is evaluated and discussed later in this report when analysing the results of the 3D numerical modelling.

This report has been compiled to assist Hume Coal formulate their full response to the independent EIS reviews undertaken on behalf of DP and E and contains the following sections:

1. A summary of the design process that was used in developing the EIS mine layout design parameters.
2. A description of the numerical modelling study and interpretation of the results.
3. A displacement-based mine stability assessment.
4. A summary of the in-house assessment of the effect of weathering of the Hawkesbury Sandstone (HBSS) in western parts of the proposed mining areas where the Wianamatta Shale is absent, thereby exposing the HBSS at surface.

2.0 SUMMARY OF INITIAL LAYOUT DESIGN LOGIC

The design process utilised to develop EIS mine layout parameters was based on conducting what was considered to be a credible worst-case 2D analysis of the most relevant coal pillars within the mine layout from a global mine and overburden stability perspective (i.e. the web pillars and intra-panel barriers), any potential stability benefits from the third dimension in plan being ignored at this time. Nonetheless, it was fully recognised and intended that mine layout optimisation would be addressed during pre-production planning or mining operations using numerical modelling, assisted by knowledge as to actual mining outcomes from as-formed mine workings.

The design approach for the limiting coal pillars that was used for EIS purposes, was founded on the application of an established 2D empirical model referred to as ARMPS-HWM, (NIOSH 2012) derived from a large case-history database (in the order of 3000 HWM drives and associated pillars that constitute largely stable outcomes) from surface HWM operations in the United States. The justification for adopting this approach at the outset is several-fold, but is fundamentally found within the following quotation from **Esterhuizen 2014**:

"Empirical models, based on the analysis of large numbers of case histories, have found wide acceptance as a tool for engineering design. The application of empirical models is limited by the restriction that they should not be used beyond the limits of the empirical base from which they were developed." (underline added by Mine Advice)

In order to justify applying the ARMPS-HWM method to the design of an underground mine layout, three independent criteria needed to be met, namely:

1. that the layout geometries for the limiting pillars within the layout were broadly similar to those used in surface HWM.
2. that the ARMPS-HWM method directly addressed the design of those limiting pillars.
3. any fundamental differences between a surface HWM and underground mine using a surface HWM layout designed using ARMPS-HWM, would not negatively influence the reliability of the design method and associated layout design outcomes.

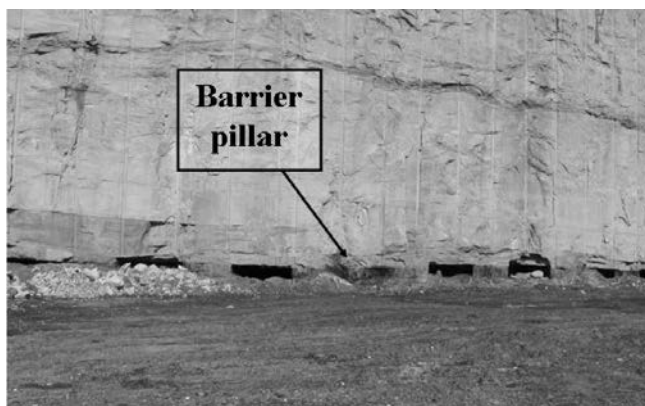


FIGURE 2. Typical Highwall Miner Holes and Web Pillars with Barrier Pillar or "skip hole" Indicated by Arrow (Zipf and Bhatt 2004)

ARMPS-HWM addresses the stability of both web pillars and barrier pillars between panels of web pillars (see **Figure 2**), these being comparable to the web pillars and intra-panel barrier pillars that are both contained within the proposed Hume EIS mine layout (**Figure 1**) and defined as the limiting coal pillars in terms of overall mine stability. This satisfies the first criteria set out above.

In addressing the second criteria, the specific design aspects for ARMPS-HWM that were applied to the mine layout at Hume are as follows (**NIOSH 2012**):

- (a) No more than 20 plunges should be mined before leaving a barrier pillar - in the case of the proposed Hume Coal layout, the maximum span between barriers was set at 60 m which will contain substantially less than 20 plunges (see point (b) below).
- (b) When the distance between barrier pillars is 60 m or less, the ARMPS Stability Factor (SF) on the web pillars can be as low as 1.3 as the barrier pillars will likely be able to prevent a collapse from initiating. Also it should be noted that very slender web pillars with width:height ratios much less than 1 may be troublesome, even if their SF appears to be adequate.
- (c) Research conducted by **Mark et al 1997** into coal pillar collapses concluded that pillars with a width:height in excess of 4 were highly unlikely to collapse. The ARMPS-HWM methodology suggests that barrier pillars with w/h ratios of greater than 4 need only maintain an SF of 1.5. In the case of the proposed Hume Coal layout, the barrier pillars have been designed to a minimum SF of 2.0.
- (d) Once the web pillars and barrier pillars have been sized, the overall system SF needs to be checked and should be in excess of 2.0

It is noted that despite its inclusion in both the ARMPS and ARMPS-HWM methodologies developed by NIOSH, the concept of a "system" SF remains a point of debate within the Australian industry. Therefore, in order to ensure that this does not become a point of contention in the EIS assessment process, it is confirmed that the proposed EIS mine layout does not rely on a system SF in the assessment of stable design outcomes, as will be demonstrated by the numerical modelling results that are provided later in this report.

The EIS mine layouts utilised the above design "rules", plus the specific requirement that web pillars must have a minimum w/h of 1, the distance between intra-panel barriers must not exceed 60 m, and intra-panel barriers must have a minimum SF of 2.0 and a minimum w/h ratio of 4, whichever results in the wider barrier pillar. These are more conservative design criteria than the minimums allowed by ARMPS-HWM and were utilised in recognition of the specific need for long-term remnant pillar stability at Hume.

Demonstrably, ARMPS-HWM provides design guidelines for not only web pillars and intra-panel barrier pillars, but also the span or distance between those barriers as a third design variable. This therefore satisfies the second defined design method criteria.

In terms of whether using ARMPS-HWM in an underground mine setting poses pillar stability design risks that are not inherent within surface HWM, this was considered carefully at the outset whereby it was realised that the proposed underground mine at Hume actually contains several mine stability advantages as compared to surface HWM, as follows:

- (i) Drives are being limited to a maximum length of 120 m as compared to the much longer drives of up to 500 m that are used in surface HWM. Therefore overall mine stability is more likely to be directly influenced by four coal pillar types acting in combination, not just the web pillars and intra-panel barrier pillars that are considered by the ARMPS-HWM analysis. This hypothesis will be tested by the 3D numerical modelling study detailed later in the report.
- (ii) The deliberate use of "sub-critical" panels of drives and web pillars between intra-panel barriers to prevent the pillar collapse scenario eventuating of both (a) low width:height web pillars being loaded under full tributary area loading to surface, and critically, (b) the overburden being unstable to surface so that it has the ability to drive web pillars to a state of full collapse once their peak strength is exceeded.
- (iii) The lack of a highwall in an underground mine has two stability benefits: firstly a highwall represents a substantial sub-vertical discontinuity that inevitably assists the overburden above HWM pillars formed from a surface mine become unstable to surface as required in point (ii)(b) above, and secondly, accepting that lower levels of horizontal stress within the overburden promote decreased overall overburden stability (as discussed in detail in **Frith and Reed 2018a**), a highwall acts to reduce the level of retained *in situ* horizontal stress within the overburden, which is potentially detrimental to pillar stability in a HWM, but not relevant to the proposed underground mine at Hume.

These attributes are judged to satisfy the third criteria in that if anything, an underground mine should be more stable than a surface HWM formed from an open cut highwall (all other factors being equal).

The application of ARMPS-HWM to the design of both web pillars and intra-panel barriers gave Hume Coal an initial basis for putting together a mine layout according to varying cover depth and an assumed working height of 3.5 m.

D	t	x	y
80	3.5	14	3.5
120	3.5	16.8	4.1
160	3.5	20.9	5.5

where: D = cover depth (m), t = working height (m), x = barrier width (m) and y = web pillar width (m)

TABLE 1. Sample Panel and Pillar Design Outcomes using ARMPS-HWM

Three specific layout design outcomes from ARMPS-HWM (see Table 1) were subsequently analysed utilising the pillar strength equations of the University of New South Wales Pillar Design Procedure (UNSW PDP), but not the UNSW PDP itself due to the supporting case-history database being substantially different to that of HWM in terms of assumed mining geometries. The reason for doing this was solely to provide NSW regulators with pillar stability indicators via resultant Factors of Safety (FoS) that they are more familiar with, as compared to Stability Factors returned from ARMPS-HWM.

As part of the assessment using the UNSW PDP pillar strength equations, two pillar load distribution cases were applied, these being the two scenarios contained within Version 6 of ARMPS (Mark 2010)

relating to the development of a pressure arch within the overburden for higher depth, sub-critical panels of pillars in the case of bord and pillar more generally (see Figures 3 and 4).

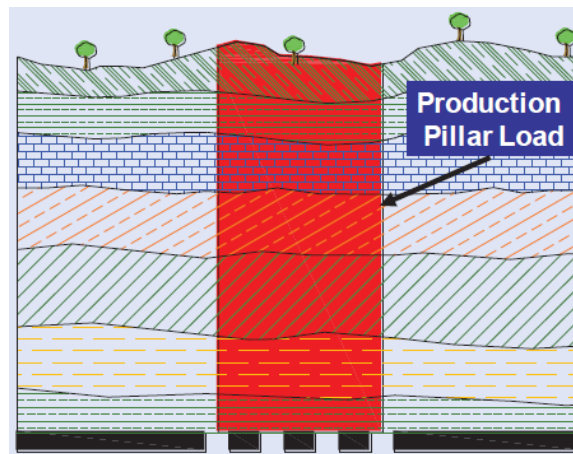


FIGURE 3. Tributary Area Loading Models for Development Mining (Mark 2010)

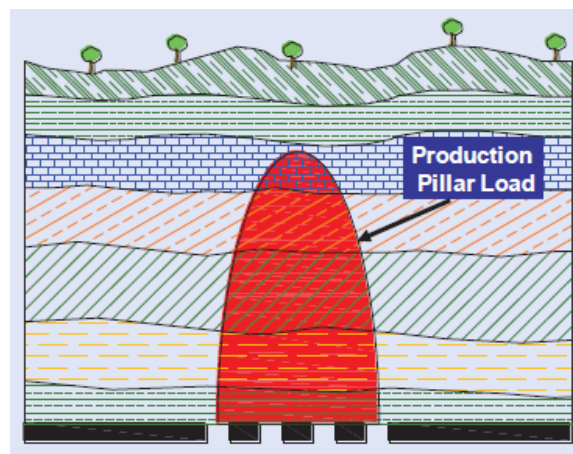


FIGURE 4. Pressure Arch Loading Models for Development Mining (Mark 2010)

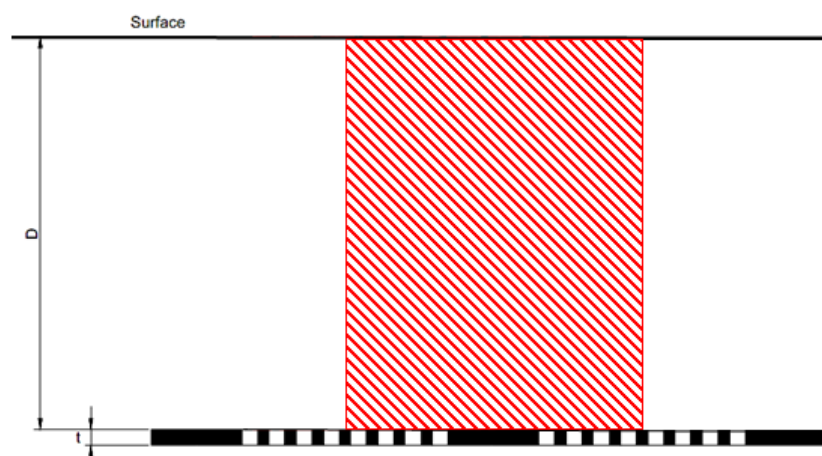


FIGURE 5. Bord and Pillar Type Assessment of Pillar Stability (Pillar Load Distribution Based Solely on Individual Pillar Width)

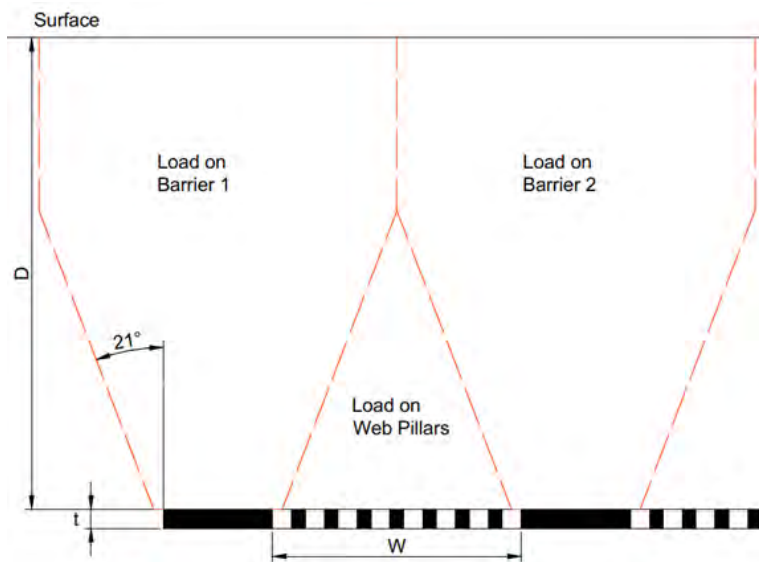


FIGURE 6. "Double Goaf Loading" of Intra-Panel Barrier Pillars (Worst Case Unequal Pillar Load Distribution)

Depth (m)	Web Width (m)	Barrier Width (m)	Number of Drives	Number of Webs	Span Between Barriers (m)	Web Pillar FoS (w/h)	Barrier Pillar FoS (w/h)	System FoS
80	3.5	14	8	7	56.5	1.33 (1)	4.95 (4)	2.25
120	4.1	16.8	7	6	52.6	1.04 (1.2)	4.05 (4.8)	1.94
160	5.5	20.9	6	5	51.5	1.04 (1.6)	3.94 (6)	2.03

TABLE 2. Two-Dimensional Pillar Stability Review using UNSW PDP and Pillar Load Distribution According to Pillar Width (refer Figure 5)

Depth (m)	Web Width (m)	Barrier Width (m)	Number of Drives	Number of Webs	Span Between Barriers (m)	Web Pillar FoS (w/h)	Barrier Pillar FoS (w/h)	System FoS
80	3.5	14	8	7	56.5	2.69 (1)	2.0 (4)	2.25
120	4.1	16.8	7	6	52.6	3.4 (1.2)	1.53 (4.8)	1.94
160	5.5	20.9	6	5	51.5	4.62 (1.6)	1.57 (6)	2.03

TABLE 3. Two Dimensional Pillar Stability Review using UNSW PDP and Worst Case Unequal Pillar Load Distribution (refer Figure 6)

Figures 5 and 6 show the manner by which the two pillar loading scenarios in Figures 3 and 4 were applied, with Tables 2 and 3 providing the range of coal pillar stability outcomes for the various cases using the UNSW PDP pillar strength equations.

The design outputs shown in **Tables 2 and 3** were intended to illustrate that the pillar system as a whole, is robust in that significant overburden load can be transferred from the web pillars to the intra-panel barrier pillars to increase the SF of the web pillars, but without the barriers being driven towards a yield and/or collapse condition. It was also recognised that the actual load distribution between the web and intra-panel barriers would vary within the mine due to differences in geotechnical conditions, the point of these two design assessments being to understand the significance of a credible range of overburden loading distributions to the suitability of the proposed pillar layouts.

The final aspect of the EIS layout design was to qualitatively consider the likely influence of the overburden in further promoting sub-critical overburden conditions between intra-panel barriers, the initial design work using ARMPHS-HWM having only considered layout geometry in terms of the distance between intra-panel barriers as a function of cover depth (W/H). It was fully recognised that the overburden of the Wongawilli Seam at Hume is dominated by the Hawkesbury Sandstone, which is tens of metres thick, such that it was likely to offer substantial assistance in ensuring sub-critical overburden conditions across a span between intra-panel barriers of no more than 60 m.

The influence of flooding of the mine workings over time, as well as unspecified levels of CHPP reject emplacement back into the workings, were also considered in general terms in the context of the long-term stability of the remnant mine workings.

The proposed mine layout design parameters as presented in the EIS submission, were justified solely on the 2D ARMPHS-HWM analyses that were further evaluated using two extreme load-distribution cases and the pillar strength equations of the UNSW PDP. The long-term integrity of the proposed EIS mine layout relies solely on the layout geometry, with the geology of the overburden, CHPP reject backfilling and longer-term flooding of the workings being additional mine stability considerations, as detailed in **Mine Advice 2016a**.

3.0 INTERPRETATION OF NUMERICAL MODELLING OUTCOMES

Both DP&E experts called for numerical modelling to be undertaken, primarily in order to better understand overburden load distributions and remnant mine stability as a pillar system, as contained within the proposed EIS mine layout. Mine Advice commissioned Dr Keith Heasley of the University of West Virginia to undertake this work on behalf of Hume Coal (Heasley 2018).

This section of the report details:

- (i) A summary description of the chosen numerical modelling software, LaModel, and the reasons for its selection.
- (ii) The significance, if any, of vertical joints and horizontal stress within the overburden not being included within LaModel.
- (iii) The coal pillar behaviour model used by LaModel as compared to that in ARMPS-HWM.
- (iv) The logic behind the different modelling runs.
- (v) The outcomes and interpretation of the five phases of the modelling work, including:
 - a. Confirmation of the model element characterisation using what is termed as the "Coal Wizard"
 - b. Back-analysis of overburden properties using measured surface subsidence behaviour at the adjacent Berrima Colliery.
 - c. 2D numerical modelling parameter sensitivity analysis
 - d. 3D numerical modelling parameter sensitivity analysis
 - e. Scenario analysis representing various anomalous conditions.

3.1 Description of the Chosen Numerical Modelling Package

The numerical modelling tool chosen was LaModel, with Doctor Keith Heasley (the developer of the model) of the University of West Virginia in the United States being commissioned to set-up and run the various required models.

Key attributes of LaModel that resulted in it being selected as the most appropriate numerical model to use in this instance, include:

- It has its genesis in the prediction of surface subsidence above bord and pillar mines, albeit potash mines in the UK rather than coal mines *per se*.
- It has been widely used to analyse subsidence and pillar stability in coal mines in the United States and elsewhere around the world.
- It utilises the Mark-Bieniawski coal pillar strength equation, which is consistent with ARMPS-HWM.

- It incorporates an overburden behavioural model (based on a frictionless laminated beam) that uses only two overburden parameters, Young's Modulus (E) and unit thickness (t), which makes it highly amenable to back-analysis type calibration.
- It has a credible history of being used as part of both coal pillar research and consulting in the US coal industry.
- It has been used and accepted in NSW as part of coal mine design for surface subsidence control when protecting sensitive surface and sub-surface features, including at Clarence Colliery.
- It uses a mathematical algorithm that substantially decreases run times for individual models, which in the case of large-grid 3D models is a beneficial attribute as it allows parameter sensitivity studies to be conducted within reasonable timeframes.

In terms of specific aspects of LaModel that need to be commented on herein for completeness, two are judged to be of particular importance:

- (i) the overburden model not including vertical jointing or horizontal stress
- (ii) the use of a load distribution function across each pillar which is different to the average pillar loading assumption used within ARMPS-HWM.

Both require specific comment.

3.1.1 Absence of Vertical Joints and Horizontal Stress in the Overburden

Vertical joints and horizontal stresses are an integral part of the overburden above an underground coal mine, yet LaModel includes neither within its overburden model. This could be taken as a model limitation without logical reasoning to the contrary.

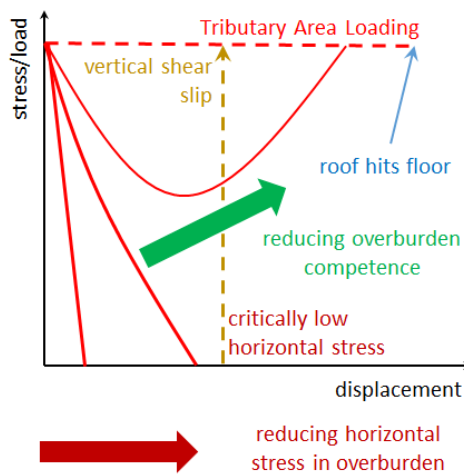


FIGURE 7. Varying Influence of Overburden Lithology, Vertical Joints and Horizontal Stress on GRC's (Frith and Reed 2018a)

Frith and Reed 2018a (copy attached as **Appendix A**) describe a model for overburden behaviour and stability/instability that is founded in the Ground Reaction Curve (GRC) concept and includes specific

consideration of the impact of vertical joints and horizontal stress. The model is outlined in more detail in **Section 4.1**, the relevant issue in relation to this study being found in **Figure 7** which contains a schematic illustration of how GRC's should change as a direct function of overburden type, vertical jointing and horizontal stress levels.

The critical point of **Figure 7** is that once the overburden displaces sufficiently to cause horizontal stresses within the overburden to reduce to critically low levels whereby vertical shear slip along sub-vertical joints occurs, overburden collapse and the development of full-tributary area loading is inevitably initiated. Conversely, when joints are horizontally confined so that vertical shear slip does not occur, the overburden will tend to behave more as a horizontally extensive continuum, with vertical jointing playing a substantially less significant role in overburden behaviour and stability/instability.

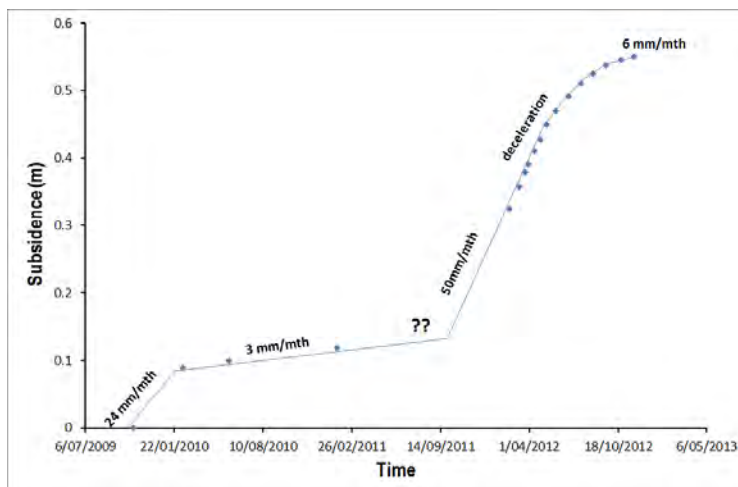


FIGURE 8. Time Dependent Variation in S_{\max} Within 3 North Subsidence Exceedance Area (Frith and Reed 2018b)

Frith and Reed 2018b (copy supplied in **Appendix B**) refer to a range of measured field data, including surface subsidence behaviour from above remnant partial extraction areas, in order to both establish that such a rapid transition is mechanistically correct, which it appears to be based on measured subsidence behaviour such as that shown in **Figure 8** as an example, as well as gain an estimate as to surface subsidence magnitudes at which it commonly occurs, 150 mm and greater being the reported finding.

LaModel modelling results can be checked for conformance with continuum-type overburden behaviour by comparing predicted levels of surface subsidence from the model with measured values of the transition to vertical joint-controlled overburden instability. Providing that predicted surface subsidence levels from LaModel are substantially lower than the known transition values, it can be reliably inferred that the absence of vertical joints and horizontal stresses within the overburden model used by LaModel, is of no significance to the reliability of the modelling outputs.

3.1.2 The Significance of Pillar Load Distributions within LaModel

Empirical models such as the UNSW PDP and ARMPS-HWM utilise average pillar loads as part of the design analysis, this being due to the fact that pillar strength equations such as the Mark-Bieniawski equation (as used in ARMPS-HWM) and those of the UNSW-PDP, were derived from collapsed cases whereby pillar loading at collapse was taken to be the average pillar stress as determined from full-

tributary area loading to surface. The distribution of load across an individual coal pillar that had subsequently failed could neither be determined, nor was deemed to be of any relevance in this general approach.

With numerical modelling subsequently being applied to coal pillar design, it was necessary to subdivide coal pillars into discrete smaller elements as part of the model grid. This, combined with the knowledge that coal pillars were rarely if ever loaded evenly across their full width, led to pillar load distribution functions being applied whereby each element in the coal pillar is taken to be loaded according to its location within the pillar, the associated technical challenge being to link this approach back to the empirically-derived pillar strength equations that are still used to evaluate overall pillar stability.

The coal pillars in LaModel are defined with concentric rings of elements, the strength of each element or element ring, being set based on its minimum distance from a mine entry. To determine the strength of each element, the stress gradient implied by the Mark-Bieniawski pillar strength formula is applied, namely:

$$S_p = S_i (0.64 + 2.16(x/h)) \quad [1]$$

where:

S_p is the assigned peak strength of an element

S_i is the *in situ* coal strength (6.205 MPa being the default value in the Mark-Bieniawski pillar strength equation)

x is the minimum distance to the centre of the element from the edge of the pillar,

h is the seam height (assumed to be 3.5 m in this case).

Using this approach, it was confirmed by Dr Heasley that:

- 1) Whilst elements towards the extremity of a pillar will have peak strengths less than given by the Mark-Bieniawski pillar strength equation, those at the centre will have higher strength values.
- 2) In the aggregate, each pillar will have a peak strength exactly equal to that derived by the Mark-Bieniawski pillar strength index. The average Stability Factor (SF)¹ for all elements within any pillar is identical to the SF that would be derived from an average pillar stress approach, as used within ARMPS-HWM.
- 3) Should pillar yield occur, they realistically yield from the rib in toward the middle of the pillar.

¹ The terms *Stability Factor* and *Factor of Safety* are mathematically identical as the calculation of pillar strength divided by pillar load. *Stability Factor* is used to identify an ARMPS-HWM outcome and differentiate it from a *Factor of Safety (FoS)* as determined using UNSW pillar strength formulae, which within the UNSW Pillar Design Procedure (PDP) is used to determine an associated Probability of Failure (PoF). Therefore, SF and FoS are substantially different in their derivation and application and so cannot be objectively compared numerically.

A possible “perceived” disadvantage of this approach is that elements in the pillar are assumed to maintain their peak-load until the pillar in its entirety has exceeded its average strength, this being the first instance that the post-peak behaviour of the pillar rather than individual elements, needs to be applied to the modelling process.

Whilst this is almost certainly not fully representative of post-peak pillar behaviour in the field, the need to model post-peak pillar behaviour only becomes a necessity once the pillar in its entirety has exceeded its average post-peak strength, as would be indicated by the average element SF being < 1. Subsequent to this point, further pillar compression would need to account for either substantial strain-softening or conversely work-hardening according to pillar w/h ratio as a minimum. As will become apparent when the numerical modelling results are reviewed, none of the coal pillars come close to meeting such a failed pillar criterion and therefore inevitably largely remain within the elastic portion of their overall stress-strain curve. This is assessed as rendering non-elastic pillar behaviour and in particular, post-peak strain softening behaviour for low w/h ratio pillars, as being irrelevant to this analysis.

Furthermore, as will be conclusively demonstrated by the scenario analysis, the key structural feature of the layout design are the intra-panel barrier pillars. The characterisation of these pillars, including elastic-plastic behaviour, is taken to be a reasonable approximation of the behaviour of these pillars which have width to height ratios of between 4 and 6.5.

3.2 Assessment Logic in Terms of the Modelling Process

Referring back to **Esterhuizen 2014**, the following quotation is taken from that paper in relation to the use of numerical models to complement empirical models:

Numerical models are based on the mechanics of rock behaviour and can be used to answer questions about rock mass response under given loading conditions and to extend the empirical models... Numerical models must be validated against empirical data. The process of first calibrating numerical models against specific case histories is required because of the uncertainty associated with rock mass strength parameters. The validity of the models can then be tested against empirically based models.

This quotation justifies two of the key numerical model preparation aspects:

- A back-analysis “calibration” of the overburden against known measurement data from the adjacent Berrima Colliery (rather than a model calibration against an empirical database).
- A validation test of the resultant overburden calibration using the 2D version of LaModel and a direct comparison of the outputs against the ARMPS-HWM designs listed in **Table 1**.

With overburden parameters having been determined using a credible back-analysis of known outcomes and LaModel having been shown to produce outcomes in 2D that are consistent with those from ARMPS-HWM (specifics to be discussed later), the model can be deemed as being suitable for use in analysing actual large-scale mine layouts in three-dimensions. The 3D modelling runs evaluated the proposed EIS mine layouts at cover depths of 80 m, 120 m and 160 m using overburden parameter variations for both Young’s Modulus, E, based on laboratory-based test data and unit thickness, t, based on the Berrima back-analysis.

A final series of numerical models were undertaken to evaluate various hypothetical scenarios associated with different levels of reduced web pillar stability, varying from the loss of one complete web pillar to all of the pillars within a web pillar panel between intra-panel barriers being removed so that they provide no contribution to pillar system stability. It is emphasised that these are both artificial scenarios, since even structure-affected or yielded web pillar(s) will provide some level of on-going support to the overburden, whereas the modelled scenarios remove yielded pillars in their entirety from the model, effectively reducing their load-bearing capacity (and therefore their SF) to zero. It is also highly unlikely that web pillars would be subjected to sufficient overburden load to cause them to go into yield at their inbye ends, or adjacent to intra-panel barrier pillars, given the Stability Factors that have been determined using the 3D numerical modelling.

As will be discussed later, the scenario analysis model runs provide for very high levels of confidence that a number of the major concerns raised by DP&Es independent experts (e.g. web pillars having a low w/h, the influence of roof falls in drives over time etc.) are not materially significant and that consequently, the proposed EIS mine layout is suitably robust and conservative to be able to accommodate such variations without overall mine stability being put at risk.

3.3 Calibration with Measured Surface Subsidence at the Adjacent Berrima Colliery

The adjacent Berrima Colliery (**Figure 9**) contains a number of areas of total pillar extraction (accepting that some amount of remnant coal inevitably exists in such areas) that are in the same coal seam, at comparable cover depths, comparable extraction widths (between solid coal pillars - this being equivalent to the distance between intra-panel barriers in the EIS mine layout at Hume), and with the same generic overburden lithology dominated by the Hawkesbury Sandstone (see **Figure 10**). Detailed surface subsidence measurements are also available for these specific mined-out areas. It is assessed that these areas of Berrima Colliery are suitable examples by which to back-calculate overburden parameters (E, t) for subsequent use by LaModel at Hume.

E and t both influence the stiffness of the overburden, with higher values of either parameter indicating a stiffer overburden and lower values indicating a softer overburden.

Data from Berrima Colliery used for overburden back-calculation included three subsidence cross-lines covering 404 panel and Southwest 1 panel. The links between extraction panel geometry and measured maximum subsidence at surface (S_{max}) are shown in **Table 4**, these outcomes allowing LaModel to be set up incorporating both the specific geometrical parameters of the mine layout as well as credible and suitably conservative (i.e. softer) overburden parameters, E and t , based on having matched the predicted S_{max} in LaModel with measured values in the order of 10 mm from Berrima.

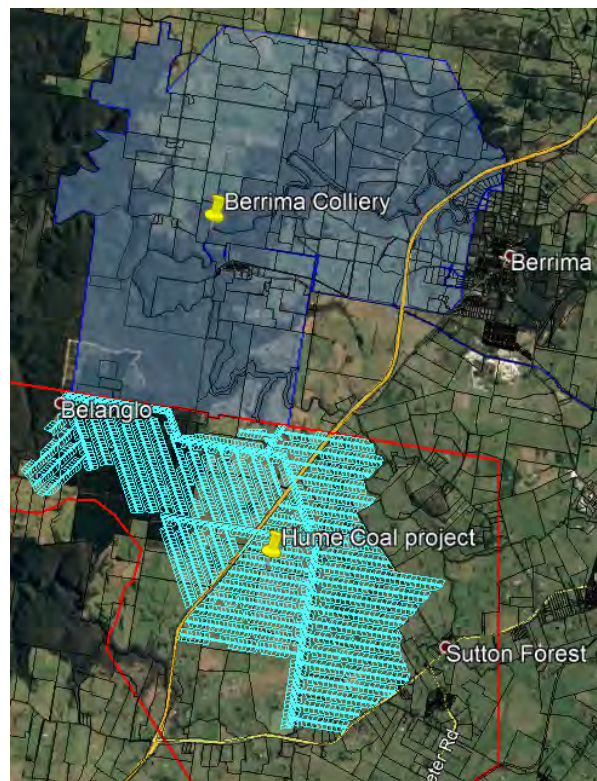


FIGURE 9. Location Plan of Berrima Colliery and the Hume Coal Project Area

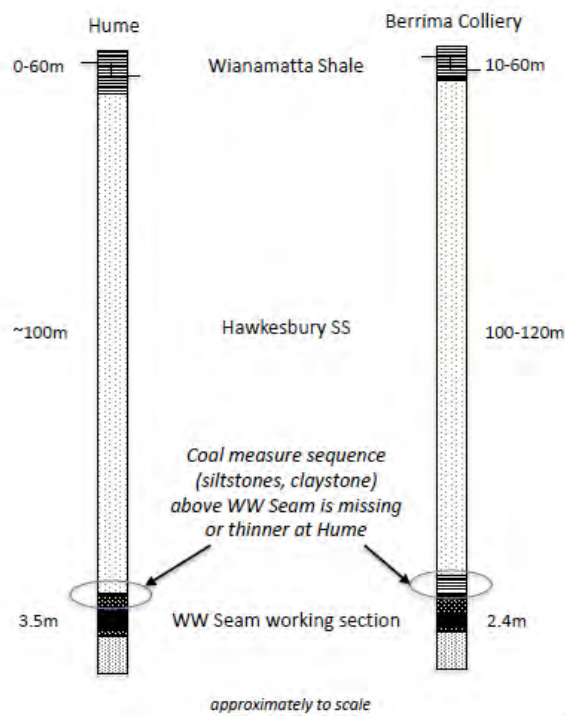


FIGURE 10. Comparison of Generic Overburden Lithology, Wongawilli Seam, (Hume and Berrima Colliery)

Panel cross line	Mining Height (m)	Void width (m)	Mining Depth (m)	Width to depth ratio	Max CL Sag (mm)
404 panel (prior to widening in 2008)	2.4	106	135	0.78	~10 nom.
SW1 cross line 1	2.4	120	160	0.75	~10 nom.
SW1 cross line 2	2.4	120	170	0.71	~10 nom.

TABLE 4. Total Extraction Geometrical Parameters and Measured S_{max} Values, Berrima Colliery

404 Panel was mined in two stages, approximately coinciding with calendar years 2007 and 2008. Extraction was initially undertaken in 2007 on the southern side of the panel, which was then widened to approximately double the initial width in 2008. It was necessary herein to only analyse the subsidence data obtained prior to panel widening when the panel still retained a sub-critical geometry (i.e. panel W/H < 1), since this is consistent with the sub-critical geometries between barrier pillars that have been proposed by Hume Coal. Subsequent to widening to a super-critical panel width, measured surface subsidence rapidly accelerated to around 0.5 m before stabilising at this level. This data will provide additional support to the displacement-based analysis presented in Section 4 of this report.

With two independent variables, E and t, being required by the LaModel overburden model, it was necessary to gain an estimate of one from another source so that the back-analysis process only had to match the *in situ* value of t to an independently determined range of E.

Laboratory testing data of the Hawkesbury Sandstone from Hume Coal surface boreholes returned E values ranging from 8.2 GPa to 23.2 GPa, with a mean value of 16.5 GPa, this being based on 15 individual tests. It is noted that Dr Heasley has confirmed that it is appropriate to utilise laboratory-based values for E in this instance, with the back-analysis process to determine associated values of t setting up the overburden in LaModel as a calibrated "rock mass".

E (Gpa)	t (m)	Smax (mm)
16.5	200	9.2
23.2	200	7.5
16.5	30	93.1

TABLE 5. Berrima Colliery Overburden Back-Analysis Results

Table 5 contains the results from the Berrima back-analyses, the key finding being that for the defined range of E, the value of t needed to be in the order of 200 m for the predicted value of S_{max} to be in the order of 10 mm, 200 m being greater than the cover depth at the various subsidence observation sites. In practical terms this is taken to indicate that the overburden at Berrima is not breaking-down at total extraction widths of up to 120 m and so tends to act as a single overburden unit.

The use of t = 30 m and E = 16.5 GPa results in a predicted S_{max} of 93 mm, or an order of magnitude higher than was measured at Berrima for the same mining geometry parameters.

In order to understand the response of the pillar and overburden system to variations in overburden stiffness (i.e. a parameter sensitivity analysis), it was decided to use the laboratory-determined range of E values in combination with t values ranging from 20 m to 40 m, the applied logic being that if such highly conservative overburden assumptions still resulted in discernible load re-distribution away from the web pillars onto surrounding barrier pillars, then there could be no rational argument for the LaModel modelling results being disputed based on the overburden assumptions used being overly optimistic.

t (m)	E (GPa)	t x E (GN/m)	De-rating from LaModel Back-Analysis
20	8.2	164	5% (20.1 x de-rating)
20	16.5	330	10% (10.0 x de-rating)
20	23.2	464	14% (7.1 x de-rating)
40	16.5	660	20% (5.0 x de-rating)
40	23.2	928	28% (3.6 x de-rating)

TABLE 6. Significance of Overburden De-Rating Assumptions Used in LaModel (based on initial modelling results only)

It is also necessary to note that the influence of overburden properties E and t on overburden stiffness is multiplicative. This means that a model using E = 10 GPa and t = 20 m will return the exact same results as a model using E = 5 GPa and t = 40 m.

A combination of E = 16.5 GPa and t = 200 m (as contained in Table 5 as being consistent with back-analysed S_{max} in the order of 10 mm) results in $E \times t = 3300$, this being used as a basis for estimating the level of conservatism associated with the actual overburden parameter assumptions used for design purposes. Table 6 contains the E x t values used in the EIS mine layout assessment, the relativity with $E \times t = 3300$ being the basis for the quoted overburden “de-rating” in the far right column.

In the parameter sensitivity analyses, Hume Coal has analysed overburden conditions that vary from the back-analysed properties of E = 16.5 GPa and t = 200 m, by as much as a 20 times de-rating, and no less than a 3.6 times de-rating.

3.4 2D LaModel Results Compared to ARMPS-HWM Designs

The aim of the 2D modelling was to make an objective comparison to the ARMPS-HWM designs, the inclusion of overburden lithology being predicted to generate discernible vertical load re-distribution away from the web pillars and onto the intra-panel barriers.

Before considering the 2D modelling results in terms of pillar SF values, it is worth re-stating that ARMPS-HWM uses full tributary area loading when designing web pillars, but adds in abutment angles defined by an Abutment Angle of 21°, on both sides of an intra-panel barrier pillar. This means that ARMPS-HWM double-counts a portion of the overburden load in the pillar design analyses. The result of this is that there will inevitably be a significant difference in barrier pillar SF between the recommended design value used within ARMPS-HWM (2) and those returned from the numerical modelling (which are much higher than 2), this same influence also being clearly evident in Tables 2 and 3. Tables 7, 8 and 9 provide ARMPS-HWM design summaries for the three cover depth cases contained in Table 1, the substantially higher SF values at shallow cover depth due to the setting of minimum w/h ratios of 1 and 4 for web and intra-panel barrier pillars respectively.

	width (m)	Actual SF v ARMPs-HWM Recommended SF	Actual w/h v recommended w/h	Actual v recommended (m)	W/H (NB 1 = approximate sub to super-critical transition)
<i>web pillars</i>	3.5	1.68 v 1.3	1 v 1		
<i>barrier pillars</i>	14	2.69 v 1.5	4 v 4		
<i>system stability</i>		2.95 v 2.0			
<i>distance between barriers (skin to skin)</i>				56.5 v 60	
<i>width to depth ratio (W/H) between barriers</i>					0.71
<i>width to depth ratio (W/H) due to drive length (NB 113 m perpendicular to gates)</i>					1.4

TABLE 7. Layout Design Assessment Parameters, 80 m Cover Depth

	width (m)	Actual SF v ARMPs-HWM Recommended SF	Actual w/h v recommended w/h	Actual v recommended (m)	W/H (NB 1 = approximate sub to super-critical transition)
<i>web pillars</i>	4.1	1.3 v 1.3	1.17 v 1		
<i>barrier pillars</i>	16.8	2.03 v 1.5	4.8 v 4		
<i>system stability</i>		2.51 v 2.0			
<i>distance between barriers (skin to skin)</i>				52.6 v 60	
<i>width to depth ratio (W/H) between barriers</i>					0.44
<i>width to depth ratio (W/H) due to drive length (NB 113 m perpendicular to gates)</i>					0.94

TABLE 8. Layout Design Assessment Parameters, 120 m Cover Depth

	width (m)	Actual SF v ARMPs-HWM Recommended SF	Actual w/h v recommended w/h	Actual v recommended (m)	W/H (NB 1 = approximate sub to super-critical transition)
web pillars	5.5	1.31 v 1.3	1.57 v 1		
barrier pillars	20.9	2.0 v 1.5	5.97 v 4		
system stability		2.56 v 2.0			
distance between barriers (skin to skin)				51.5 v 60	
width to depth ratio (W/H) between barriers					0.32
width to depth ratio (W/H) due to drive length (NB 113 m perpendicular to gates)					0.71

TABLE 9. Layout Design Assessment Parameters, 160 m Cover Depth

Depth (m)	Lamination Thickness (m)	Rock Mass Elastic Modulus (Gpa)	Average Web Pillar Safety Factor	Centre Web Pillar Safety Factor	Barrier Pillar Safety Factor
80	20	8.2	1.798	1.726	5.695
80	20	16.5	1.843	1.769	5.374
80	20	23.2	1.864	1.796	5.233
80	40	8.2	1.842	1.768	5.377
80	40	16.5	1.885	1.825	5.105
80	40	23.2	1.903	1.853	4.999
120	20	16.5	1.408	1.362	4.737
120	40	8.2	1.408	1.361	4.739
120	40	16.5	1.450	1.414	4.518
120	40	23.2	1.468	1.438	4.432
160	20	16.5	1.414	1.379	3.739
160	40	16.5	1.446	1.416	3.603
160	40	23.2	1.460	1.432	3.549

TABLE 10. 2D LaModel Results for Specific EIS Layout Designs (refer Table 1)

Table 10 provides a summary of the various 2D LaModel runs, with the following comments being made based on a comparison with the ARMPs-HWM designs as contained in Tables 7, 8 and 9:

- (a) SF values for the centre web pillar are all greater than 1.3, those at 80 m cover depth ranging from around 1.75 to 1.85 according to variations in overburden stiffness parameters.
- (b) Average web pillar SF values are higher than the centre web pillar value, due to not all web pillars within a web pillar panel being loaded equally. At 80 m cover depth, the average SF value ranges from 1.798 to 1.903, with those at 120 m and 160 m cover depth being lower at 1.408 to 1.468.

- (c) Barrier pillar SF values varying according to changing cover depth (as is also evident in **Table 2**) and varying overburden stiffness assumptions, the lowest SF value (3.549) being directly linked to the stiffest overburden condition at 160 m depth, and the highest SF value (5.695) being related to the softest overburden condition at 80 m depth. This all makes sense in terms of the varying influence of assumed overburden stiffness on overburden load re-distribution away from the web pillars and onto the barrier pillars. This same basic effect is also evident in **Table 2**

The 2D LaModel results demonstrate that the web pillars are likely to be loaded to a lower level than under full-tributary-area loading (as assumed in ARMPS-HWM) across the full range of assumed overburden stiffness. Therefore as a direct and inevitable consequence, slightly higher levels of overburden load are being carried by the intra-panel barriers. This overburden load-transferring mechanism is directly driven by the sub-critical nature of each panel of web pillars between intra-panel barriers and is consistent with the EIS layout design report whereby this effect was deliberately included within the panel layouts, albeit not fully quantified at that time (**Mine Advice 2016a**). The additional load carried by intra-panel barriers does not lead to a credible risk of barrier pillar failure, since they retain SF values in the range of 3.55 to 5.695.

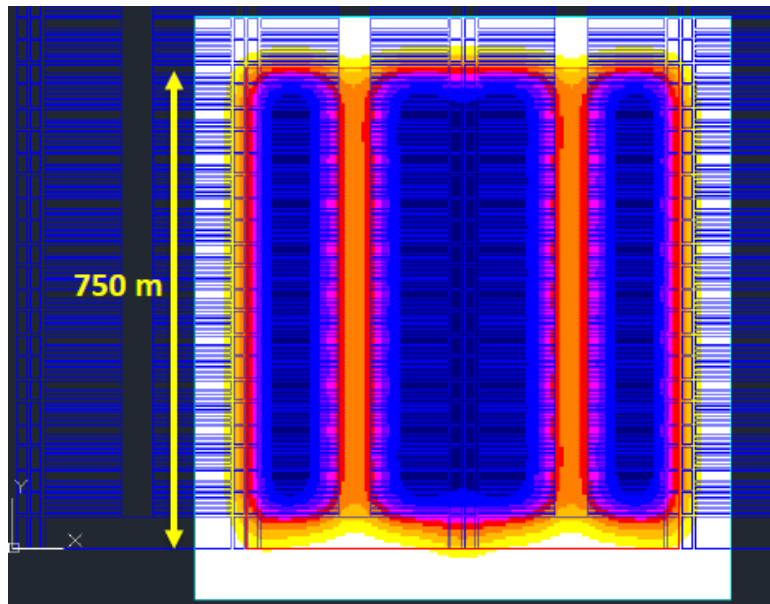
The comparison of the 2D modelling results with the original ARMPS-HWM designs, satisfies the second aspect of the **Esterhuizen 2014** statement, namely to evaluate the “calibrated” numerical model from specific case histories, against an empirical database. It also demonstrates that despite being significantly de-rated from likely reality, the range of overburden stiffness assumptions all return conclusive evidence of sub-critical overburden behaviour between intra-panel barriers, this adjoining web pillars and intra-panel barrier pillars together as part of a larger pillar system, this being the basis for ARMPS-HWM applying a System Stability Factor approach to the overall layout design in addition to the individual pillars within the system.

3.5 3D Model Results

3D modelling runs incorporating a much more extensive mine layout (see **Figure 11**) were undertaken subsequent to the 2D model runs in order to (i) determine the relative distribution of pillar loads in 3D over a series of panels, (ii) gain insight into the global stability behaviour of the pillar-overburden system in 3D, and (iii) provide a further complement to the empirical design methodology used in the original EIS mine layout design process.

Fewer modelling runs were conducted in 3D (**Table 11**) as compared to 2D, in order to reduce the time required to complete the 3D modelling, since individual models were still taking several days to run despite the mathematical processing speed of LaModel.

At 80 m cover depth, it was decided to include the softest possible overburden condition ($E = 8.2$ GPa and $t = 20$ m) to evaluate the effect on mine stability resulting from a twenty-fold de-rating of back-analysed overburden stiffness in the shallowest parts of the mine, where the panels have the highest width to depth (W/H) ratios. Otherwise, each cover depth was evaluated according to lower and upper overburden stiffness limits as defined by $E = 16.5$ GPa and $t = 20$ m (least stiff overburden) and $E = 23.2$ GPa and $t = 40$ m (most stiff overburden) respectively.



Model for DoC = 80m

FIGURE 11. Sample 3D Model Area of Influence Within the Mine Layout

Depth (m)	E (GPa)	t (m)
80	8.2	20
80	16.5	20
80	23.2	40
120	16.5	20
120	23.2	40
160	16.5	20
160	23.2	40

TABLE 11. Cover Depth and Overburden Parameters used in 3D Modelling Runs

3.5.1 80 m Cover Depth

Figure 12 shows vertical stress isopachs for the three overburden cases, which range from a 20 times to 3.6 times stiffness de-rating as compared to the likely true overburden conditions acting at the Berrima observation or control sites. Each of the three layouts in Figure 12 confirm the stabilising influence of the solid inter-panel barrier pillars via incrementally reducing vertical stress magnitudes on each web pillar with increasing proximity to the inter-panel barrier pillar. This is also the case for the softest overburden condition ($E = 8.2$ GPa and $t = 20$ m), although the level of influence is not as substantial as for the stiffer overburden cases, as would logically be expected.

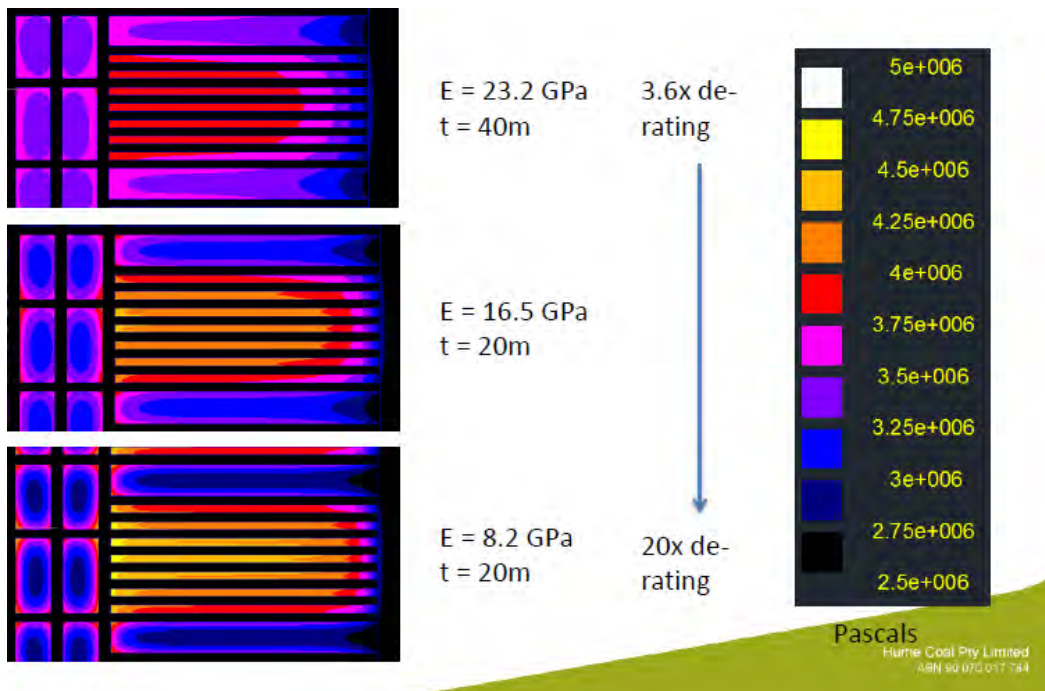


FIGURE 12. Vertical Stress Distributions, 80 m Cover Depth Cases

The stabilising influence of the chain pillars at the opposite end of the web pillars becomes clearer as the overburden stiffness de-rating is reduced back to levels that are closer to the back-analysed overburden properties. The overburden needs to be de-rated by at least ten-fold or an order of magnitude before even a small length of a web pillar contains a stability condition less than that of the ARMPS-HWM design at 80m depth of cover. This effect is judged to be a direct consequence of the presence of 5.5 m wide gateroads at the end of each web pillar, which will inevitably tend to cause overburden load from above the roadway to be re-distributed onto the ends of the adjacent web pillars. Such an influence is obviously not relevant in surface HWM from an open cut highwall, however the 3D modelling parameter sensitivity study has identified this influence so it is therefore now included in the resultant stability analyses.

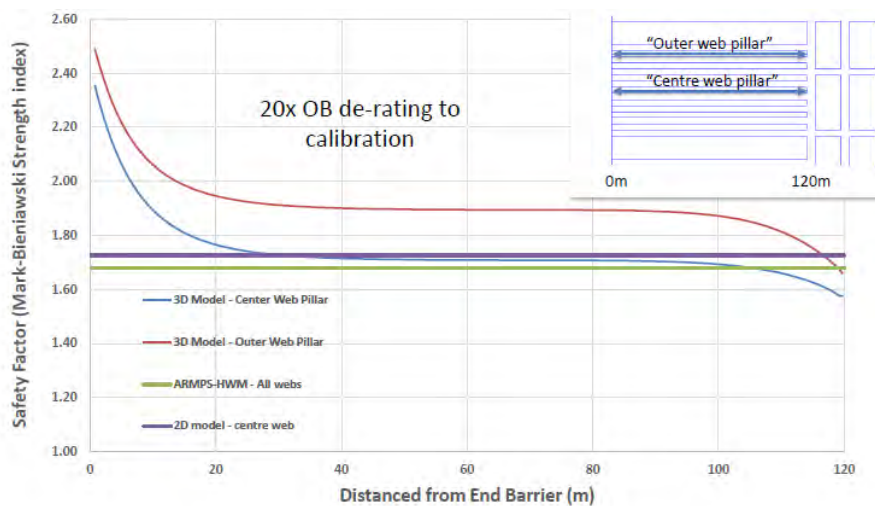


FIGURE 13. Web Pillar Section Showing Varying SF along Web Pillars According to Different Methods of Analysis ($H = 80 \text{ m}$, $E = 8.2 \text{ GPa}$, $t = 20 \text{ m}$)

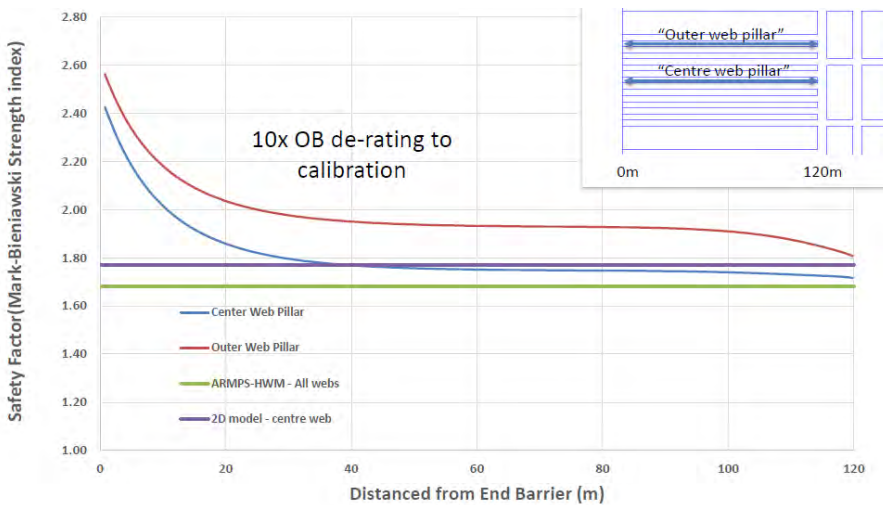


FIGURE 14. Web Pillar Section Showing Varying SF along Web Pillars According to Different Methods of Analysis ($H = 80$ m, $E = 16.5$ GPa, $t = 20$ m)

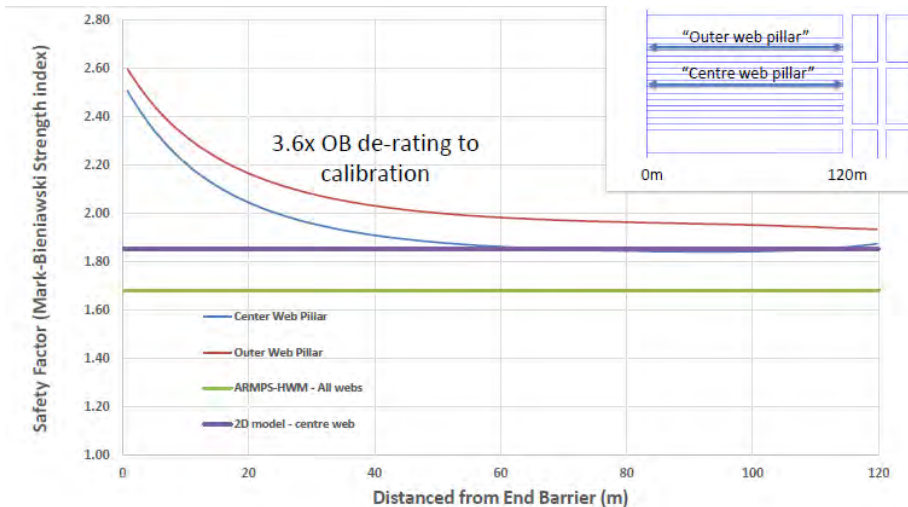


FIGURE 15. Web Pillar Section Showing Varying SF along Web Pillars According to Different Methods of Analysis ($H = 80$ m, $E = 23.2$ GPa, $t = 40$ m)

Figure 13 shows the variation in SF along both the centre and outer web pillars for a cover depth of 80 m, $E = 8.2$ GPa and $t = 20$ m, the influence of bringing in the overburden in 2D initially and the full 3D problem analysis being evident. For this case, the average web pillar SF for an entire web pillar panel is found to be 1.8, this being only marginally higher than the average value found using the 2D model (1.798 – Table 10), but more significant when compared to the ARMPMS-HWM design value in Table 7 of 1.68.

The intra-panel barrier pillars in Figure 13 have an average SF of 5.67, which is as expected given the very minor difference between the web pillar SF values, and is only marginally lower than that given by the 2D analysis of 5.695 (Table 10). The chain pillars have a SF of 5.102.

At the other end of the overburden range, Figure 15 shows the varying SF values along web pillars for $E = 23.2$ GPa and $t = 40$ m, the changes in web pillar stability in both the 2D and 3D models being more obvious, as compared to Figure 13. For this case, the average web pillar SF for an entire web pillar

panel is found to be 1.93, this being only marginally higher than the average value found using the 2D model (1.903 – **Table 10**), but more significant when compared to the ARMPS-HWM design value in **Table 7** of 1.68.

The intra-panel barrier pillars in **Figure 15** have an average SF of 5.092, which is almost identical to that given by the 2D analysis of 4.999 (**Table 10**). The chain pillars have a SF of 4.841.

Whilst a stiffer overburden results in greater vertical load re-distribution from the web pillars onto the surrounding barrier pillars, in both overburden cases the overall difference in both web and intra-panel barrier pillar stability outcomes from both the 2D and 3D models is small and the intra-panel barriers retain very high SF values between 5 and 5.67. The 3D models also provide confirmation of the 2D modelling outcomes for the webs and intra-panel barriers, and demonstrate stable design outcomes for the chain pillars and the inter-panel barrier pillars, via their high Stability Factors.

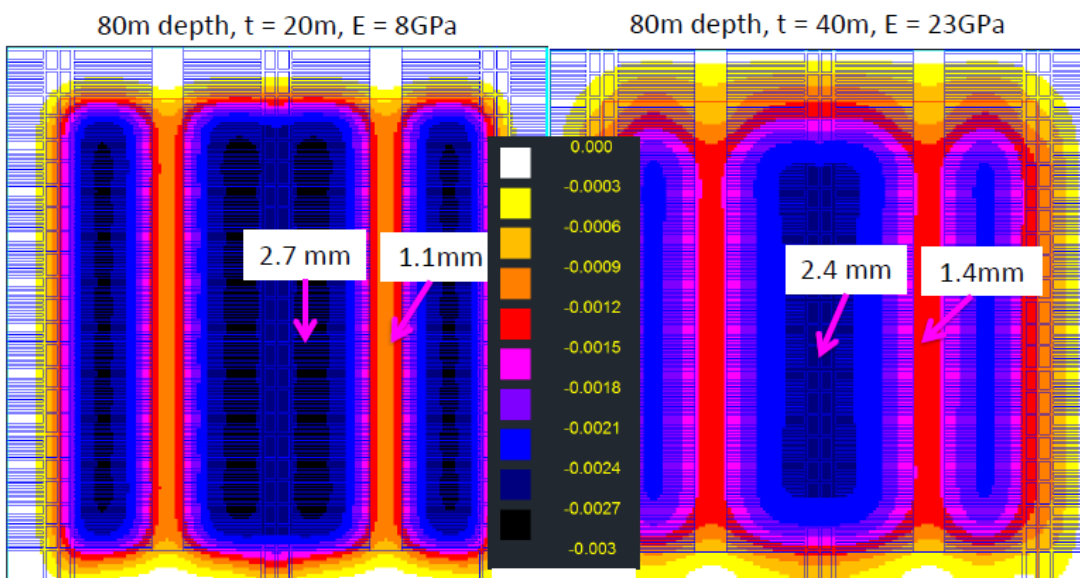


FIGURE 16. Surface Subsidence Isopachs (in metres) and Spot Values (in mm)

In terms of surface subsidence, **Figure 16** shows the outcomes for the two extreme 80 m deep cases, the spot values included in the figure indicating that the predicted magnitudes are very low (< 5 mm).

3.5.2 160 m Cover Depth

Whilst 3D modelling runs were conducted for a cover depth of 120 m, results from the 160 m deep cases are more useful in discussing the modelling outputs, as when combined with those from 80 m depth the full layout design range is effectively covered.

Figure 17 shows vertical stress isopachs for the three overburden cases, ranging from a 10 times to 3.6 times stiffness de-rating as compared to the likely true overburden conditions acting at the Berrima back-analysis sites.

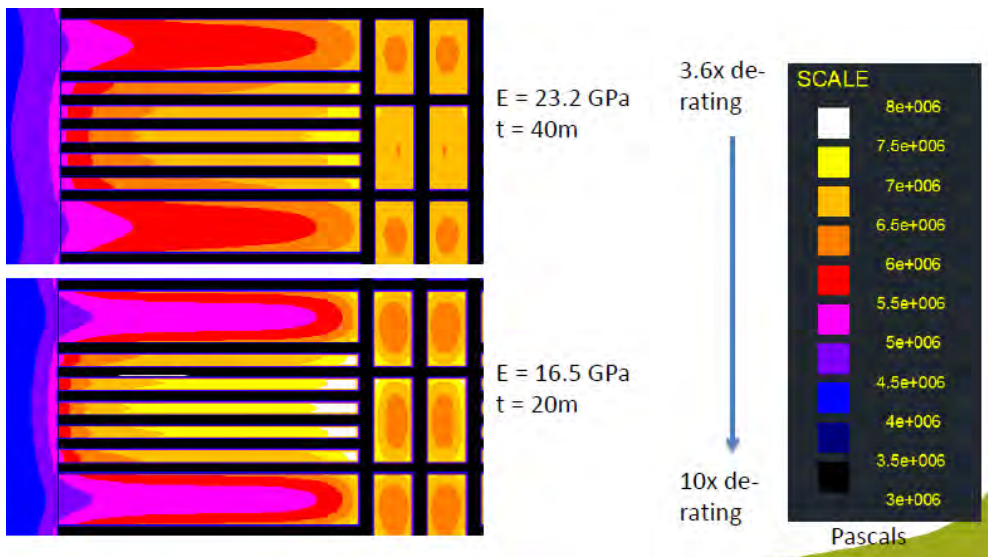


FIGURE 17. Vertical Stress Distributions, 160 m Cover Depth Cases

The two layouts shown in Figure 17 again demonstrate the stabilising influence of the solid inter-panel barrier pillars via an incrementally reducing vertical stress towards the inter-panel barrier on each web pillar, the level of influence being lower with the less stiff overburden case (i.e. $E = 16.5 \text{ GPa}$, $t = 20 \text{ m}$).

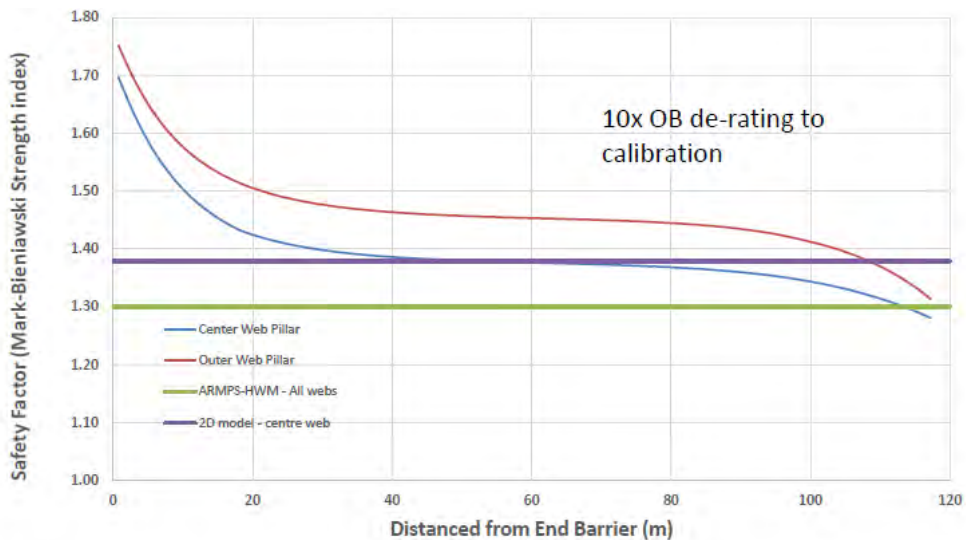


FIGURE 18. Web Pillar Section Showing Varying SF along Web Pillars According to Different Methods of Analysis ($H = 160 \text{ m}$, $E = 16.5 \text{ GPa}$, $t = 20 \text{ m}$)

Figure 18 shows the variation in SF along both the centre and outer web pillars for a cover depth of 160 m, $E = 16.5 \text{ GPa}$ and $t = 20 \text{ m}$, the influence of bringing in the overburden in 2D initially and the full 3D problem analysis being evident. For this case, the average web pillar SF for an entire web pillar panel is found to be 1.43, this being close in magnitude to the average value found using the 2D model (1.414 – Table 10), and only marginally increased as compared to the ARMPS-HWM design value in Table 9 of 1.31.

The intra-panel barrier pillars in Figure 18 have an average SF of 4.356, which is slightly higher than that given by the 2D analysis of 3.739 (Table 10). The chain pillars have an SF of 2.589.

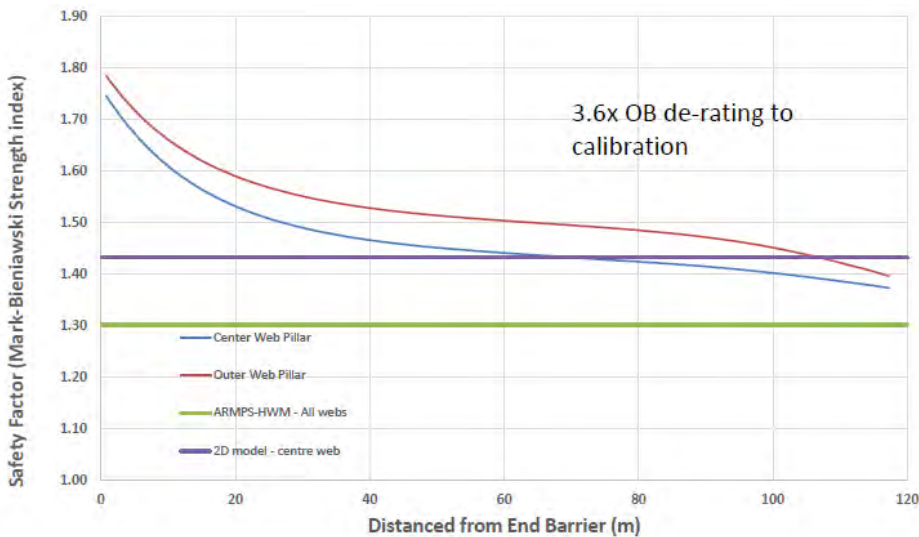


FIGURE 19. Web Pillar Section Showing Varying SF along Web Pillars According to Different Methods of Analysis (H = 160 m, E = 23.2 GPa, t = 40 m)

As the overburden stiffness is increased closer to the back-analysed values, **Figure 19** shows the varying SF values along web pillars for $E = 23.2 \text{ GPa}$ and $t = 40 \text{ m}$ – representing a 3.6 times de-rating. For this case, the average web pillar SF for an entire web pillar panel is found to be 1.458, this being almost identical to the average value found using the 2D model (1.46 – **Table 10**), but more significant when compared to the ARMPS-HWM design value in **Table 9** of 1.31.

The intra-panel barrier pillars in **Figure 19** have an average SF of 4.174, which is marginally higher than that given by the 2D analysis of 3.549 (**Table 10**). The chain pillars have a SF of 2.587.

As per the 80 m cover depth cases described in **Section 4.5.2**, whilst a stiffer overburden results in greater vertical load re-distribution from the web pillars onto the surrounding barrier pillars, in both overburden cases the overall difference in both web and intra-panel pillar stability outcomes between the 2D and 3D models is small and the 3D models provide support to the 2D modelling outcomes.

Stable design outcomes for the chain pillars and the interpanel barrier pillars are also demonstrated in the 3D model outcomes via their high Stability Factors.

In terms of surface subsidence, **Figure 20** shows the outcomes for the two extreme 160 m deep cases, the spot values included in the figure indicating that the predicted magnitudes remain very low (< 5 mm).

Overall, the 3D LaModel runs show changing vertical load distributions between web pillars, intra-panel barriers, inter-panel barriers and gate road pillars due to varying overburden stiffness. However, the overall finding is that the differences in average SF for both the web pillars and intra-panel barrier pillars in both the 2D and 3D cases, is small, with the 2D models providing the same basic insight as the more complex 3D models as to the influence of overburden lithology and load distributions between web pillars and intra-panel barrier pillars, as compared to the ARMPS-HWM designs where overburden lithology is not included. The 3D models provide additional insight in terms of the effect of and stability outcomes for the inter-panel barrier and chain pillars, which in all cases exhibit stable outcomes as inferred from their respective Stability Factors.

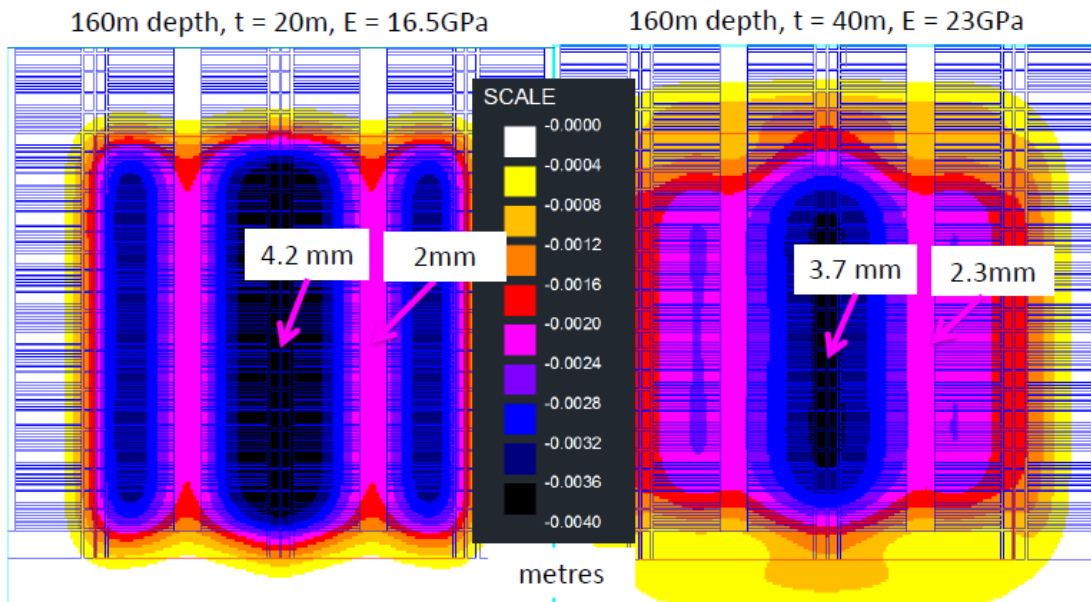


FIGURE 20. Surface Subsidence Isopachs and Spot Values (in metres)

Predicted values of surface lowering are < 5 mm in all cases, although reasons as to why these model predicted values are substantially less than the maximum value for S_{\max} of 20 mm used for EIS purposes in **Mine Advice 2016b**, will be discussed in more detail in a later section of the report.

3.6 Scenario Analysis

The scenario analysis was achieved by running two hypothetical scenarios in 3D for two cover depths (a total of four models) in order to analyse the sensitivity of global mine stability to localised variations in web pillar stability of varying severity, namely:

- (i) the complete removal of a single web pillar from a web pillar panel, and
- (ii) the removal of all web pillars from a web pillar panel.

These runs were done for the two cover depths of 80 m and 160 m representing the low and high end of the range of cover depths present within the proposed mining footprint. These models also utilised the lowest level of overburden stiffness for each specific cover depth as per the standard 3D modelling runs (i.e. $E = 8.2 \text{ GPa}$ and $t = 20 \text{ m}$ for 80 m depth and $E = 16.5 \text{ GPa}$ and $t = 20 \text{ m}$ for 160 m depth).

3.6.1 80 m Cover Depth

Figure 20 shows the panel cross-line used for developing surface subsidence curves from LaModel. Table 12 contains key stability parameters for the “before and after” conditions relating to specific changes in web pillar configuration, Figures 22 and 23 showing the resultant change in surface subsidence for the single and complete web pillar removal scenarios respectively, the location of solid inter-panel barriers and chain pillars being indicated relative to the subsidence profile.

The scenario analysis modelling run for 80 m cover depth and least stiff overburden, indicate that the removal of a single web pillar has only a minimal negative impact on the SF values for the various coal pillars within the system, and the impact on surface subsidence is limited to the general vicinity of the web pillar that has been removed, being in the order of 1 mm in terms of increased S_{\max} magnitude.

Parameter	Before	After – single web pillar removal	After – web pillar panel removal
Average Web SF – all webs within a panel	1.8	1.6	N/A
Average Intra-Panel Barrier SF	5.7	5.5	2.9
Chain Pillar SF	5.1	4.9	3.3
S _{max} (mm)	2.7	3.7	23.5

TABLE 12. Key Stability Parameter Summary – 80 m Cover Depth

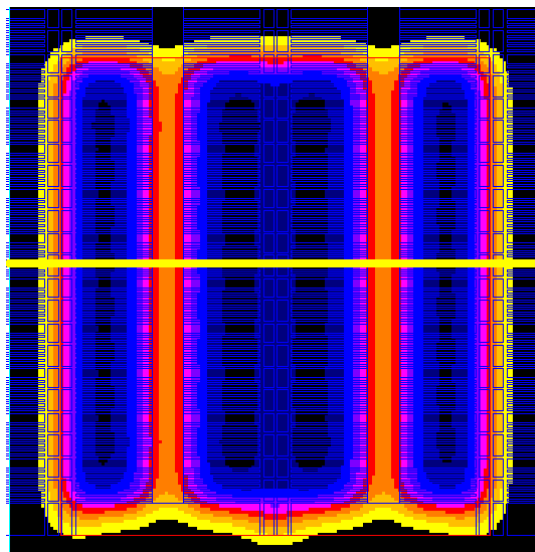
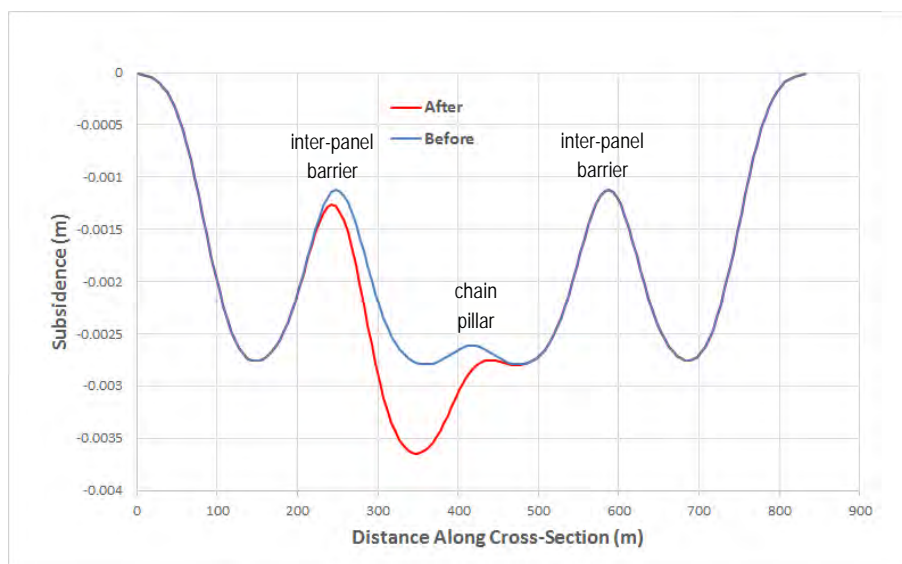


FIGURE 21. Panel Cross-Line Used for Surface Subsidence Curves

FIGURE 22. Surface Subsidence Profile Change Along a Centre Web Pillar, Single Web Pillar Removed ($H = 80$ m, $E = 8.2$ GPa, $t = 20$ m)

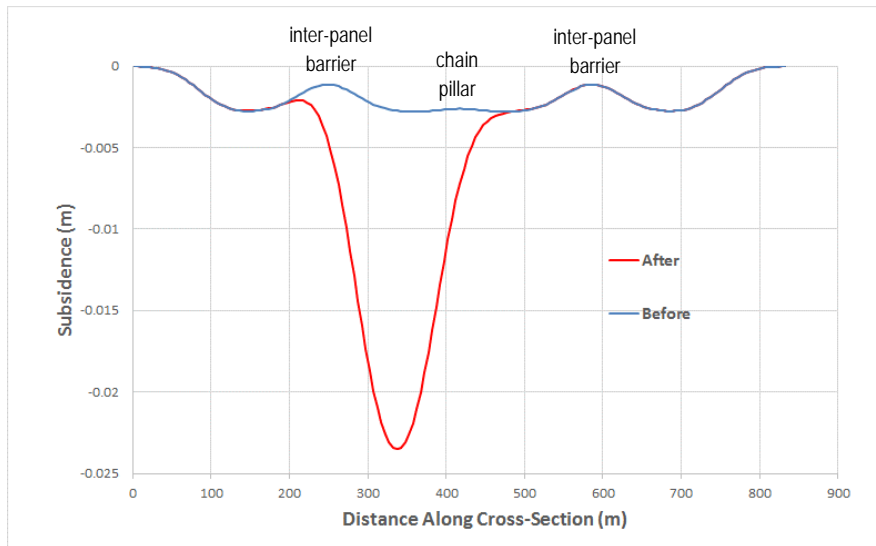


FIGURE 23. Surface Subsidence Profile Change Along Centre Web Pillar, Full Web Pillar Panel Removed ($H = 80 \text{ m}$, $E = 8.2 \text{ GPa}$, $t = 20 \text{ m}$)

The removal of a full web pillar panel (7 web pillars in this case), results in far more significant changes to pillar SF values although with both the intra-panel barriers and chain pillars retaining SF values in the order of 3, their on-going integrity can be inferred despite the artificial and unrealistic removal of the stabilising influence of all web pillars in a panel. Surface subsidence increases to 23.5 mm above the centre of the web pillar panel that has been removed, with adjacent areas being largely unaffected in practical terms.

The significance of $S_{\max} = 23.5 \text{ mm}$ in terms of its likely impact upon the stability of the overburden remote from the coal pillars will be discussed in more detail later in the report, suffice to state that differential surface subsidence of this magnitude is not considered to indicate a substantial change in overall overburden condition above the area of removed web pillars. The EIS utilised a "credible worst-case" subsidence value of 20 mm for vertical surface lowering, the difference between 20 mm and 23.5 mm being considered to be immaterial from a subsidence impact assessment perspective, remembering again that the 23.5 mm prediction is based on what is considered to be a totally unrealistic scenario where web pillars are completely removed from the numerical model.

Parameter	Before	After – single web pillar removal	After – web pillar panel removal
Average Web SF	1.3	1.1	N/A
Average Intra-Panel Barrier SF	4.4	4.1	2.7
Chain Pillar SF	2.6	2.5	1.9
S_{\max} (mm)	4.2	5.1	16.4

TABLE 13. Key Stability Parameter Summary – 160 m Cover Depth

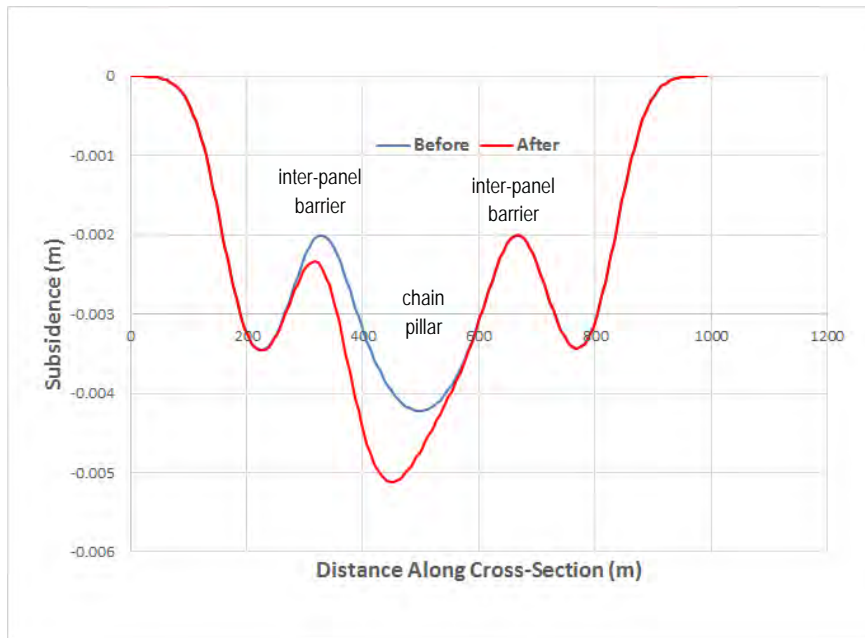


FIGURE 24. Surface Subsidence Profile Change Along Centre Web Pillar, Single Web Pillar Removed ($H = 160$ m, $E = 16.5$ GPa, $t = 20$ m)

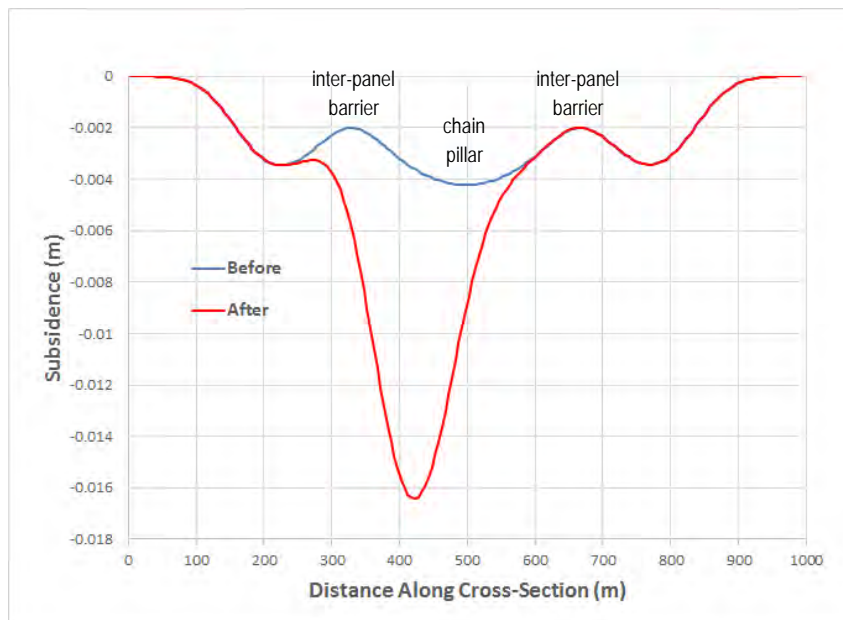


FIGURE 25. Surface Subsidence Profile Change Along Centre Web Pillar, Full Web Pillar Panel Removed ($H = 160$ m, $E = 16.5$ GPa, $t = 20$ m)

3.6.2 160 m Cover Depth

Table 13 contains key stability parameters for the “before and after” conditions in relating to the specific change in web pillar configuration, Figures 24 and 25 showing the resultant change in surface subsidence for the single and complete web pillar removal scenarios respectively, the location of solid inter-panel barriers and chain pillars being indicated relative to the subsidence profile.

The scenario analysis modelling runs for 160 m cover depth and the least stiff overburden, indicate that the removal of a single web pillar has only a minimal negative impact on the SF values for the various coal pillars within the system, and the impact of surface subsidence is limited to the general vicinity of the web pillar that has been removed and is in the order of 1 mm in terms of increased magnitude.

The removal of a full web pillar panel (5 web pillars in this case) results in more significant changes to pillar SF values with the chain pillars dropping to an SF in the order of 1.9. Surface subsidence increases to 16.4 mm above the centre of the web pillar panel that has been removed, with adjacent areas being largely unaffected in practical terms. The significance of $S_{max} = 16.4$ mm in terms of its likely impact upon the condition of the stability of the overburden remote from the coal pillars will be discussed in more detail later in the report, suffice to state that differential surface subsidence of this magnitude is not considered to indicate a substantial change in overall overburden condition above the area of removed web pillars.

It is noted that the only time that any of the defined barrier pillars within the system drop below an SF of 2 is for the chain pillars at 160 m depth in association a complete panel of web pillars being removed from the system (see **Table 13**). However when it is remembered that the loss of load-bearing ability for a complete panel of web pillars is judged to be a totally unrealistic scenario in reality, and that with the loss of only one web pillar, the chain pillars retain an SF of 2.5, it is concluded that based on the numerical modelling results there is no obvious requirement to re-design the chain pillars for deeper cover areas of the proposed mine.

4.0 DISPLACEMENT-BASED STABILITY CRITERIA

The idea of evaluating global mine stability via displacement criteria in addition to pillar loading criteria, was raised by Emeritus Professor Jim Galvin during the experts meeting, his comment being that it had been raised by Emeritus Professor Ted Brown (who chaired the experts meeting) during his peer review of Emeritus Professor Jim Galvin's recently published text book.

The same issue was recently addressed in some detail in **Frith and Reed 2018a and 2018b** (see **Appendices A and B**), with both a behavioural model for the stability/instability of a vertically jointed overburden and measured overburden displacement data that allows the model to be tested and the magnitude of key overburden stability parameters estimated, the primary parameter being the magnitude of differential vertical subsidence across an area of standing coal pillars. It is assessed that this model and the associated published field data provides a displacement-based method by which mine stability for the proposed EIS layouts at Hume can be assessed in a meaningful manner.

Prior to assessing remnant mine stability for the proposed EIS mine layout at Hume, it is necessary to outline in detail, the technical basis of the overburden stability/instability model and the supporting field data.

4.1 A Conceptual Cause and Effect Model for Overburden Stability/Instability

If the influence of the overburden above collapsed mine workings supported with coal pillars is to be quantified, a conceptual model is required that incorporates all of the primary controls. Such a model was first suggested in **Frith and Reed 2018a**, which is developed further herein to produce a Ground Reaction Curve (GRC) representation that incorporates the associated principles.

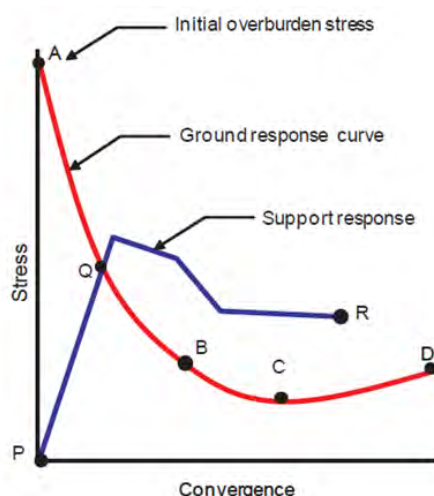


FIGURE 26. Generic Ground Reaction Curve (GRC) Representation

The GRC concept (Figure 26) was originally developed in the early 1960's to assist tunnellers ensure that permanent, and often, stiff permanent tunnel linings were not damaged by excessive ground strains. This has since been applied by others to coal mining problems, such as tailgate standing support design and longwall shield design.

Figure 26 shows that a significant element of a GRC is the installation of ground support following excavation, however in this instance it is only the ground curve that is of interest. The ground curve

(ABCD in Figure 26) contains both a section of negative slope (ABC) whereby the overburden is losing its natural stability due to increasing vertical movement, and a subsequent section of positive slope (CD) whereby natural stability has been effectively lost with self-weight or dead-loading then dominating the condition of the overburden.

A series of simple thought-experiments relating to super-critical mining widths can demonstrate the direct influence of key geotechnical parameters on overburden stability or instability. Super-critical mining geometry is simply the geometry at which the mining excavation width to cover depth ratio exceeds one, as stated in Galvin 2006.

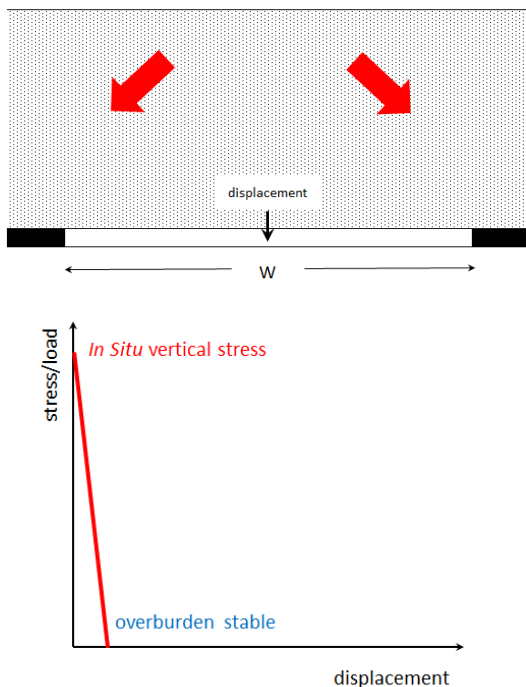


FIGURE 27. Thought-Experiment and Ground Curve: Massive Overburden with No Vertical Joints or Horizontal Stress

Figure 27 represents a massive, stiff sandstone with no vertical joints or horizontal stress. Under this scenario, it is obvious that the overburden will remain stable across a wide extraction span, with the associated GRC rapidly reducing to zero stress (i.e. a self-supporting condition).

Figure 28 is identical to Figure 27 but contains laminated material. Under this scenario, the overburden would initially "sag" downwards and eventually exceed a "critical" level of movement marking the onset of instability to full overburden collapse to surface (i.e. Tributary Area Loading in coal pillar design terminology).

Figure 29 contains the overburden representations of Figures 27 and 28, but introduces vertical joints and horizontal stress. Vertical jointing is omnipresent in coal measures strata sequences and is characterised by zero cohesion and a friction angle that varies according to surface conditions along the joint. Therefore, vertical shear resistance cannot develop along the joint without a normal confining stress, which is horizontal in this case. Therefore irrespective of overburden lithology, without the presence of horizontal stress the presence of vertical jointing will inevitably result in a GRC as shown in Figure 30, namely an unstable overburden with zero stiffness from the outset.

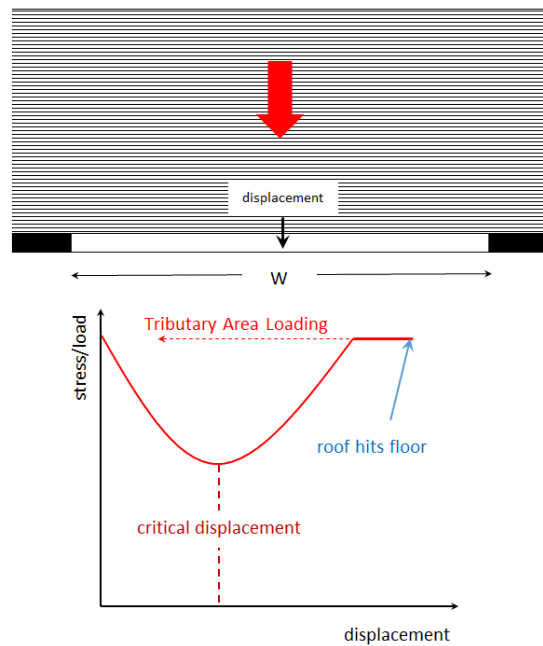


FIGURE 28. Thought-Experiment and Ground Curve: Laminated Overburden with No Vertical Joints or Horizontal Stress

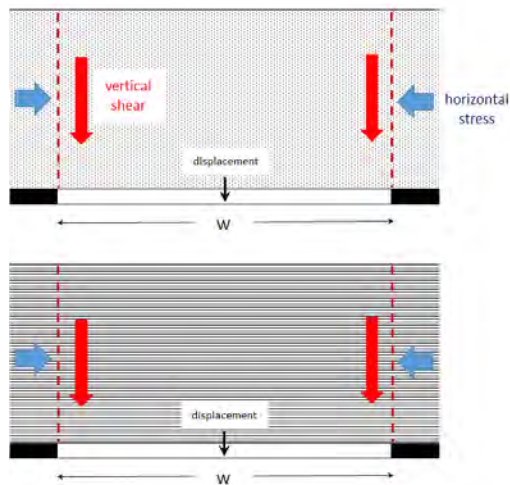


FIGURE 29. Thought-Experiment Representations: Massive and Laminated Overburdens Including Vertical Joints and Horizontal Stress

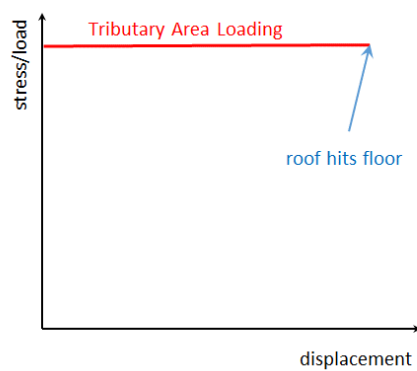


FIGURE 30. GRC: Vertical Joints Present without Horizontal Stress

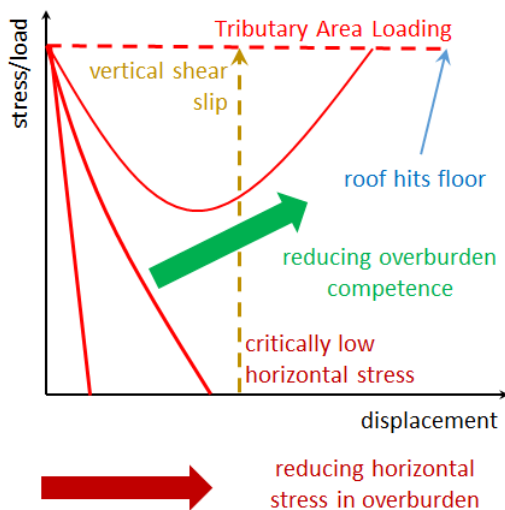


FIGURE 31. Varying Influence of Overburden Lithology, Vertical Joints and Horizontal stress on GRC's

Once overburden horizontal stress is included, the influence of overburden lithology and vertical shear resistance along vertical joints can be combined, resulting in a range of possible GRC outcomes as generally illustrated in **Figure 31**.

For any given span between either barriers or solid coal, overburden stability or instability is directly influenced by the presence or absence of massive strata units etc. and the horizontal stress generating a stabilising influence across vertical joints. In combination, these two geotechnical parameters logically give rise to two distinctly different mechanisms associated with overburden instability and eventual collapse:

- (i) delamination and/or associated sag whilst ever vertical joints remain horizontally "clamped", or
- (ii) a "plug" type collapse due to vertical joints becoming unstable from insufficient horizontal confinement.

The first point of this conceptual overburden model is to justify the idea that overburden conditions dictate the importance of the coal pillars in maintaining stable mine workings, not the other way round.

4.2 Measurement Data that Supports the Basis of the Conceptual Overburden Model

In order for **Figure 31** to be useful as an engineering design tool, magnitudes need to be assigned to at least some of the elements. In this case the key issue is the magnitude of vertical overburden displacement at which shear slip along vertical joints occurs due to the horizontal stress in the overburden becoming critically low. This is taken to be the transition from a stiff to soft overburden condition, this representing the onset of full tributary area loading conditions to surface whereby the stability of the low w/h web pillars would be isolated from that of the various surrounding barrier pillars. It is the degree to which the proposed EIS layout avoids this occurring by maintaining sub-critical overburden conditions between intra-panel barriers that is the absolute crux of the layout designs that have been developed.

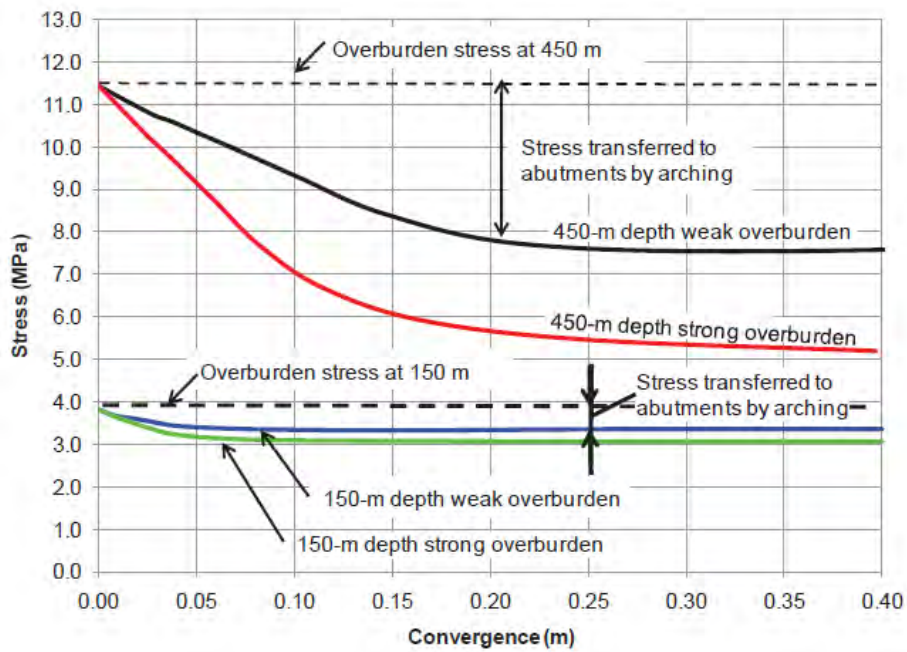


FIGURE 32. Ground Response Curves at the Centre of a 300 m wide Panel in Weak and Strong Overburden Strata at 150 m and 450 m Depth of Cover (Esterhuizen et al 2010)

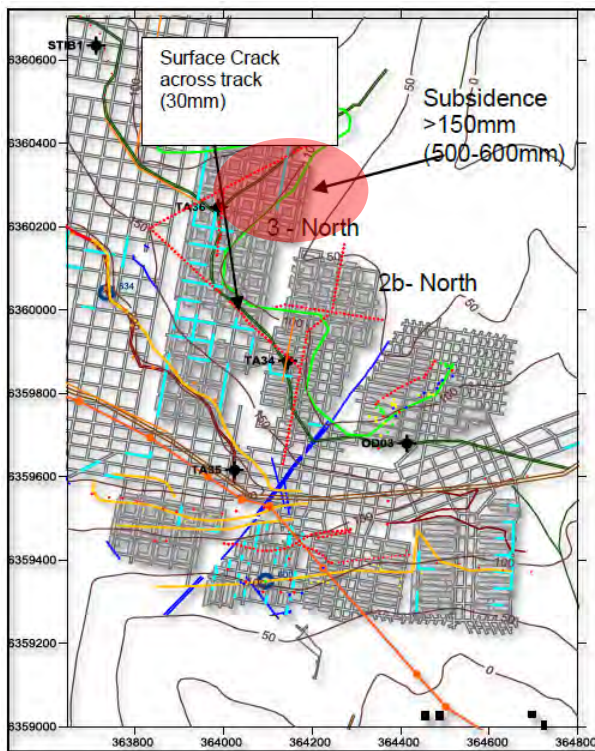


FIGURE 33. Modified Duncan Panels (2b-North, 3 North & 4 South) to West of Transition Zone and Cover Contours (Ditton and Sutherland 2013) – *shaded area added by author*

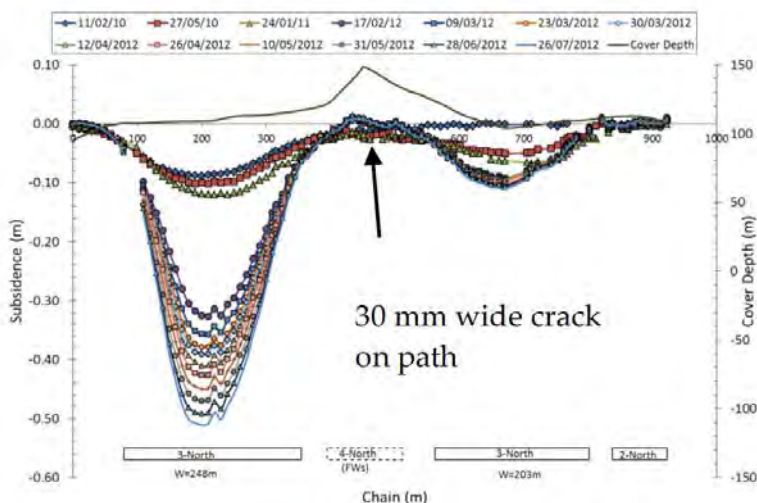


FIGURE 34. Delayed Subsidence above 3 North in Level 1 Area (Ditton and Sutherland 2013)

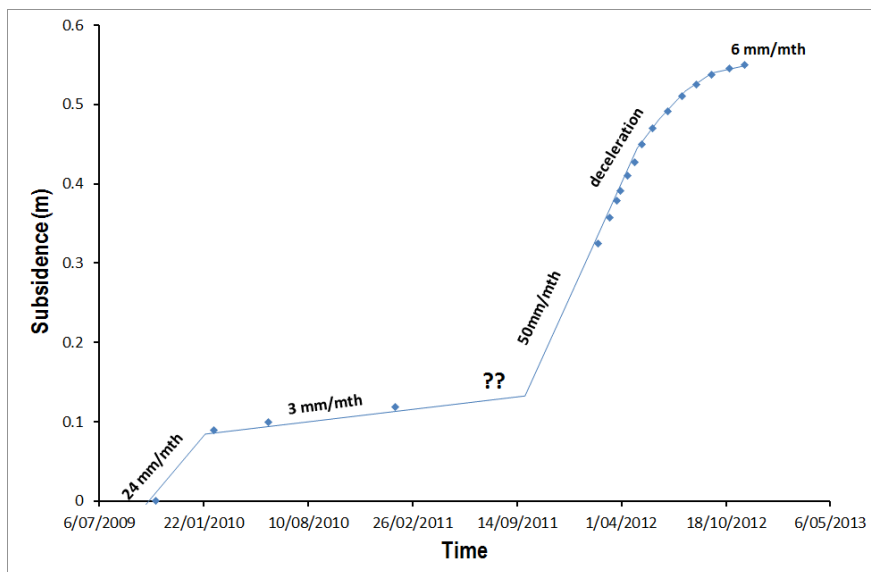


FIGURE 35. Time Dependent Variation in S_{\max} Within 3 North Subsidence Exceedance Area

The fundamental work of Esterhuizen *et al* 2010 in this subject area provides only limited assistance as the study was undertaken without field data validating the numerically produced GRC's (see Figure 32). They state that "*it is difficult to measure the ground response curve in actual underground excavations because of the significant loads that would have to be applied to balance the original ground pressure*". This is correct, but it doesn't alter the need for field data to validate GRCs if they are to be used in the design of underground mines using coal pillars.

A literature search has been undertaken to identify surface subsidence data from above coal pillar systems that have allowed overburden collapses. Fortunately, such subsidence data exists from the Lake Macquarie Area of NSW in Australia relating to partial extraction layouts, and despite pillar system failure relating to floor rather than pillar failure, as it is the GRC of the overburden that is of specific interest, this makes no material difference.

Ditton and Sutherland 2013 describe a significant unexpected subsidence exceedance related to completed Duncan Method partial extraction workings in the Fassifern Seam with a soft claystone floor at the Tasman Mine. The exceedance was within the 3 North Panel and was limited to an area whereby the standard 5 heading development layout was extended to 6 headings over a panel length of four pillars (i.e. approximately 180 m) – see **Figure 33**.

Figure 34 shows the variation in vertical subsidence across the exceedance area of 6 headings and the adjacent area of 5 headings, **Figure 35** containing a time-dependent plot of S_{\max} above the 6 heading area as estimated from **Figure 34**. Based on these two figures and what is known about the Tasman geotechnical environment (including from McTyer and Sutherland 2011), the following comments are made:

- (i) Immediately post-mining, the development of S_{\max} follows a trend of a high rate that decelerates to a longer-term condition, in this case very slow creep at an average rate of 3 mm/month.
- (ii) Based on extrapolation, once S_{\max} reached 150 mm to 200 mm, an obvious change of state occurred via a substantial increase in settlement rate (to around 50 mm/month) followed by a deceleration back to a second longer-term condition with $S_{\max} > 450$ mm (NB questions-marks have been included in **Figure 35** as reading frequencies do not allow the exact nature of the transition to be reliably identified).
- (iii) The floor of the mine workings was soft and heaved following mining (**Figure 36**), coal pillars remaining relatively intact.
- (iv) The overburden included the Teralba Conglomerate in the order of 20 m thick.
- (v) The subsidence exceedance was restricted to the 6 headings area with an extraction width between solid coal of 248 m, as compared to the 5 heading area at a width of 203 m – see **Figure 34**.
- (vi) Both 5 and 6 heading areas were at a cover depth in the order of 130 m (see **Figure 34**) and so using the selection criterion used by Salamon and Munro as well as UNSW, both were under full tributary area loading to surface and presumably had identical pillar loadings.
- (vii) The increased subsidence did not extend into adjacent 5 heading areas, indicating that the "event" was controlled by the excavation geometry and overburden stability, rather than pillar stability.
- (viii) With a seam outcrop around three sides of the mine (see **Figure 37**), tectonic horizontal stress levels were low, as discussed by **McTyer and Sutherland 2011**.

The conclusion reached is that the increased subsidence in the 6 heading area was likely caused by the onset of "plug" type overburden instability within the Teralba Conglomerate once a critical or threshold level of overburden movement had been reached (around 150 mm) due to on-going overburden creep over time via floor instability.



FIGURE 36. Moderate Floor Heave in 3-North Panel (outbye)

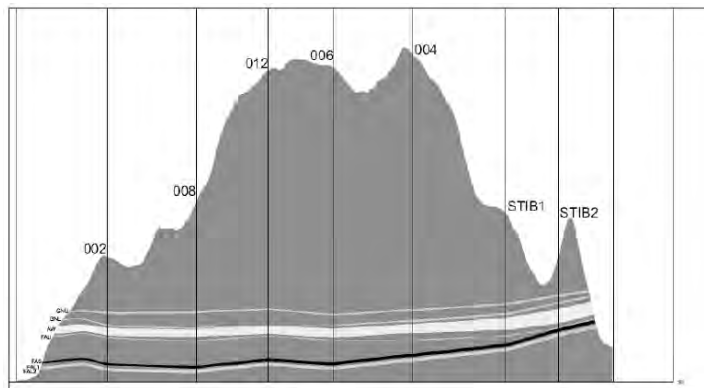


FIGURE 37. North-South Section Across the Tasman Mine Lease Showing the Fassifern Seam Outcrop around the Sugarloaf Range (H:V = 20:1) - Fassifern Seam is shown in black (McTyer and Sutherland 2011)

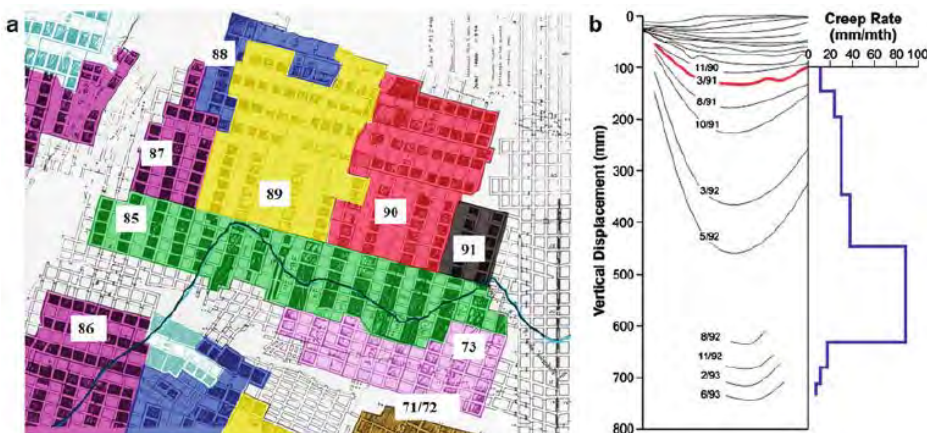


FIGURE 38. An Example of the Rate of Development and Magnitude of Vertical Surface Displacement Due to Bearing Capacity Failure of the Floor In Partial Extraction Workings at a Depth of 160 m (Galvin 2016)

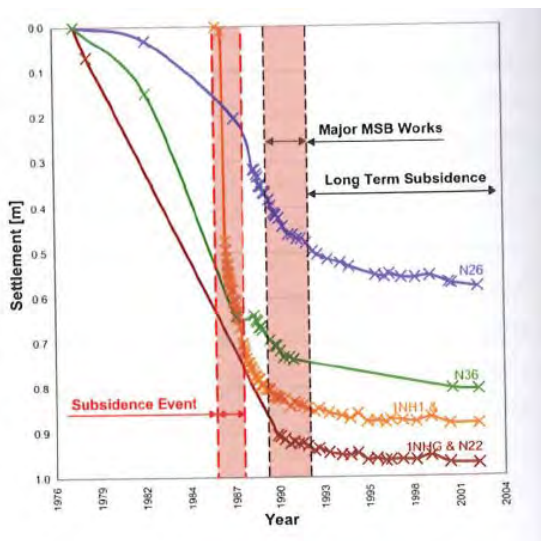


FIGURE 39. Surface Settlements from Newvale Colliery (Shirley and Fagg 2017)

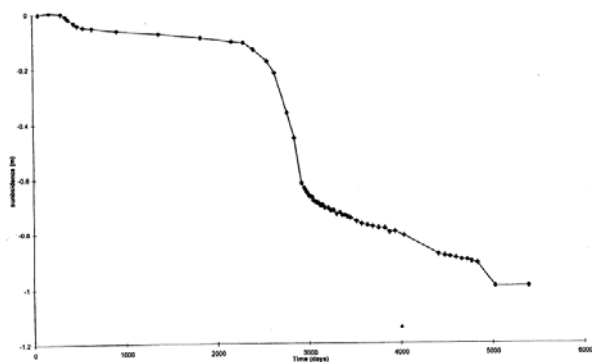


FIGURE 40. Subsidence vs Time Plot for 5NE Panel, Newvale 2 Colliery (Vasundhara et al 1998)

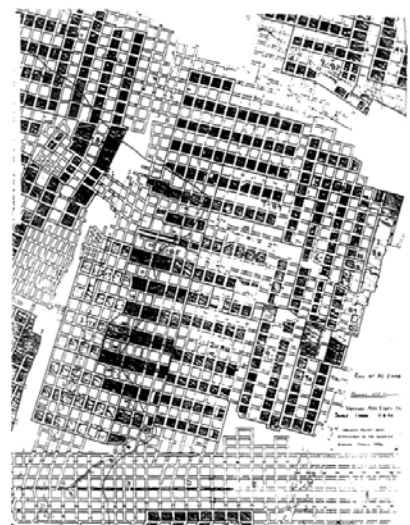


FIGURE 41. Remnant Mine Layout, NE Panels, Newvale 2 Colliery (Vasundhara et al 1998)

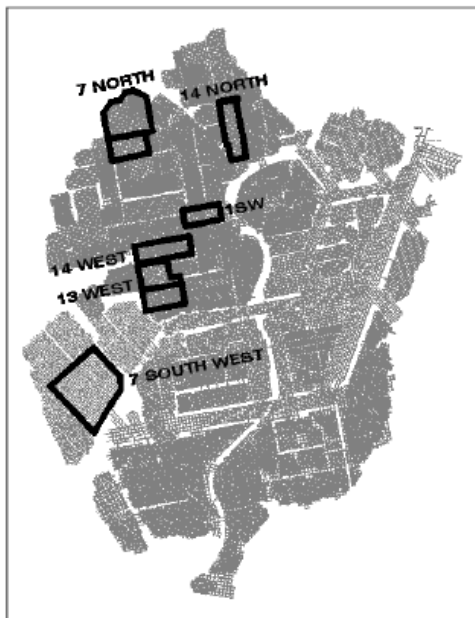


FIGURE 42. Some of the Known Rapid Floor Heave and Subsidence Events in the Great Northern Seam at Awaba Colliery (Seedsman 2008)

Four similar examples to that described for the 3 North Panel at Tasman Mine have been found in the published literature.

Figure 38 is taken from Galvin 2016 and Figure 39 from Shirley and Fagg 2017 relating to the section of the Newvale Mine associated with the well-publicised lowering of the lake foreshore in Chain Valley Bay in the late 1980's/early 1990's. Figure 40 contains measured surface settlements vs time above the 5NE Panel at Newvale 2 Colliery (Vasundhara *et al* 1998) with Figure 41 showing the remnant mining layout in the NE Panels. Figure 42 is taken from Seedsman 2008 whereby he back-analysed what were described as "*rapid floor heave and subsidence events*" at Awaba Colliery, noting that some of these events occurred at depths as low as 60 m with coal pillars on 20 m centres having pillar Factor of Safety (FoS) values in excess of 3.

All of the listed case histories have a number of common characteristics that are of particular interest in the context of the proposed layout design at Hume:

- (i) The partially extracted areas are all super-critical in that W/H values are $\gg 1$. The partial extraction areas shown in Figures 38 and 41 are in the order of 600 m x 600 m with cover depths in the order of 160 m to 180 m, resulting in W/H values in the order of 3 to 4.
- (ii) Following the completion of partial extraction, initial subsidence levels were low with longer-term trends consisting of very low rates of creep with time (where sufficient measurements were taken to allow time-dependent trends to be reliably identified).
- (iii) At subsidence values of 150 mm and greater, the rate of subsidence with time rapidly increased with longer-term subsidence levels approaching 1 m.
- (iv) Longer-term settlement rates commonly return to low values with no evidence of further sudden increases, even several years later.

- (v) As Great Northern Seam workings, the presence of thick, massive conglomerate units in the overburden as well as soft tuffaceous floor material, can be reliably inferred.

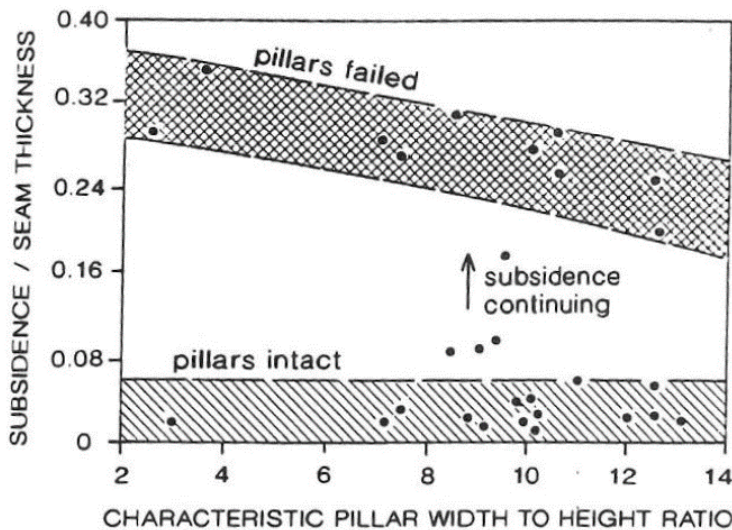


FIGURE 43. Subsidence as Function of Pillar Width to Height Ratio for Soft Floor Failures (Mills and Edwards 1997)

Figure 43 (Mills and Edwards 1997) succinctly summarise some 29 remnant pillar case histories incorporating soft floor measures in the Lake Macquarie area, whereby measured surface subsidence magnitudes clearly polarise into two distinctly different categories, namely "pillars intact" for $S_{\max}/T < 0.075$ and "pillars failed" with S_{\max}/T varying as a direct function of pillar w/h. A step-wise transition between the two conditions can also be inferred via the presence of two distinct "intact" and "failed" populations with few case examples in-between. With the stated seam thickness involved being 2.2 m to 2.5 m, provides for an upper S_{\max} value for "pillars intact" (or overburden stable in more general terms) in the order of 165 mm to 187.5 mm.

Using these specific case histories and relevant geotechnical characteristics, a technical discussion on mechanistic causation can be developed.

The majority of the investigative work that accompanied these delayed and unexpected surface settlement events above partial extraction areas, focused on the failure and compression of soft floor material beneath remnant coal pillars. This is fully understandable given the nature of the floor material and commonly observed floor heave in the workings.

The technical issue that received almost no attention was determining the cause of the rapid increase in the rate of subsidence months after the completion of mining, this being a common feature of the case histories.

Seedsman 2008 makes the statement that "massive conglomerates may span and delay evidence of imminent over-loading of pillars – temporarily stiff loading system". However when the mined-out areas have widths and lengths in the order of 600 m at cover depths < 200 m, conventional subsidence thinking would inevitably eliminate the possibility that even thick massive conglomerates could span across such areas, this being consistent with the periodic weighting classification for longwalls (Frith and McKavanagh 2000) whereby a 30 m thick conglomerate can only span across an extraction width

of 200 m (see **Figure 44**), certainly not 600 m. Clearly there is a major problem or disconnect using overburden caving behaviour from total extraction panels such as longwalls, to estimate the overburden stability to instability point when substantial remnant coal pillars are left in place.

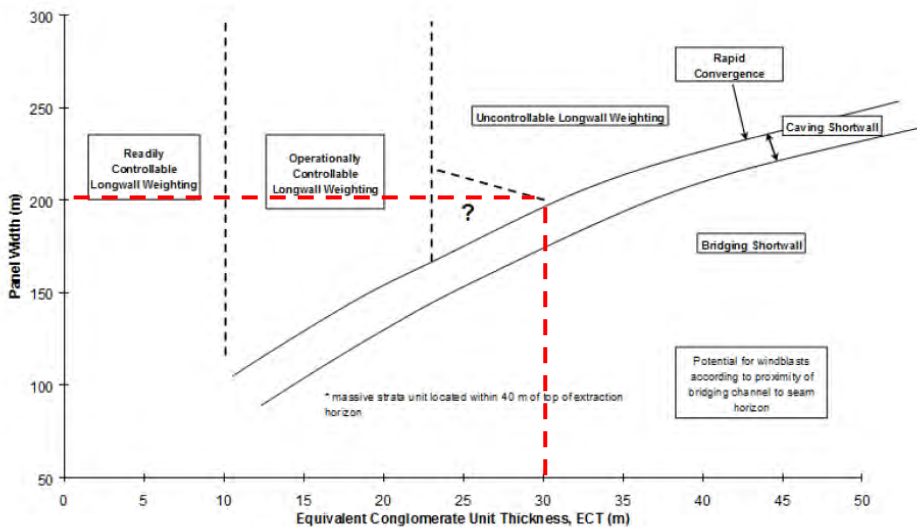


FIGURE 44. Near-Seam, Massive Strata Weighting Classification (Frith and McKavanagh 2000)

The suggested solution to this conundrum, which is as per as that stated by **Van de Merwe 2006** and addressed in **Frith and Reed 2018a** in relation to the non-collapsed area at Coalbrook, is found in two aspects of bord and pillar workings and/or partial pillar extraction that either are absent or substantially diminished in longwall extraction once full caving has been established, namely:

- (i) the contribution of the remnant coal pillars to overburden stability, and
- (ii) the stabilising influence of horizontal stress within the overburden.

In other words, the GRC for the overburden must be being altered by remnant coal pillars, this being consistent with the idea that coal pillars "reinforce" rather than "suspend" the overburden, as was discussed in **Frith and Reed 2018a**.

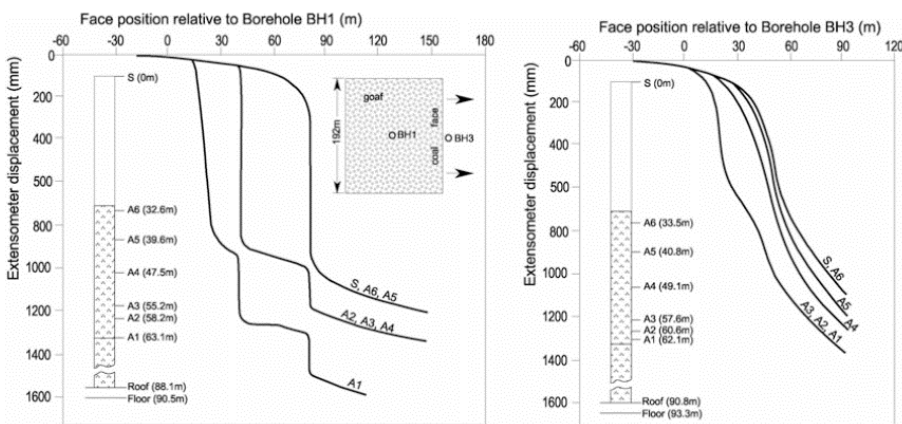


FIGURE 45. Graphs Showing Progressive Step-Failure of a Dolerite Sill as Recorded using Surface to Seam Borehole Extensometers (reproduced from Galvin 2016)

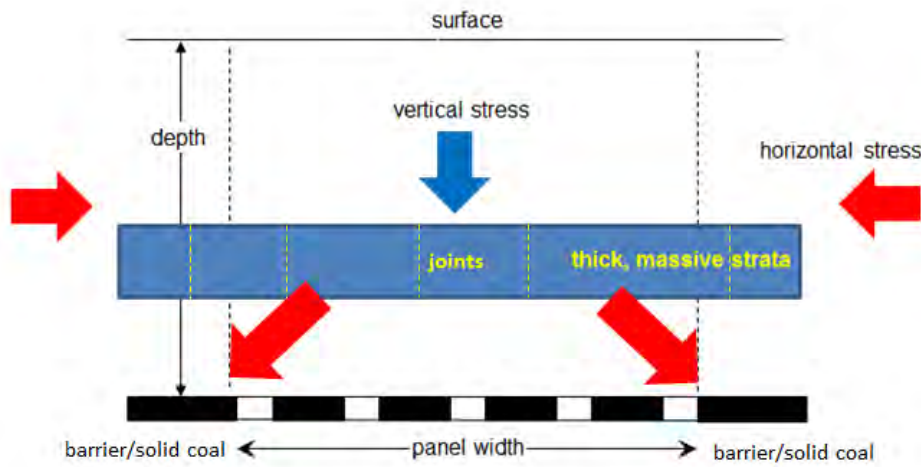


FIGURE 46. Schematic Illustration of a Reinforcing Problem Representation for Coal Pillar Design Including Super-incumbent Load Transfer to Solid Coal or Barrier Pillars

As indicated in Figure 31, it is postulated that the onset of super-critical overburden conditions to surface is dictated by the overburden exceeding a critical level of subsidence, which based on data published by Mills and O'Grady 1998 and Ditton and Frith 2003 was suggested as being in the order of 200 mm by Frith and Reed 2018a. Surface extensometry data published by Salamon *et al* 1972 further indicates the onset of rapid subsidence for values exceeding 150 mm to 200 mm (see Figure 45). The close correlation with measured subsidence magnitudes at the onset of rapid subsidence in the previously described partial extraction cases from the Lake Macquarie area of NSW, is noted.

Re-defining the role of coal pillars as reinforcing rather than suspending the overburden, a general arrangement for the pillar design problem including a more detailed overburden representation containing thick massive strata units, vertical joints and *in situ* horizontal stresses, being shown in Figure 46. It is noted and accepted in this representation, that the *in situ* vertical stresses acting on the production pillars cannot be re-distributed out to any flanking barrier pillars by the action of the overburden, as this would require said pillars to vertically expand or extend due to mining. Therefore, it is only the *in situ* vertical stress that is released by the formation of mining excavations that can be re-distributed, either in full or more likely, in part.

The controlling influence of overburden horizontal stress on surface subsidence was recognised by Mills 2012, who concluded that "sag" subsidence increases in the presence of high horizontal stress, based on subsidence data from the Newcastle Coalfield in NSW. The explanation for this phenomenon is beyond the scope of this report, but inevitably leads into the significance of high horizontal stress in roadway roof control as being the driver for uncontrolled buckling of the roof strata, the control and limiting of which is a reinforcing rather than suspension roadway roof support design problem.

Based on the available field data from a wide variety of sources, it would appear that as a general condition, differential vertical subsidence within the overburden needs to be at least in the order of 150 mm before horizontal stresses become critically low, thereby allowing vertical joint-controlled overburden instability to occur. At subsidence levels < 150 mm, the overburden appears to retain a stiffness such that the role of coal pillars is likely one of reinforcing the overburden, and at > 150 mm, the likelihood of the overburden becoming soft (i.e. zero stiffness) therefore needing to be carried or

suspended by the remnant coal pillars, increases with ever-increasing overburden displacement. It is noted that this type of overburden model is entirely consistent with the GRC concept, which contains both reinforcing and suspension mechanisms according to a critical displacement level having been reached.

4.3 Comments in Relation to the EIS Mine Layout at Hume

In order to make meaningfully assess long-term remnant mine stability for the proposed EIS mine layouts at Hume, two displacement-based parameters are required:

- (i) The critical level of differential vertical subsidence at surface, above which global overburden instability can be reasonably inferred.
- (ii) The likely maximum levels of differential vertical subsidence at surface that are directly associated with the proposed remnant mine layout.

These can be combined into a Factor of Safety (FoS) against overburden instability by dividing (i) by (ii), this being analogous to the definition of a load-based FoS for coal pillars being pillar strength/pillar load.

The preceding discussion has argued that based on various forms and sources of field data, (i) is in the order of 150 mm as a minimum.

In terms of (ii), there are two sources of predicted surface subsidence levels above remnant workings, the first as outlined in the EIS subsidence report itself ([Mine Advice 2016b](#)), the second being from the LaModel numerical simulations.

The LaModel derived values as detailed in [Section 4.5](#), are substantially lower than the S_{\max} value of 20 mm that was stated in the EIS. The primary reason for this difference is that La Model did not take account of the compression of floor measures, a thick coal roof and de-pressurisation effects, whereas the 20 mm value stated in EIS included all of these influences, and was also rounded up to represent a credible worst-case scenario for the proposed mining area as a whole.

As a result of this, despite the LaModel-derived values being linked to a holistic assessment of the mine layout, it is still judged to be prudent to assume that S_{\max} could be as high as 20 mm for the purpose of subsidence impacts and in this case, overburden stability.

With (i) and (ii) defined, it is found that an overburden displacement FoS against the onset of mass instability to surface is given by $150/20 = 7.5$. This is a substantial FoS against overburden instability being initiated in conjunction with the proposed EIS mine layout and allows for significant parameter variation in terms of horizontal stress levels and overburden lithology between that at Hume and the various case histories that were used in the determination of the 150 mm minimum displacement criterion.

5.0 WEATHERING OF THE HAWKESBURY SANDSTONE (HBSS)

Due to the Wianamatta Shale being absent in some parts of the western extent of the proposed mining area, the HBSS unit that dominates the overburden from a lithological perspective, contains varying amounts of natural weathering. This was known when the proposed EIS mine layout was compiled but has been raised by the independent review as requiring further details to be provided. Hume Coal have carried out a geological review of the available borehole information in affected areas, which forms the primary input to the geotechnical discussion herein.

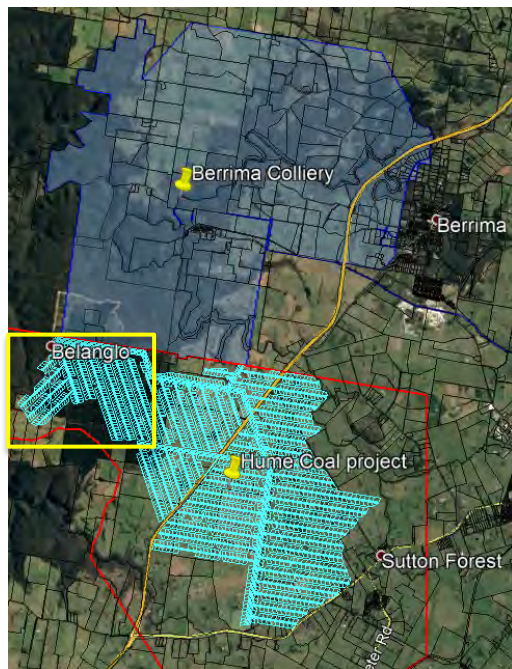


FIGURE 47. Location of Known Weathered HBSS Area



FIGURE 48. Weathered HBSS Area and Associated Surface Boreholes

Figures 47 and 48 locate both the area of weathered HBSS within the overall proposed mine layout and the surface boreholes that have been used to evaluate its significance.

Of the 18 cored holes within the defined area, only 7 were fully cored through the HBSS, these having been used to evaluate the full effect of weathering on the structural competency of the HBSS. Of the core recovered from these surface boreholes, 79% is classified as being unaffected by weathering (UA), faintly weathered (FW) or slightly weathered (SW). Only 3% of the core is classified as either highly

weathered (HW) or completely weathered (CW) – Figure 49. As a general rule, all of the boreholes show alternating bands of weathered and fresh rock material, such that the impact of weathering is effectively limited to the formation of relatively thin, weaker horizons within otherwise largely unweathered to only slightly weathered material.

weathering categorisation (%)

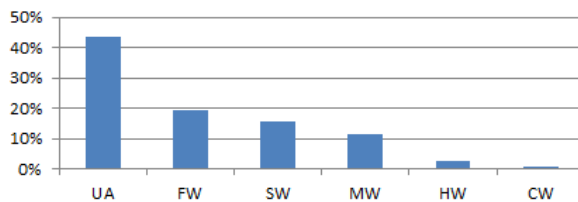


FIGURE 49. Weathering Categorisation for HBSS in Defined Area at Hume

weathering categorisation (%)

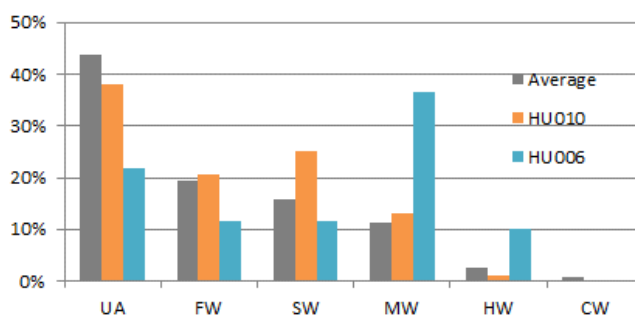


FIGURE 50. HBSS Weathering Categorisation for HU010 and HU006 As Compared to Typical Conditions in the Defined Area

Two of the surface boreholes in the defined area of weathered HBSS were selected for comparison with HBSS conditions in other parts of the mine, HU010 being close to “typical” of the area and HU006 representing what is judged to be the worst-case example of weathered HBSS in this part of the mining area. Figure 50 demonstrates the above stated borehole weathering assessments by comparing the various proportions of different levels of weathering in both boreholes with the average or typical proportions from the entire area.

HBSS SONIC DATA

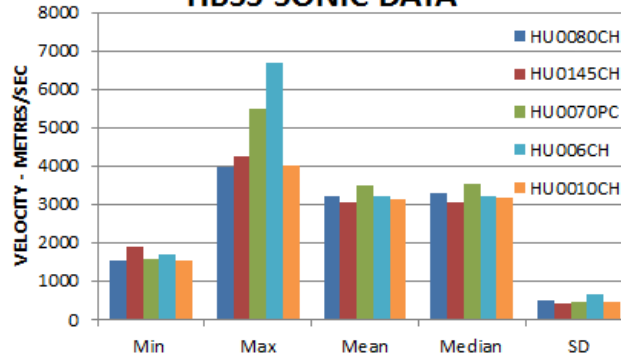


FIGURE 51. Sonic Velocity Comparison Between Weathered and Non-Weathered HBSS

As there is no engineering basis by which different degrees of weathering can be quantified in terms of their geotechnical significance to overburden stability, a direct comparison was made between HU010 and HU006 and other surface boreholes from the proposed mining area as a whole, using sonic velocity, this being established as an indicator of material strength, which if significantly compromised should stand out clearly in sonic velocity data.

Figure 51 shows the comparison for the two boreholes containing varying degrees of HBSS weathering with three other surface boreholes that are outside of the defined area of weathered HBSS and are distributed across the rest of the proposed mining area. From the sonic velocity summary data in **Figure 51**, it is evident that minimum, mean, median and standard deviation (SD) values do not show any obvious variation as a function of whether the borehole is located within the defined area of HBSS weathering or not, with the highest measured sonic velocity in the order of 6800 m/s being from the most weathered borehole, HU006.

It is concluded from the analysis conducted by Hume Coal as to the actual range of known weathered HBSS material in a number of surface boreholes from one specific part of the proposed mining area, that the overall impact on the structural competence of the HBSS is no worse than "minor" given the analyses presented herein.

In terms of the significance of this finding to the design of the mine layout in affected areas, several relevant points need to be made:

- (i) that ARMPS-HWM does not utilise the lithology of the overburden as a design variable, only the geometry of the mine layout.
- (ii) as HWM is a generally shallow cover depth mining method from either open cut excavations or around seam outcrops on hillsides, some level of near-surface overburden weathering is inevitably contained within many of the case-histories within the ARMPS-HWM database. Therefore it is to some degree included within the ARMPS-HWM design rules.
- (iii) web pillar panels of no more than 60 m width at shallow cover depth with a maximum W/H of 0.75, are likely to be influenced by more stable overburden conditions in general terms, than say a 200 m wide extraction panel at 267 m depth (i.e. also with a W/H = 0.75) due to the fact that overburden lithology does not change scale in line with changing layout geometry.
- (iv) the western area of the Hume Project is largely beneath state forest with many of the surface boreholes containing no evidence of significant groundwater in the HBSS. Therefore this area of the mine is relatively low risk in terms of any impact of mining on sub-surface aquifers, this being the primary environmental impact issue that the mine layout has been designed to mitigate.

The severity of weathering of the HBSS within a defined part of the proposed mining area has been evaluated in detail by Hume Coal and found to be minor in terms of the change on the overall structural competency of the HBS. When combined with the fact that the primary design method, ARMPS-HWM, does not rely on the nature of the overburden lithology and the HBSS in the area affected by weathering is not a significant aquifer, it is concluded that the known weathering of the HBSS does not represent a significant threat to either the integrity of the remnant mine workings or the environmental impact due to the proposed mining.

6.0 OVERALL SUMMARY

The 2D and 3D numerical modelling study conducted by Dr Keith Heasley using LaModel has confirmed the following in relation to the proposed Hume EIS mine layout:

1. That the simple 2D design analyses using ARMPS-HWM upon which the EIS layout was based, were indeed worse-case scenarios in terms of the inferred stability of the low w/h ratio web pillars and adjacent intra-panel barrier pillars as a pillar system.
2. That when credible, but conservative assumptions in relation to the nature of the overburden were utilised in the design analysis, varying levels of overburden load were re-distributed from above web pillars to the adjacent barrier pillars. This confirmed that the proposed EIS mine layouts contain a range of coal pillar types that behave as a combined pillar system in promoting global mine stability, rather than as individual pillars.
3. Predicted levels of surface subsidence (due to coal pillar compression only) were generally consistent in magnitude with those derived analytically from within the EIS impact assessment process.
4. An evaluation of remnant mine stability based on estimated critical levels of overburden lowering whereby mass instability of the overburden could be initiated as compared to predicted values, has returned FoS values in excess of 7 for the proposed mine layout.
5. The insensitivity of global mine stability to such local variations as minor geological structures within the coal seam, localised roof falls in web pillar drives and deviations in the as-formed web pillar geometries, has been demonstrated in the 3D numerical modelling by removing both single web pillars and also an entire panel of web pillars, the modelling outcomes still returning stable overall remnant mine workings.

With the 2D and 3D numerical modelling study being completed and having confirmed the general suitability of the proposed EIS mine layouts, it is concluded that the mine layout design process is essentially complete, the only remaining task being to establish an operational management plan for implementation, as was also highlighted in the EIS documentation.

7.0 REFERENCES

- Canbulat, I. (2017). **Review of the Mine Plan and the Subsidence Risks Associated with the Proposed Mine Plan – Hume Project.** Report prepared for NSW Department Of Planning And Environment, Report No. DPE/2017-1.
- Ditton, S. and Frith, R. (2003). **Influence of Overburden Lithology on Subsidence and Sub-Surface Fracturing on Groundwater.** Final Project Report. Brisbane, Queensland: ACARP Project C10023.
- Ditton, S. Sutherland, T. (2013). **Management of Subsidence at the Tasman and Abel Mines - Issues and Outcomes.** Proceedings of COAL 2013, University of Wollongong.
- Esterhuizen, G.S. Mark, C. Murphy, M. (2010). **The Ground Response Curve and Its Impact on Pillar Loading in Coal Mines.** Proceedings 3rd International Workshop on Coal Pillar Mechanics and Design. Morgantown, West Virginia. pp. 123-131.
- Esterhuizen, G.S. (2014). **Extending Empirical Evidence through Numerical Modelling in Rock Engineering Design.** The Journal of The Southern African Institute of Mining and Metallurgy, Vol. 114, October.
- Frith, R C. McKavanagh, B. (2000). **Optimisation of Longwall Mining Layouts under Massive Strata Conditions and Management of the Associated Safety and Ground Control Problems.** End of Grant Report, ACARP Project C7019.
- Frith, R. Reed, G. (2018a). **Coal Pillar Design When Considered a Reinforcement Problem Rather Than a Suspension Problem.** Proceedings of COAL 2018, University of Wollongong and AusIMM.
- Frith, R. Reed, G. (2018b). **The Limitations and Potential Design Risks When Applying Empirically-Derived Coal Pillar Strength Equations to Real-Life Mine Stability Problems.** To be published in Proceedings of 37th ICGCM, Morgantown, West Virginia.
- Galvin, J. (2016). **Ground Engineering: Principles and Practices for Underground Coal Mining.** Switzerland: Springer International Publishing, pp. 684.
- Galvin, J. (2017). **Independent Assessment: Hume Coal Project.** Report prepared for NSW Department of Planning and Environment, Report No. 1716-12/1b.
- Heasley, K. (2018). **Pillar Design Analysis Using LaModel.** Commercial consulting report to Mine Advice.
- Mark, C. Chase, F. Zipf, K. (1997). **Preventing Massive Pillar Collapses in Coal Mines.** Proceedings of the New Technology for Coal Mine Ground Control in Retreat Mining, NIOSH IC 9446, pp. 35 - 48.
- Mark, C. (2010). **Pillar Design for Deep Cover Retreat Mining: ARMPS Version 6 (2010).** 3rd International Workshop on Coal Pillar Mechanics and Design, University of West Virginia, pp. 106-122.
- Mine Advice (2016a). **Mine Design Justification Report, Hume Project.** Report to Hume Coal, Report No. HUME12/2.
- Mine Advice (2016b). **Environmental Impact Statement Subsidence Assessment.** Report to Hume Coal, Report No. EMM01/2.

McTyer, K. Sutherland, T. (2011). **The Duncan Method of Partial Pillar Extraction at Tasman Mine.** Proc. 30th Int. Conference on Ground Control in Mining, West Virginia.

Mills, K. Edwards, J. (1997). **Review of Pillar Stability in Claystone Floor Strata.** Symposium on Safety in Mines, The Role of Geology, Sydney, NSW, pp. 161-168.

Mills, K. and O'Grady, P. (1998). **Impact of Longwall Width on Overburden Behaviour.** In: Proceedings of the Coal Operators' Conference. Brisbane, Queensland: University of Wollongong.

Mills, K. (2012). **Observations of Ground Movements Within the Overburden Strata Above longwall Panels and Implications for Groundwater Impacts.** 38th Symposium on the Advances in the Study of the Sydney Basin, Coalfields Geology Council of New South Wales.

NIOSH (2012). **Analysis of Retreat Mining Pillar Stability – Highwall Mining (ARMPS-HWM).** User Manual for ARMPS-HWM software version 1.3.

Salamon, M. D. G. Oravecz, K.I. Hardman, D. (1972). **Rock Mechanics Problems Associated with Longwall Trials in South Africa.** Research Report No. 6/72 (pp. 35). Chamber of Mines of South Africa Research Organisation.

Seedsman, R. (2008). **Awaba – Understanding Soft Floors And Massive Conglomerates.** Presentation to Mine Managers Association, May 2008.

Shirley, A. Fagg, S. (2017). **Subsidence Events, Investigation and Litigation: The Need for a Forensic Approach.** Proceedings 10th Triennial Conference on Mine Subsidence.

Van Der Merwe, J. N. (2006). **Beyond Coalbrook: Critical Review of Coal Strata Control Developments in South Africa.** Proceedings of the 25th International Conference on Ground Control in Mining. Morgantown, WV: West Virginia University, pp. 335–346.

Vasundhara, Galvin, J, Hebblewhite, B. (1998). **Geomechanical Behaviour of Soft Floor Strata in Underground Coal Mines.** ACARP Report, Project C4026.

Zipf, R.K. Bhatt, S. (2004). **Analysis Of Practical Ground Control Issues In Highwall Mining.** Proceedings of 23rd ICGCM, Morgantown, West Virginia, pp. 210-219.

APPENDIX A

Copy of Frith and Reed 2018a

COAL PILLAR DESIGN WHEN CONSIDERED A REINFORCEMENT PROBLEM RATHER THAN A SUSPENSION PROBLEM

Russell Frith¹, Guy Reed

ABSTRACT: Current coal pillar design is the epitome of suspension design. In principle, this is seemingly no different from early roadway roof support design. However, for the most part, roadway roof stabilisation has progressed to reinforcement, whereby the roof strata is assisted in supporting itself. Suspension and reinforcement are fundamentally different and, importantly, lead to substantially different requirements in terms of roof support hardware characteristics and their application. This paper presents a prototype coal pillar and overburden system representation where reinforcement, rather than suspension, of the overburden is the stabilising mechanism via the action of *in situ* horizontal stresses within the overburden, the suspension problem potentially being an exception rather than the rule, as is also the case in roadway roof stability. Established principles relating to roadway roof reinforcement can potentially be applied to coal pillar design under this representation. The merit of this assertion is evaluated according to documented failed pillar cases in a range of mining applications and industries found in a series of published databases. Based on the various findings, a series of coal pillar system design considerations and suggestions for bord and pillar type mine workings are provided. This potentially allows a more flexible and informed approach to coal pillar sizing within workable mining layouts, as compared with common industry practices of a single design Factor of Safety (FoS) under defined overburden dead-loading to the exclusion of other potentially relevant overburden stabilising influences.

INTRODUCTION

The simplest model for coal pillar loading consists of an unstable overburden to the surface, known as Tributary Area Theory (TAT), overburden stability then being entirely controlled by the load-bearing ability of the coal pillars formed in the workings (Figure 1). For bord and pillar type mining design purposes, the TAT model to the surface has been and can be modified (by the application of either pressure-arch concepts or by considering the sub- or super-critical nature of the overburden at the surface) to modify pillar loading magnitudes, it is still generally true to state that the stability of coal pillars is evaluated via a defined unstable section of overburden imparting dead loads onto the coal pillars beneath. The level of confidence in the design remaining stable is then determined according to the design Factor of Safety (FoS) over and above the assumed coal pillar strength(s).

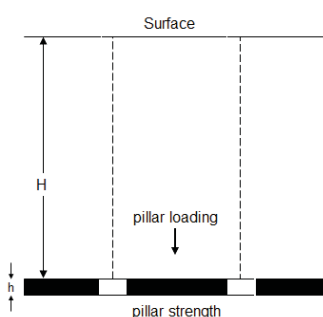
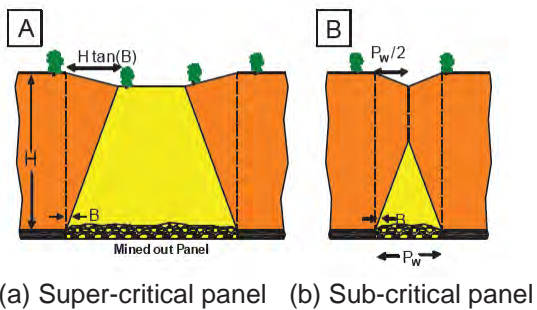


Figure 1: Tributary Area Theory (TAT) loading arrangement for coal pillars

Since the Coalbrook disaster in 1960, the basic model of full TAT to surface has been applied in empirical studies attempting to define the strength of coal pillars by back-analysing failed cases (e.g. Salamon and Munro 1967). Figure 2 shows how pillar loading can be modified

¹ Mine Advice Pty Ltd, New South Wales, Australia. Email: russell.frith@mineadvice.com Tel: +61 409 056 514

according to panel width to cover depth considerations (W/H ratio) as part of what may be termed as partial TAT [Mark *et al* 2010]. In both cases, vertical dead-loading of the overburden onto the coal pillars is the key pillar design assumption.



(a) Super-critical panel (b) Sub-critical panel

Figure 2: Abutment angle concept used to estimate loads in ARMPS [Mark *et al* 2010]

Van Der Merwe 2006 makes the following statement in relation to what occurred in the immediate aftermath of Coalbrook: “*The attention was focused on pillar strength research, very little attention initially being paid to overburden strength. This is not an unreasonable approach: if the pillars are strong enough to support the overburden, it doesn’t matter how weak the overburden is—failure cannot occur. This is especially true if the [TAT] is used to determine pillar load because TAT predicts the maximum load on the pillar*”.

The fact that this statement was made as recently as 2006, over 40 years after Coalbrook, is taken to be evidence that the TAT pillar loading model has persisted, whether it be full TAT to the surface or a modified/partial version.

At the 35th ICGCM, Reed, McTyer, and Frith 2016 posed a question, asking whether it was possible for coal pillar research to follow what had already occurred in roadway roof control research. Roadway roof control was initially founded on the belief that roadway roof support needed to be designed to hold in place an otherwise critically unstable roof mass, using suspension roof support [Figure 3(a)]. However, this was eventually superseded by the prevailing concept that roadway roof stability could be far more efficient and reliable by retaining some or all of the self-supporting ability of the roof strata via reinforcement using roof bolting and longer cables and tendons (Figure 3(b)). The reinforcing approach considers the competence of the roof mass (as given by the Coal Mine Roof Rating or CMRR for example), the horizontal stresses acting across the roof, the width of the roadway and the installed roof support in formulating design outcomes. The roadway roof stability design problem was forever changed from the simple and often far too simplistic assumption of “dead-load” suspension when the problem became one of roof reinforcement. Frith and Colwell 2011 outline details of the various problems and potential risks of continuing to apply a dead-load suspension approach to roadway roof support design in reinforcing design situations.

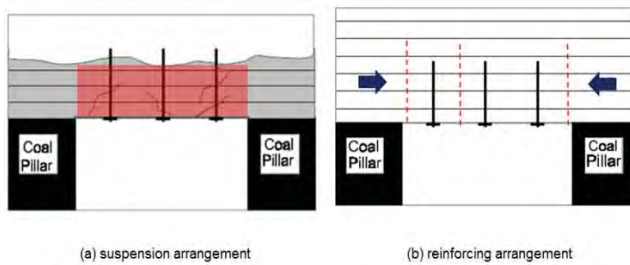


Figure 3: Schematic illustrations of suspension and reinforcing problem representations for roadway roof control

This paper debates the application of full or modified TAT dead-load pillar loading to bord and pillar coal pillar design nearly 60 years after Coalbrook. Figure 1 shows the suspension arrangement for coal pillars. The similarity with Figure 3(a) for roadway roof support is evident; the only difference being that the unstable strata mass is held in place

by roof bolts anchored into stable overlying strata, as compared to a coal pillar being founded on the floor of the roadway.

In stark contrast, Figure 4 outlines a suggested reinforcing problem representation for coal pillars similar to that shown in Figure 3(b) for the roof of a mine roadway. In the reinforcing coal pillar design representation, the horizontal stress acting within the overburden, the competence of the overburden in terms of its self-supporting ability across the panel, and the panel width are all brought into the problem representation. These are directly analogous to the horizontal stress in the roof of a roadway, the competence of the roof strata (e.g. the CMRR), and the roadway width, respectively. Each is a primary variable in the reinforcing roadway roof stability problem.

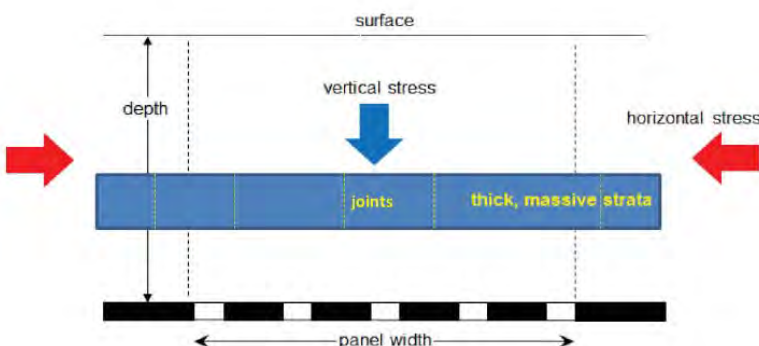


Figure 4: Schematic illustration of a reinforcing problem representation for coal pillar design

This then leads to the fundamental question as to whether, albeit with many years of hindsight, the mechanics of coal pillar design are comparable to that of reinforcing roadway roof support. Do coal pillars control the overburden through reinforcement rather than suspension? Do pillars work to allow the overburden to stabilise itself, rather than simply support the overburden?

The paper seeks to demonstrate that the overburden reinforcement scenario is the more likely answer in many instances with some specific exceptions and offers views on the implications on bord and pillar layout design involving coal pillars.

JUSTIFICATION FOR A REINFORCING APPROACH TO COAL PILLAR DESIGN

In addressing whether the coal pillar design problem is one of suspension or reinforcement, it must be determined which becomes unstable first: the overburden to surface or the pillar? This question is derived by considering suspension design for roadway roof support where by definition, the installed roof support must remain load-bearing well after the roof strata has failed and become critically unstable, a roof collapse being solely dictated by the structural state and associated load-bearing capacity of the installed roof support.

The earlier quotation from Van Der Merwe 2006 implies that as long as the overburden becomes critically unstable before a correctly designed coal pillar reaches its maximum load-bearing capacity, it does not matter how weak the overburden is at face value this makes perfect sense, but leaves one critical issue unanswered: "Will in fact the overburden become critically unstable before the coal pillar goes post-peak"?

If the answer to the question is generally "no", it must logically be concluded that the manner by which the suspension approach to pillar design as outlined in Figures 1 and/or 2, whereby an unstable amount of overburden is controlled by coal pillars prior to their peak strength being reached, is a worst, a flawed and at best, a limiting view. Therefore, how and why the overburden becomes critically unstable relative to the coal pillar becoming unstable becomes of significant interest.

Useful thought-experiments

Before presenting detailed technical arguments, it is useful to consider a number of basic “thought-experiments” whereby the significance of the horizontal stress in the overburden can be justified as a problem variable, both conceptually and numerically.

The Ground Reaction Curve (GRC) concept (Figure 5) was originally developed in the early 1960’s to assist tunnellers ensure that permanent, and often, stiff permanent tunnel linings were not damaged by excessive ground strains. This has since been applied by others to coal mining problems, such as tailgate standing support design and longwall shield design.

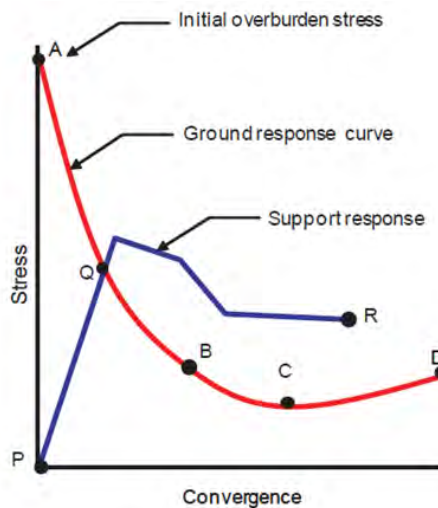


Figure 5: Generic Ground Reaction Curve (GRC) representation

Figure 5 shows that a significant element of a GRC is the installation of ground support following excavation; however in this instance it is only the ground curve that is of interest. The ground curve (ABCD) contains both a section of negative slope (ABC) whereby the strata is losing its natural stability due to increasing vertical movement and a section of positive slope (CD) whereby natural stability is effectively lost with self-weight or dead-loading then dominating the stability problem.

A series of simple thought-experiments relating to super-critical extractions (i.e. $W/H > 1$) will now be used to demonstrate the direct influence of key geotechnical parameters on initial overburden caveability. Figure 6 presents a simple situation whereby the overburden consists solely of massive sandstone to the surface with no vertical joints. Under this scenario, it is self-evident that the overburden will retain its stability across the extraction span with the ground curve rapidly reducing to zero stress (i.e. self-supporting) following extraction.

Figure 7 is geometrically the same as Figure 6 but the overburden now solely consists of laminated material, albeit still with no vertical joints. Under this scenario, the overburden initially flexes via vertical downwards movement, but eventually exceeds some undefined “critical” level of overburden movement which marks the onset of mass instability back to full overburden collapse (under tributary area loading in coal pillar design terminology).

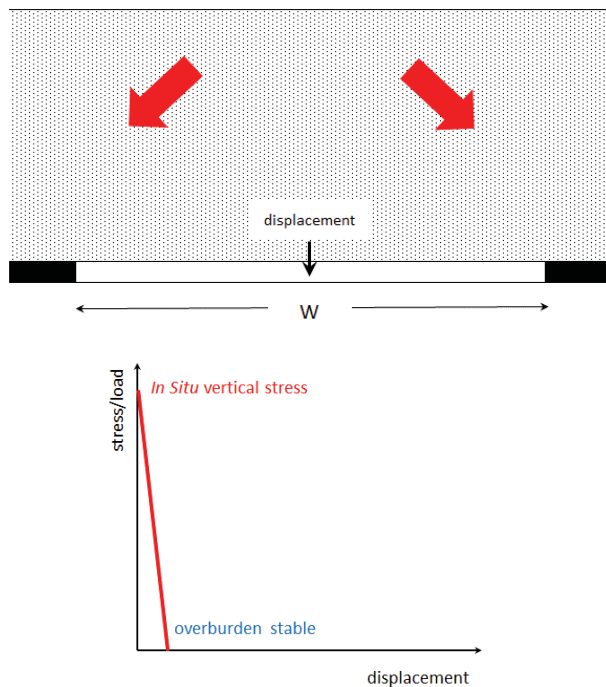


Figure 6: Thought-experiment and ground curve: massive overburden with no vertical joints

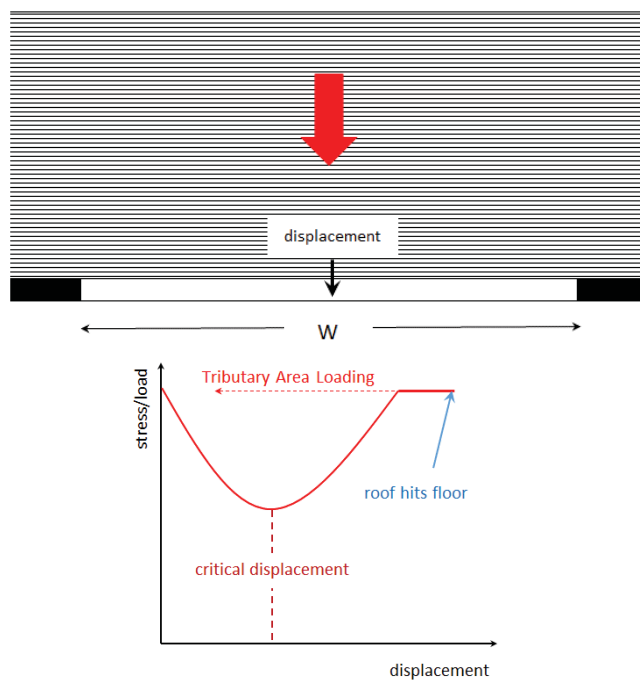


Figure 7: Thought-experiment and ground curve: Laminated overburden with no vertical joints

Figure 8 contains the massive and laminated overburden representations used in Figures 6 and 7, but introduces both vertical joints and horizontal stress.

Vertical jointing is almost always present in coal measures strata sequences (although spacings, orientations and persistence vary) and is typically characterised by zero cohesion and a friction angle that varies according to surface conditions along the joint. Under such joint conditions, no vertical shear resistance can be developed along the joint without the influence of a normal confining stress (horizontal stress in this case). Therefore irrespective of the overburden type, without the presence of horizontal stress vertical jointing results in a

ground curve as shown in Figure 9, namely the overburden is an unstable detached block from the outset.

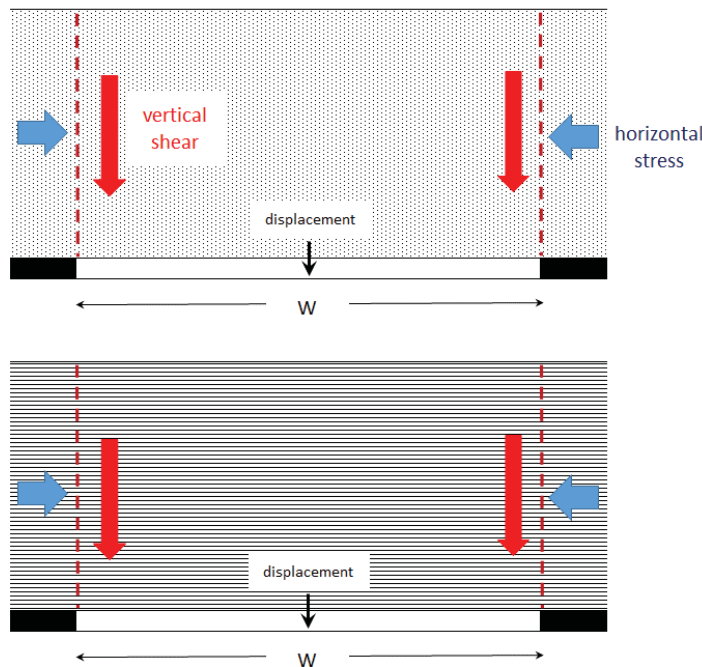


Figure 8: Thought-experiment representations: Massive and laminated overburdens including vertical joints and horizontal stress

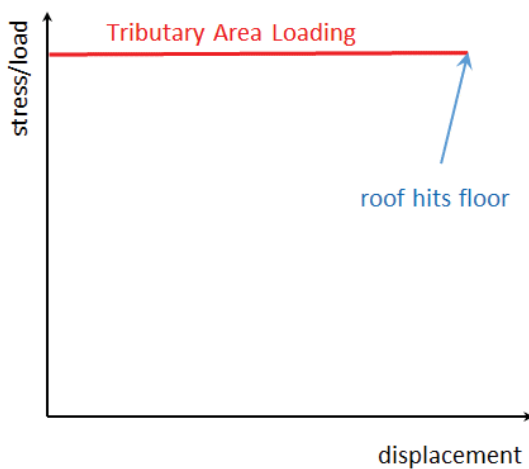


Figure 9: Ground curve: Vertical joints present without horizontal stress

Once horizontal stress is included into the representation, it allows the varying influence of overburden lithology and vertical shear along vertical joints to be combined, resulting in a range of possible ground curve outcomes as generally illustrated in Figure 10. To provide context as to what may be a significant level of horizontal stress in this regard, assuming a joint friction angle of 45° only 2.5 MPa of horizontal stress is required for limit equilibrium in terms of shear slip along vertical joints at the extremities of a 200 m wide extraction span. This is a relatively low level of horizontal stress in general coal mining terms.

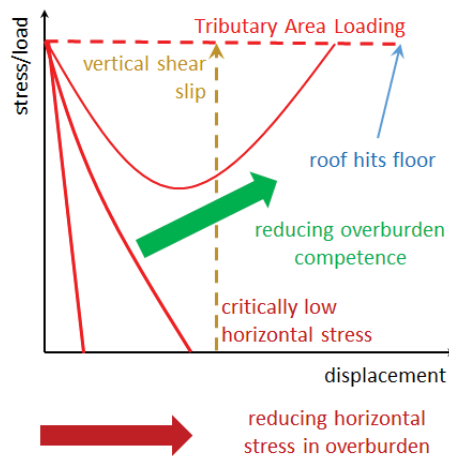


Figure 10: Varying influence of overburden lithology, vertical joints and horizontal stress on GRC's

In general terms, for any given extraction span, initial caveability is directly influenced by both the structural competence of the overburden in terms of the presence or absence of massive strata units etc. and also the level of horizontal stress acting within the overburden which defines the level of stabilising influence along vertical joints. The important point to make is that in combination they can result in two distinctly different caving mechanisms, namely:

- delamination and incremental overburden collapse whilst ever vertical joints do not undergo vertical shear slip, as opposed to;
- a "plug" type collapse of otherwise intact overburden material due to vertical shear slip along vertical joints.

The point of these thought-experiments and simple calculations is to justify that it is almost certainly overburden condition above coal pillars, which dictate their importance in maintaining the overall stability of mine workings. More to the point, the full TAT representation of Figure 1 is clearly only one possible pillar loading and overburden condition scenario and as will be now further argued, it is potentially quite uncommon for the peak-strength of the coal pillar solely controlling whether a pillar collapse (low w/h) or pillar creep (higher w/h) occurs or not.

Which generally fails first—overburden or coal pillars?

The starting point for an assessment of which is more likely to fail first - overburden or coal pillar- is again found in the (GRC) concept (Figure 5). The GRC concept was originally developed around the same time as the Coalbrook disaster to assist tunnellers to ensure that permanent, and often, stiff permanent tunnel linings were not damaged by excessive ground strains. Others have since applied this to coal mining problems, such as tailgate standing support design and longwall shield design.

Figure 5 implies that a significant element of GRC is in the installation timing of different types of ground support following excavation in that:

1. They should be installed before the surrounding strata becomes critically unstable. In reality, the surrounding strata becoming critically unstable is the onset of the suspension design problem, this being where the ground curve starts to rise with ever-increasing strata displacement.
2. They should be installed sufficiently early so that the ground and support loading curves coincide at some point. This is the point that overall equilibrium or stability is achieved.

It is suggested that applying the GRC concept to coal pillar design is a perfect analogy to attempting to protect a permanent tunnel lining from excessive ground strains. The reinforcement design problem for a permanent civil excavation for example is about

controlling ground movements within acceptable limits, particularly if a key supporting structure could be overloaded as a direct result of being installed too early. However, two major differences are apparent when applying the GRC concept to coal pillars rather than excavation support, namely:

3. The pillars are already installed at the time of excavation (i.e. their installation cannot be delayed).
4. They are inevitably pre-loaded to a pre-determined level by the action of the in situ vertical stress, therefore their maximum elastic straining ability post-mining is inevitably reduced as cover depth increases (all other factors being equal).

Defining the initiation point for overburden instability

Considering the issue of the overburden first, the relevant question is how much vertical movement is required for the overburden to become critically unstable to surface at a super-critical panel width? (See Scenario A in Figure 2). For the purpose of demonstration, a panel width range between 150 and 200 m will be considered, these generally resulting in a super-critical mining geometry at relatively shallow (<150 m depth) bord and pillar mining ($W/H > 1$).

Two sources of guidance will be used in addressing this question: (a) surface subsidence data with respect to the transition from sub-critical to super-critical surface behaviour (as illustrated in Figure 2), and (b) overburden extensometry data relating to measured overburden movements following the extraction of longwall panels in the same panel width range.

Figure 11 shows the standard S_{max}/T vs W/H representation for a series of varying width longwall panels in the Newcastle Coalfield, the cover depth ranging between 70 and 150 m [Ditton and Frith 2003]. This is also a common bord and pillar mining cover depth range. The data indicates that the onset of full overburden instability and associated collapse at the surface commences at an S_{max}/T value of around 0.1, the mid-point of the transition to super-critical being 0.25 to 0.3, and full collapse at surface at a value in the order of 0.5. For an assumed mining height of 2 m, these represent vertical overburden movements at the surface of 200, 600, and 1000 mm respectively. In other words, overburden collapse at the surface does not typically commence under this scenario before 200 mm of vertical movement and is only reliably complete by 1000 mm. It is accepted that these values change according to varying extraction height and may also be influenced by overburden characteristics and goaf bulking behind a longwall. However, they are a useful starting point for this discussion.

Also of interest is the amount of vertical movement in the immediate overburden above the mine workings that is required to initiate overburden collapse across the full panel width, this section of strata directly interacting with the coal pillars that are left in place.

Figure 12 shows overburden movement isopachs in vertical section behind a longwall face as a function of both distance into the overburden above the working horizon and distance behind the face [Mills and O'Grady 1998]. While the figures themselves are not particularly clear, statements from the paper are worth re-quoting herein.

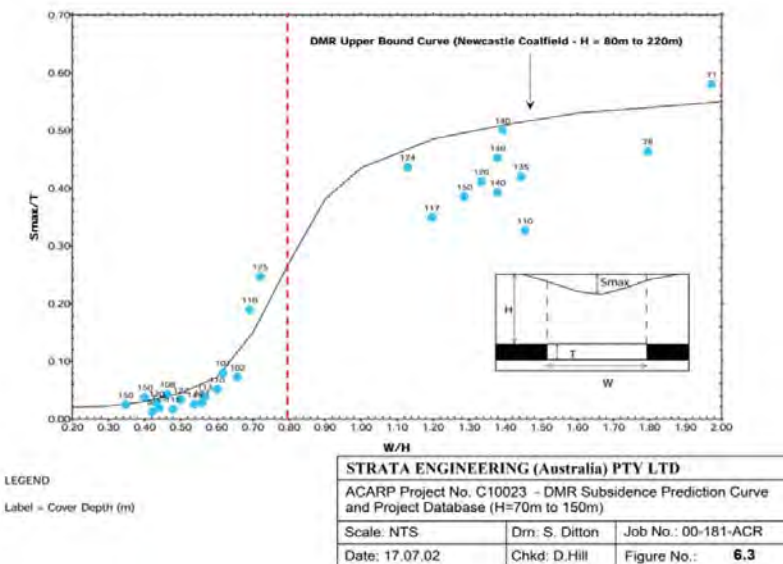


Figure 11: Measured S_{max} values analysed according to extraction height (T), panel width (W) and cover depth (H) for depths ranging from 70 to 150 m [Ditton and Frith 2003]

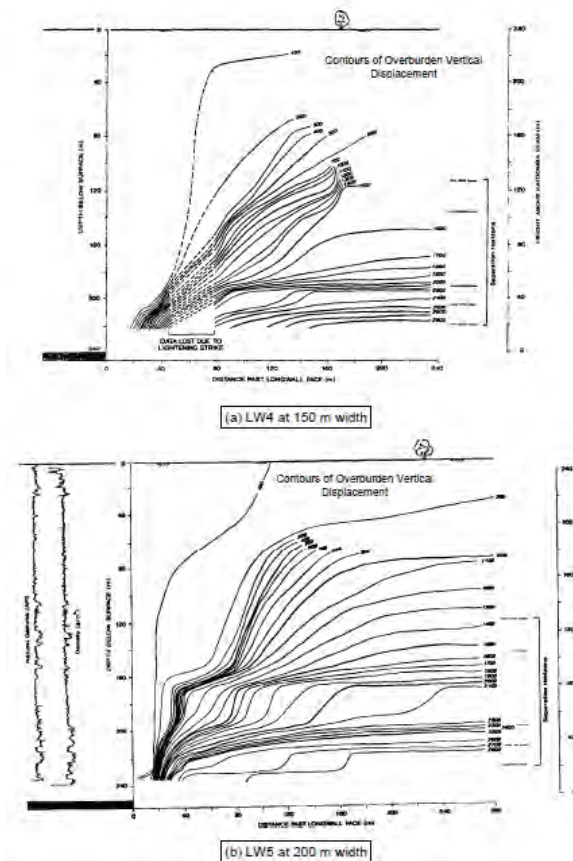


Figure 12: Surface extensometry data, LW's 4 and 5, Clarence colliery [Mills and O'Grady 1998]

The following is in relation to Figure 12(a) for a 150-m-wide longwall panel: "the 200 mm contour represents the line below which, downward movements accelerate rapidly. The transition between relatively small displacements (<200 mm) and much larger displacements occurs within a relatively narrow zone."

Regarding Figure 12(b), Mills and O'Grady (1998) state that for a 200 m wide longwall panel: "immediately below the 200 mm contour, the rate of ground separation increases rapidly as indicated by the close spacing of the 500 mm and 1 m contours".

In both instances, Mills and O'Grady (1998) are seemingly stating that the onset of rapid overburden movement following longwall extraction occurs at an overburden displacement magnitude in the order of 200 mm.

Independent and fundamentally different data sets relating to instability at the surface and within the overburden following longwall extraction, may cause minimum overburden movements prior to the onset of full overburden collapse in the order of 200 mm for panel widths in the range 150 to 200 m. This is the first requirement in determining whether the coal pillar or the overburden fails first when coal pillars are left in place between stable barriers.

Condition of coal pillar at peak loading

In terms of the coal pillar, the relevant consideration is the vertical compression at the point that it reaches its maximum or peak load-bearing ability, this being commonly termed as "pillar strength". Figure 13 provides stress-strain curves relating to the laboratory testing of coal samples according to varying w/h ratio [Das 1986]. From this data, it is estimated that for a w/h range of 1 to approximately 5, the vertical strain at peak-loading varies from 1% to 2%. Extrapolating this to a coal pillar scale means that for a 2 m high pillar, the total vertical compression at peak loading varies between 20 and 40 mm. However, as discussed by Galvin, caution needs to be used when applying laboratory test data to *in situ* pillar behaviour; therefore, some form of *in situ* coal pillar testing data would be valuable to provide real-world insight into this issue

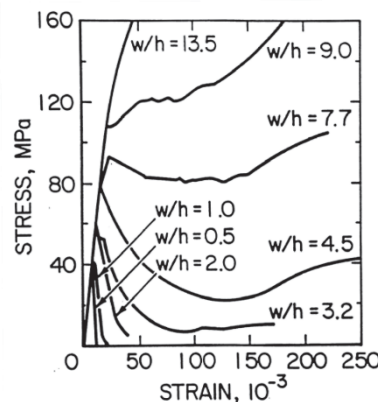


Figure 13: Stress-strain behaviour of coal for varying width to height (w/h) ratio [Das 1986]

Figures 14 and 15 contain stress-strain data for larger coal "pillars" tested *in situ* as opposed to laboratory specimens [Van Heerden 1975]. In the two cases for two different w/h ratios, the compressive strain at peak-loading is $<1\%$ (i.e. 10×10^{-3}). In the case of a 2 m high coal pillar this equates to <20 mm of vertical compression at its maximum strength.

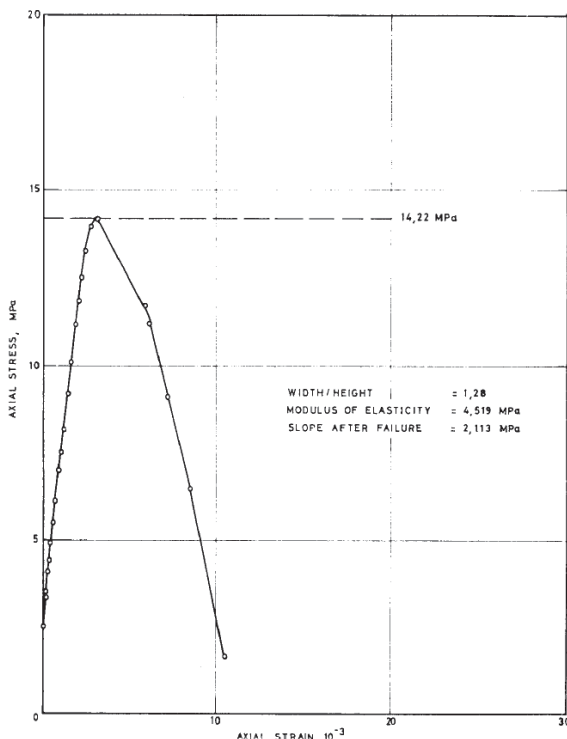


Figure 14: Stress-strain behaviour for in situ coal pillar testing [Van Heerden 1975]

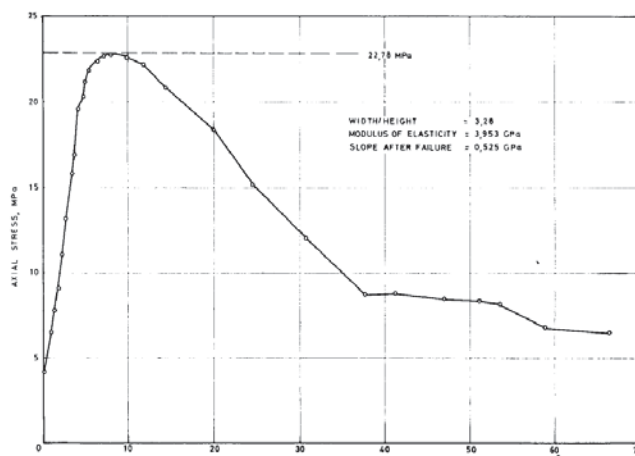


Figure 15: Stress-strain behaviour for in situ coal pillar testing [Van Heerden 1975]

Figure 16 relates to a different method of *in situ* coal pillar testing. In this test, an approximately 1.8 m-high coal pillar is incrementally reduced in size and the applied pillar load and vertical compression responses are measured [Skelly *et al* 1975]. Recognising that the coal pillar is pre-stressed before it is reduced in size due to the *in situ* pre-mining vertical stress, an additional 2.54 mm of compression is recorded when taking the pillar from its *in situ* loading under the action of vertical stress 16.5 MPa of (2,400 psi), to its measured peak load of around 2900 psi (20 MPa). This equates to 2.54 mm of pillar compression for a 3.5 MPa (500 psi) increase in average pillar stress. Extrapolating this value to the complete elastic stress-strain range of the pillar from 0 to 20 MPa, results in total vertical compression of the pillar at peak loading of only 14.7 mm for the 1.8 m high pillar in the test case. For a 2 m-high pillar, this would increase to 16 mm, all other factors being equal.

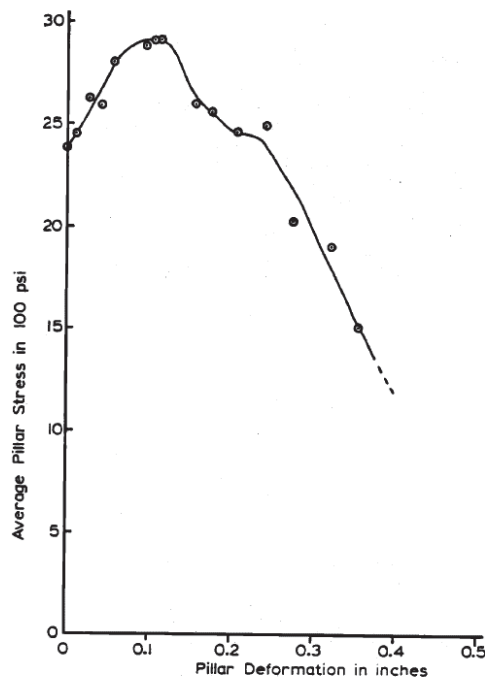


Figure 16: Stress-deformation curve for test pillar "a" [Skelly et al 1975]

In situ coal pillar testing data from both South Africa and the USA indicate that for a 2 m high coal pillar, vertical pillar compression at peak-loading or maximum strength would be in the order of 20 mm. This is of similar magnitude as that inferred from the Das 1986 lab-testing data of 20 to 40 mm, according to a varying *w/h* ratio of between 1 and up to 5.

So which fails first—overburden or coal pillar?

Even making an allowance for the elastic compression of an immediate stone roof and floor above and below coal pillars, the preceding general analysis of overburden movements above total extraction panels and vertical strains in coal at peak-strength, leads to the inevitable conclusion that it is more likely than not that coal pillars will exceed their peak strength (and so "fail") before the overburden becomes in a critically unstable state to the surface.

This general conclusion is well justified in the various reports relating to Coalbrook in that (a) surface subsidence cracks above the area of the mine that was eventually to collapse so catastrophically, were identified days before the major event (NB subsidence cracks at surface generally require hundreds of millimetres of vertical subsidence before they appear, not tens of mm), (b) various coal pillars were observed to be spalling and splitting well prior to the main collapse (which is inconsistent with the retention of an elastic pre-peak pillar state leading up to the collapse) and (c) micro-seismic events were heard and measured as part of the main collapse, a common source of micro-seismic and indeed seismic events being stress-driven shear slip along pre-existing planes of weakness (such as the vertical joints in Figure 8), rather than the compressive failure of soft material as in a coal pillar.

One case example on its own obviously does not prove that all failed pillar cases in the various coal industry databases conform to this same scenario. Weaker and less stiff roof and/or floor measures, thick soft clay bands within the coal seam, very low horizontal stress environments in mountainous terrain or in proximity to highwalls and/or the presence of mid-angled structures in the overburden above a collapsed area, would all tend to change the conditions at the point of overburden collapse towards one whereby the coal pillar may be the controlling influence, as analysed previously. However, the various observations leading up to the Coalbrook collapse certainly support the idea that the overburden failing before the coal pillar can be eliminated as a universal truth. If nothing else, this means that any coal pillar strength equations that have been empirically-derived from databases of failed pillar cases,

will only reasonably reflect the intact strength of coal pillars if all or the majority of the failed cases occurred as a direct and immediate consequence of the coal pillars first exceeding their intact strength, the Coalbrook collapse now being strongly argued to not fit this description.

This finding, in particular as it relates to Coalbrook, is seemingly quite profound and raises a question-mark as to the reliability of almost 60 years of coal pillar strength research that has utilised failed pillar cases in back-calculating intact coal pillar strengths at failure and so developing coal pillar strength equations. However, it is only based on one technical argument, namely that coal pillars can reach their peak-loading condition well before the overburden has displaced sufficiently to become critically unstable. Therefore, further supporting evidence has been sought.

Other real-world examples worth considering further

Three significant case history examples have been identified that either (1) seemingly further back the assertion that the rigid application of full TAT loading to surface (Figure 1) when back-analysing failed pillar cases contains limitations that may only manifest when the resultant pillar strength equations are used in practice, and/or (2) indicate that a key piece of the design problem has been overlooked and that we may do well to now include it. Figure 17 shows the combined Australian and South African databases of failed coal pillars, including a series of Highwall Mining (HWM) pillar failures that were back-analysed using the previously-developed pillar strength equations of the University of New South Wales Pillar Design Procedure (UNSW PDP) [Hill 2005]. The area of interest (marked by a red ellipse) contains a number of HWM pillar failures with UNSW PDP FoS values ranging from 1.7 to as high as 2.4, these all being greater than, significantly so in most cases, the range of FoS values for the failed non-HWM cases that define the majority of the two databases.

It could perhaps be argued that these HWM pillar failures are due to low pillar w/h ratios having reduced pillar strengths as compared to the predicted strengths, due to the influence of localised geological structures. In fact, this influence is commonly argued by others, although at first glance it isn't immediately obvious from Figure 17, as there are a number of non-HWM failed cases with similarly low w/h ratios (which would have also been square/rectangular underground pillars rather than continuous HWM pillars) that do not generally mirror those of HWM. Perhaps the HWM pillar failures that stand out from the general underground mining examples have a different causation entirely.

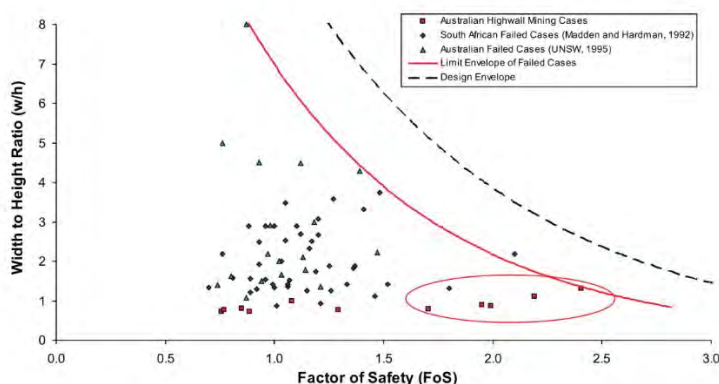


Figure 17: Database of pillar collapses—width to height ratio vs. FoS [Hill 2005]

Forming coal pillars next to an open cut highwall represents a specific and not particularly common scenario, whereby the self-supporting ability and stiffness of the overburden above the pillars is inevitably reduced due to the presence of a zero friction vertical discontinuity in the overburden with no horizontal stress acting across it, namely the highwall. If, as previously argued via the various thought-experiments and calculations, the overburden needs to overcome the stabilising influence of horizontal stress acting across vertical joints before it enters a critically unstable state, then being located adjacent to an open cut highwall is an obvious situation where this influence would logically be reduced as compared to further

into an underground mine. In other words, the HWM situation may more closely resemble that of Figure 1, as compared to that of underground mining. Therefore, if the UNSW PDP pillar strength equations as used by Hill 2005 contain a limitation that is linked back to their derivation, its presence and significance should logically show up in any case examples that significantly deviate from the majority within the founding database. To have five failed examples in the FoS range of 1.7 to 2.4 in such a small database as that of Australian HWM, strongly suggests that the coal pillar strength equations used in determining the FoS values in Figure 17, are substantially overstating coal pillar strength. In this regard, it is interesting to note that UNSW are currently undertaking a joint project with CSIRO to re-evaluate their pillar strength equations for low-width HWM pillars, presumably as a direct result of the Australian and other failed HWM examples.

The other notable aspect of Figure 17 is that, for w/h values >4 to 4.5, there is only one outlier collapsed failed case at a w/h of almost 8, which, according to Colwell 2010, is more likely to be a floor failure than a core pillar collapse based on his personal knowledge of the case history. As such, its relevance in terms of the discussion on whether the pillar or overburden fails first is judged to be minimal, as without definitive knowledge on the type of instability involved it cannot be included. The same trend is also evident in the ARMPS failed pillar database (Figure 18), where, in terms of core pillar failures there are no examples with w/h values >3 [NIOSH]. This leads the discussion into pillar squeezes or creeps and what the relevant case histories might be able to tell us about the general validity of pillar strength equations at higher w/h ratios.

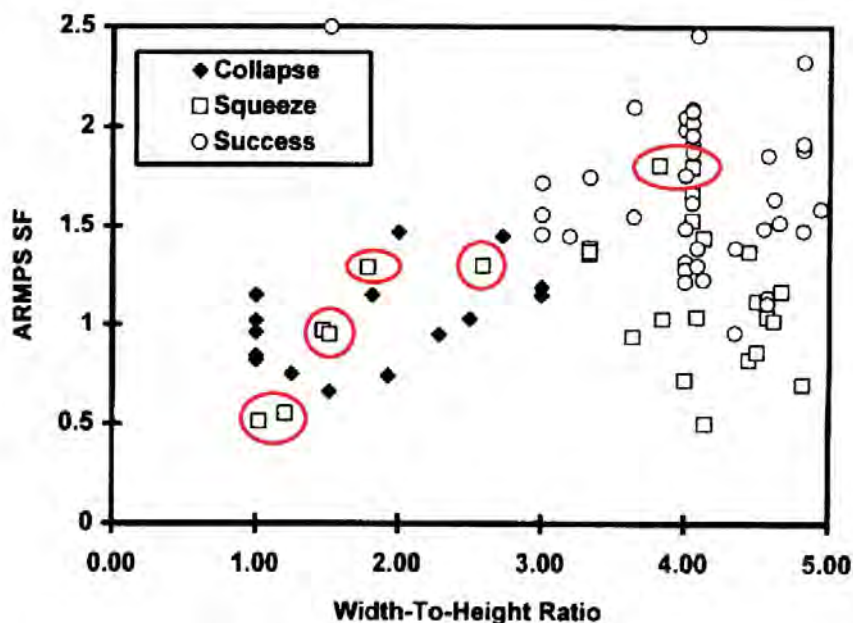


Figure 18: ARMPS SF vs pillar w/h ratio for pillar collapses and other case histories [NIOSH]

Ditton and Frith 2003 analysed the relationship between surface settlements above longwall chain pillars (under Double Goaf (DG) loading with extraction panels on both sides) that could not be explained by the superimposition of the two individual subsidence troughs on either side of the chain pillar. The resulting levels of surface lowering were plotted against the FoS of the chain pillar under DG loading as determined using the UNSW PDP pillar strength equation for w/h values >5. A relationship between the two parameters was found as shown in Figure 19.

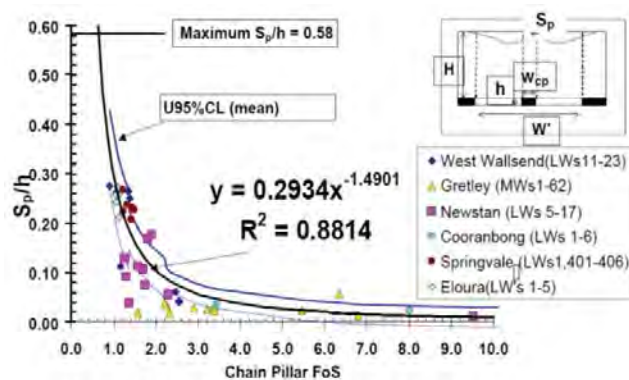


Figure 19. Surface lowering above a chain pillar under DG loading v chain pillar FoS using UNSW PDP strength equations [Ditton and Frith 2003]

This pillar loading scenario is probably quite unique in that due to the presence of extracted longwall panels on either side of the chain pillars, any stabilising influence of horizontal stress within the overburden should have been substantially reduced as compared to standing coal pillars in a bord and pillar type layout. Despite the extreme extraction geometry on either side of the pillars as compared to mine roadways, this scenario may in fact be more consistent with that of full TAT pillar loading and so provide further interesting insights. Surface lowering in above a chain pillar with longwall goaf on both sides is inevitably also influenced by the compression of the roof and floor strata, as well as that of the chain pillar itself. However, as the chain pillar controls the vertical stresses that are being applied to both the roof and floor strata, and as the coal has a Young's Modulus that is generally substantially lower than that of stone, it is perhaps not unreasonable to examine the problem, at least in the initial instance, using this data set.

What is most interesting is that the general relationship in Figure 19 indicates that the magnitude of surface lowering starts to exponentially increase for chain pillar FoS values below the range of 2 to 2.5. The chain pillars in this database are all of a high w/h ratio as a result of Australian longwall mining practice, therefore coal pillar collapse via failure of the pillar core cannot be attributed as the cause. Therefore, for the onset of what appears to be non-elastic chain pillar compression effects at FoS values in the range of 2 to 2.5, one can infer that the pillar strength equations being used may be significantly overstating the intact or elastic peak-strength of the coal pillar. This is essentially no different from what has been concluded in relation to the Australian HWM cases in Figure 17.

Having analysed two different Australian databases that contain what appear to be anomalous pillar stability outcomes with respect to either pillar strength, there is perhaps a credible argument that the pillar strength equations used in both examples tend to overestimate the true intact strength of coal pillars across a wide range of w/h ratios.

Where all of this ultimately leads to is the statement that mine layout design for bord and pillar type mining may benefit by dispensing with the idea that the overburden can be stabilised at a prescribed level of design confidence by simply assigning an FoS (or SF) to the coal pillars in isolation from the natural stability of the overburden. Furthermore, if coal pillars do indeed commonly exceed their peak strength well before the overburden becomes critically unstable, their role in preventing overburden collapse cannot be linked to their peak strength, nor therefore by definition, the traditional pillar design FoS of pillar strength/pillar load. In other words, coal pillar FoS under vertical loading may be no more than a useful surrogate for some other, more relevant consideration.

This leads to the inevitable question as to how else can coal pillars act to stabilise the overburden above either bord and pillar or partial extraction mine layouts, whereby retaining overburden stability during and post-mining is almost always the critical layout design requirement? The only credible possibility is that of overburden "reinforcement" with the coal pillars assisting the overburden support itself; in the same way that reinforcing roof support

acts to assist the roof strata above a mine roadway to support itself. This however is another topic for another time.

Another quick look at Coalbrook

Returning to Coalbrook, it is interesting to re-consider the sequence of events leading up to the disaster as outlined by Van Der Merwe 2006. Two comments, in particular, are intriguing:

1. The main collapse on January 21, 1960, was preceded by a smaller collapse on December 28, 1959, in an experimental area where top coaling had been undertaken.
2. Mine management concluded, incorrectly as it turned out, that "the weight had come off" following the first two collapses on January 21, based on the occurrence of surface subsidence. They therefore assumed that the remaining areas were safe.

If one applies the full TAT pillar loading model shown in Figure 1 it is difficult to understand how such a large area of inadequately sized coal pillars (as evidence by their eventual collapse) could stand over years without incident, yet a pillar collapse in one, small area of only 6 hectares, triggered at least three major collapses in rapid succession totalling over 324 hectares, less than 1 month later. However, if one applies the overburden reinforcement model shown in Figure 4, the focus becomes one of overburden and coal pillars working in tandem to retain horizontal stress within the overburden. With this model in mind, the events at Coalbrook can be explained quite differently.

The smaller pillar collapse in December 1959 within the trial area of top coaling, would have inevitably caused a substantial reduction in horizontal stress within the overburden above nearby surrounding mine workings that were still standing. Similar to high magnitude guttering or cutter roof in the roof of a mine roadway, with the stabilising contribution of horizontal stress being lost above part of the overall pillar system remote from any barriers, the stability of the entire overburden would have inevitably been put at risk. As it turned out, a series of major collapses occurred not long afterwards.

It is interesting to dwell on the coal pillar strength research that occurred in South Africa following Coalbrook. The most intriguing issue are the numerous changes made to coal pillar strength equations as other collapsed cases have been considered from different coalfields. Currently this process is still ongoing, with new formulae being developed in response to new pillar failures. It is still continuing in Australia today with the UNSW highwall mining pillar strength formula [Mo *et al* 2017]. Therefore, it could perhaps be argued that the process has now got to a point where selecting the appropriate pillar strength equation for design purposes is as much engineering judgement as assigning representative values to any other geotechnical parameter. This is hardly acceptable in a mine design discipline that carries the safety and business consequences associated with coal pillar failures.

With this in mind, it is instructive to further reflect on the coal pillar strengths equation developed after Coalbrook. Equation 1 is based on the in situ testing of large coal specimens with no direct link to failed cases and/or the assumption of full TAT [Bieniawski 1968] and it provides lower pillar strength values as compared with the statistically-derived Equation 2 and those of the UNSW PDP which use the assumption of full TAT as per Figure 1. However Equation 3 is the recently published strength equation for highwall mining coal pillars [Mo *et al* 2017], highwall mining being one scenario whereby the stabilising influence of horizontal stress on the overburden can logically be minimised, which is very close numerically to that of Equation 1.

$$\sigma_p = 2.76 + 1.52 w/h \quad (1)$$

$$\sigma_p = 7.176 (w^{0.46}/h^{0.66}) \quad (2)$$

$$\sigma_p = 4.66 (0.56 + 0.44 w/h) \text{ or } 2.61 + 2.05 w/h \quad (3)$$

The conundrum that emanates from Equations (2) and (3) is that they suggest that a square pillar with a w/h of say 2 [Equation 2] is actually stronger than a long strip pillar as used in

highwall mining [Equation 3]. This does not make logical sense, and so raises a very significant question regarding pillar strength determination and assignment during design for industry to address. In hindsight, perhaps coal pillar strength research should have ceased with the Bieniawski equation from 1968 [Equation 1] based on the in situ testing of coal, rather than becoming an on-going statistical battle to develop new and supposedly "improved" pillar strength equations from failed cases databases, that in reality may provide no more than a slightly better answer to what may commonly be the wrong problem and at times, can be misleading.

While this did not occur in 1968 for obvious and understandable reasons, industry might be wise to focus more intently on other relevant pillar design, or more correctly, "overburden stability" design parameters, as outlined herein and in Reed, McTyer, and Frith 2016.

The final question Van Der Merwe 2006 poses relates to why a section of similarly sized coal pillars at Coalbrook that were directly adjoined to the large collapsed area did not similarly collapse (Figure 20). He offers that the only possible reason is that as the span across the pillars was reduced as compared to the main collapse area; the collapse did not propagate into this area. However, he also makes the following statement: *"the fact that those pillars did not also fail cannot be explained by either the pillar safety factors or the presence of the dolerite sill based on current understanding. Clearly, a better understanding of the overburden stability is required. Had the overburden failed, then the pillars could not have survived, but current knowledge does not offer a method to evaluate the role of the overburden. For the time being, this question cannot be answered".*

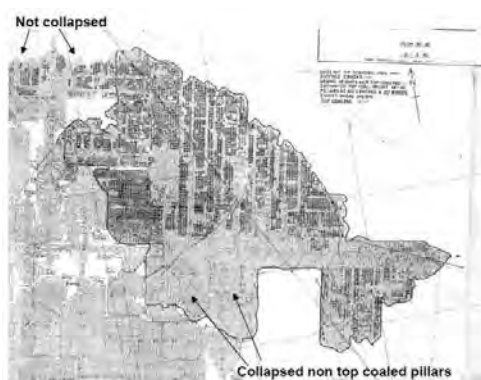


Figure 20: Details of the collapsed and non-collapsed areas at Coalbrook [Van Der Merwe 2006]

If the coal pillars in this un-collapsed area were of insufficient strength to prevent a collapse and the panel width was super-critical, even with the overburden containing a thick dolerite sill, and therefore was critically unstable to surface without the assistance of the coal pillars, only one credible possibility is seemingly left to explain why the area remained stable despite the absence of a barrier pillar between the collapsed area. Namely, the interaction between the coal pillars and the overburden maintained levels of horizontal stress within the overburden that provided a significant and critical contribution to overburden stability in addition to that of the coal pillars themselves, thereby preventing the overburden collapse.

In this regard, it is interesting to consider whether the alignment of the major horizontal stress may have coincided with the minimum span or width across the mined-out un-collapsed area. When reviewing the role of horizontal stress in South African coal mining, Frith 2002 found that the most predominant alignment of the major horizontal stress was closer to NS than EW based on observations and measurements at a number of underground mines.

Referring again to Figure 20, an alignment of the major horizontal stress east of north would closely align with the minimum span across the stable mined-out area. This combination logically represents the most stable possible overburden condition, as higher amounts of horizontal stress would need to be dissipated before the overburden could collapse via vertical shear at the extremities of the span.

Accepting the comments and judgements of Van Der Merwe 2006 as being essentially correct, this one small area that remained stable both during and after the Coalbrook collapse, conclusively proves that bord and pillar coal pillar stability problems cannot and should not be uniquely defined by full or even partial TAT representations, one exception to the rule potentially being sufficient to disprove the rule.

Decades later, it seems that the 1960 Coalbrook disaster may still provide us with valuable lessons if we are prepared to view the problem through a different lens.

Implications to mine planning, layout design, and future research

The final section of this paper considers, in general terms, the implications to future mine layout design as a result of these findings. Is there any benefit in undertaking research in order to overcome any of the limitations that are now seemingly inherent, to a varying extent, in our current bord and pillar type pillar design approaches?

The short-term answer to this question is probably “no”. Major coal mining research institutions around the world that would have the resources to do the work are now largely absent from industry. It is also the case that the statistical approach to determining coal pillar strength equations has fortuitously, if perhaps unknowingly, compensated to some degree for some of the limitations by providing statistically-derived recommendations on what FoS or SF to apply in certain mining circumstances, irrespective of how accurate or inaccurate the coal pillar strength equations that evolved from the database may happen to be.

Nonetheless, should the nature of the pillar-loading scenario differ substantially from the majority of failed cases within a database (as per the Australian HWM and longwall chain pillar compression examples herein), the mine designer needs to be aware of this to ensure that the overall layout design contains suitable measures to compensate for any threats to mine or surface stability resulting from pillar strength equations over-estimating the true intact peak strength of the coal pillars. This frames the layout design problem as one of engineering adequate overburden rather than solely coal pillar stability and considers the coal pillars as one of several component in that problem.

Given that the paper has concluded that overburden reinforcement may be generally more appropriate for coal pillar design in non-caving mining scenarios such as bord and pillar and partial extraction, some historical context is required to explain why this may not have been realised much earlier:

1. In the aftermath of the Coalbrook tragedy, the need to develop credible pillar design methodologies to prevent a recurrence would have been enormous, both technically and politically. Spending many years undertaking research studies to generate all of the various geotechnical insights that the industry is incredibly fortunate to have today, would have been prohibitive and unimaginable. There was a need to provide a reliable solution relatively quickly. In that context, the researchers at that time and since should be recognised and congratulated for their achievements both now and into the future.
2. At the time of Coalbrook in 1960, the impact of horizontal stress in coal mine strata control was barely recognised, let alone proven and accepted. In fact, a Safety in Mines Research Advisory Committee research project came about in the early 2000's as the role of horizontal stress in South African coal mine roadway roof control was still subject to industry debate at that time.
3. The insights in this paper have only come about as a result of nearly 60 years of international coal mine research and publications based on documented mining experiences—none of which were available in 1960.

The development of coal mine strata control knowledge and principles has been an on-going work-in-progress internationally for well over a century, but was undoubtedly accelerated after 1960 as a direct consequence of the Coalbrook disaster. Inevitably, as more mining experience-based research work is conducted and published, more engineers and scientists are exposed to real-world problems, rather than laboratory or computer-based simulations.

From time to time, significant realisations will inevitably emerge that challenge our views. This may be one such time. As a fraternity the question we need to consider is are we prepared to embrace a changing understanding of a problem and steer the ongoing search for improved knowledge in different directions as a direct consequence? Or conversely, do we prefer to stoically defend previous understandings, despite credible arguments that may render them incomplete, on the basis that it is perhaps more important to preserve the integrity of the past than look to the future with a new vision?

REFERENCES

- Bieniawski Z T. *The effect of specimen size on compressive strength of coal*. International Journal of Rock Mechanics and Mining Sciences and Geomechanical Abstracts 1968;5(4):325–335.
- Colwell M, 2010. *Pillar design procedures and research methodologies—Can there or should there be a unified approach?* In: Proceedings of the Second Australasian Ground Control in Mining. Sydney, Australia: AusIMM, The Minerals Institute; pp67–77.
- Frith R, 2002. *Survey of horizontal stresses in coal mines from available measurements and mapping*. Final Report. SIMRAC Project COL802.
- Das M, 1986. *Influence of width/height ratio on post-failure behaviour of coal*. International Journal of Mining and Geological Engineering 1986;4(1): 79–87.
- Ditton S, Frith R, 2003. *Influence of overburden lithology on subsidence and sub-surface fracturing on groundwater*. Final Project Report. Brisbane, Queensland: ACARP Project C10023.
- Frith R, Colwell M, 2011. *Why dead load suspension design for roadway roof support is fundamentally flawed within a pro-active strata management system*. In Proceedings of the 30th International Conference on Ground Control in Mining. Morgantown; WV: West Virginia University.
- Galvin, J, 2016. *Ground engineering: Principles and practices for underground coal mining*. Switzerland: Springer International Publishing; pp684.
- Hill, D, 2005. *Coal pillar design criteria for surface protection*. In Proceedings of the Coal Operators' Conference. Brisbane, Queensland: University of Wollongong.
- Hoek, E, Brown, E,T, 1980. Underground excavations in rock. IMM, London.
- Mark, C, Gauna, M, Cybulski, J, Carabin, G, 2010. *Application of ARMPs (version 6) to practical pillar design problems*. In Proceedings of the 30th International Conference on Ground Control in Mining. Morgantown, WV: West Virginia University; pp10.
- Mills, K, O'Grady, P, 1998. *Impact of longwall width on overburden behaviour*. In Proceedings of the Coal Operators' Conference. University of Wollongong.
- Mo, S, Canbulat, I, Zhang, C, Oh, J, Shen, B, Hagan, P, 2017. *Numerical investigation into the effect of backfilling on coal pillar strength in highwall mining*. International Journal of Mining Science and Technology.
- NIOSH.ARMPs-Analysis of Retreat Mining Pillar Stability. Version 6.2.02. <https://www.cdc.gov/niosh/mining/works/coversheet1813.html>; 201
- Reed, G, McTyer, K, Frith, R 2016. *An assessment of coal pillar system stability criteria based on a mechanistic evaluation of the interaction between coal pillars and the overburden*. International Journal of Mining Science and Technology; 27(1): pp9–15.
- Salamon, M D G, Munro, A H, 1967. *A study of the strength of coal pillars*. Journal of the Southern African Institute of Mining and Metallurgy 1967;68:56–67.
- Skelly, W A, Wolgamott, J, Wang, F D, 1976. *Coal mine pillar strength and deformation prediction through laboratory sample testing*. In Proceedings of the 18th U.S. Symposium on Rock Mechanics. Alexandria, VA: American Rock Mechanics Association; 1976.
- University of New South Wales. Graduate diploma in coal mine strata control. Course Notes; 2010.
- Van Der Merwe, J N, 2006. *Beyond Coalbrook: Critical review of coal strata control developments in South Africa*. In Proceedings of the 25th International Conference on Ground Control in Mining. Morgantown, WV: West Virginia University; pp335–346.
- Van Heerden, W L 1975. *In situ complete stress strain characteristics of large coal specimens*. Journal of the South African Institute of Mining and Metallurgy;207–217.

APPENDIX B

Copy of Frith and Reed 2018b

The Limitations and Potential Design Risks When Applying Empirically-Derived Coal Pillar Strength Equations to Real-Life Mine Stability Problems

Russell Frith (Mine Advice Pty Ltd)

Guy Reed (Mine Advice Pty Ltd)

ABSTRACT

Determining coal pillar strength equations from databases of stable and/or failed case-histories is more than 50 years old and has been applied in different countries by different researchers in a range of mining situations. Whilst common wisdom sensibly limits the use of the resultant pillar strength equations and methods to design scenarios that are consistent with the founding database, there are a number of examples whereby failures have occurred as a direct result of applying empirical design methods to coal pillar design problems that are inconsistent with the founding database.

The paper explores the reasons as to why empirically-derived coal pillar strength equations tend to be problem-specific, and so should perhaps be considered as providing no more than a pillar strength “index”. These include the non-consideration of overburden horizontal stress within the mine stability problem, an inadequate definition of super-critical overburden behaviour as it applies to standing coal pillars and the non-consideration of overburden displacement and coal pillar strain limits, all of which combine to potentially complicate and so confuse the back-analysis of coal pillar strength from failed cases.

A modified coal pillar design representation and model is presented based on coal pillars acting to reinforce a horizontally-stressed overburden, rather than suspend an otherwise unstable self-loaded overburden or section thereof, the latter having been at the core of historical empirical studies into coal pillar strength and stability.

INTRODUCTION

The inspiration for this paper is founded in three statements from two eminent persons in the field of coal pillar strength research, Jim Galvin and Essie Esterhuizen, as follows:

“Both Salamon and Munro and UNSW based the derivation of their pillar strength formulae on a criteria that the diameter of a panel of pillars, W, had to at least equal the depth of mining, H. This was thought to result in full tributary loading. It is now known that there are some mining environments included in both the South African and Australian databases in which mining span must exceed depth by a considerable margin in order to achieve full deadweight loading. Hence, it is logical to conclude that these data points may have contributed to pillar strength being overestimated by Salamon and Munro and UNSW (underline added by authors). Normally, this should be of no consequence because it is reflected in the probability of design success associated with any given safety factor.” Galvin 2006

“Empirical models, based on the analysis of large numbers of case histories, have found wide acceptance as a tool for engineering design. The application of empirical models is limited by the restriction that they should not be used beyond the limits of the empirical base from which they were developed.” Esterhuizen 2014

“Pillar design criteria based on field experience have met with mixed success” – Galvin 2016

This paper addresses three inevitable but currently unresolved questions that follow from these statements:

- (i) How significant might the overestimate of pillar strength be when the varying contribution of the overburden to the stability or instability of mine workings supported with coal pillars is ignored when back-analysing failed cases?
- (ii) How important and what are the various “*limits*” that need to be considered when determining whether an empirical method can be used with confidence or not?
- (iii) Based on (i) and (ii), in hindsight is it reasonable for empirically-derived pillar strength equations to use units (e.g. psi or MPa)?

A Conceptual Cause and Effect Model for Overburden Stability/Instability

If the influence of the overburden above collapsed mine workings supported with coal pillars is to be quantified, a conceptual model is required that incorporates all of the primary controls. Such a model was first outlined in **Frith and Reed 2017** which is developed further herein to produce a Ground Reaction Curve (GRC) representation that incorporates the associated principles.

A series of simple thought-experiments relating to super-critical extractions, as stated by **Galvin 2006** as $W/H > 1$, can demonstrate the direct influence of key geotechnical parameters on overburden stability or instability.

Figure 1 represents a massive sandstone with no vertical joints or horizontal stress acting. Under this scenario, it is obvious that the overburden will remain stable across a wide extraction span, with the associated GRC rapidly reducing to zero stress (i.e. a self-supporting condition).

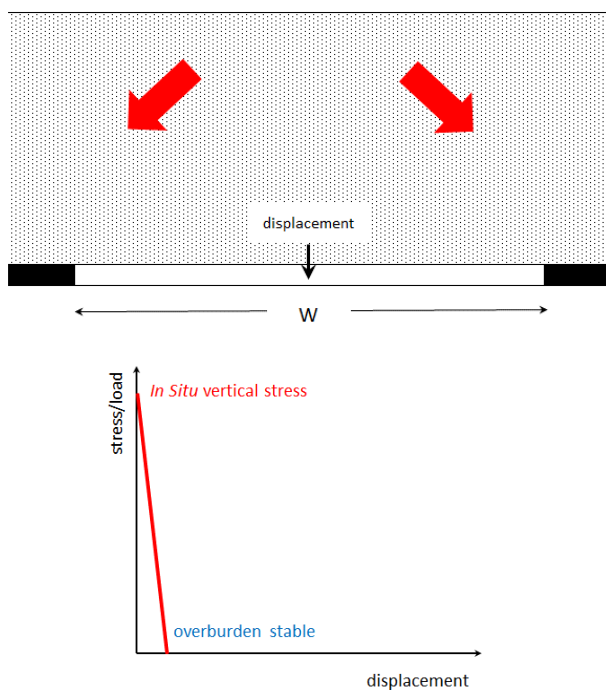


Figure 1. Thought-Experiment and Ground Curve: Massive Overburden with No Vertical Joints or Horizontal Stress

Figure 2 is identical to **Figure 1** but contains laminated material. Under this scenario, the overburden would initially “sag” downwards and eventually exceed a “critical” level of movement marking the onset of instability to full overburden collapse to surface (i.e. Tributary Area Loading in coal pillar design terminology).

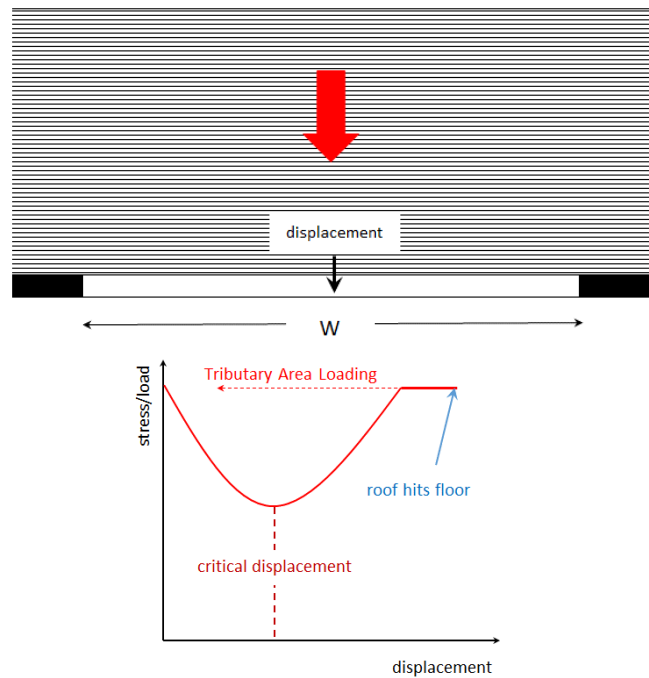


Figure 2. Thought-Experiment and Ground Curve: Laminated Overburden with No Vertical Joints or Horizontal Stress

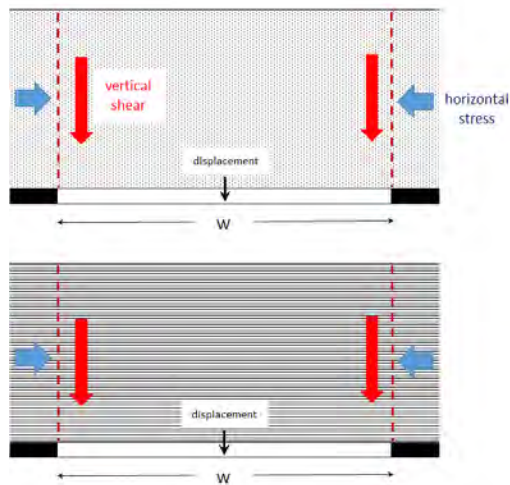


Figure 3. Thought-Experiment Representations: Massive and Laminated Overburdens Including Vertical Joints and Horizontal Stress

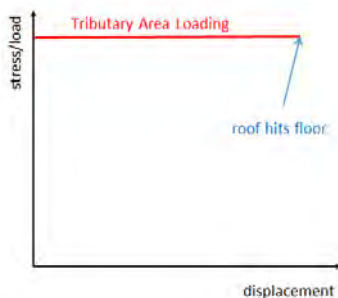


Figure 4. GRC: Vertical Joints Present without Horizontal Stress

Figure 3 contains the overburden representations of **Figures 1** and **2**, but introduces vertical joints and horizontal stress. Vertical jointing is omnipresent in coal measures strata sequences and is characterised by zero cohesion and a friction angle that varies according to surface conditions along the joint. Therefore, vertical shear resistance cannot develop along the joint without a normal confining stress, which is horizontal in this case. Therefore irrespective of overburden lithology, without the presence of horizontal stress the presence of vertical jointing will inevitably result in a GRC as shown in **Figure 4**, namely an unstable overburden with zero stiffness from the outset.

Once overburden horizontal stress is included, the influence of overburden lithology and vertical shear resistance along vertical joints can be combined, resulting in a range of possible GRC outcomes as generally illustrated in **Figure 5**.

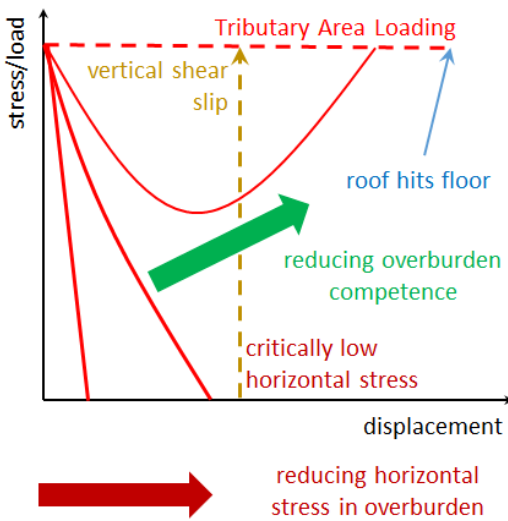


Figure 5. Varying influence of overburden lithology, vertical joints and horizontal stress on GRC's

For any given span between either barriers or solid coal, overburden stability or instability is directly influenced by the presence or absence of massive strata units etc. and the horizontal stress generating a stabilising influence along vertical joints. In combination, these two geotechnical parameters logically give rise to two distinctly different mechanisms associated with overburden instability and eventual collapse:

- Delamination and/or associated sag whilst ever vertical joints remain horizontally “clamped”, or
- A “plug” type collapse due to vertical joints becoming unstable from insufficient horizontal confinement.

The first point of developing this conceptual model is to justify that overburden conditions dictate the importance of the coal pillars in maintaining stable mine workings, not the other way round.

MEASUREMENT DATA THAT SUPPORTS THE BASIS OF THE CONCEPTUAL OVERBURDEN MODEL

At the 36th ICGCM, concern was raised with the author that without field-data substantiating the magnitude of the overburden stress drop before collapse was initiated in a GRC (as per **Figure 5**), there was no way of quantifying the extent by which the nature of the overburden may have influenced back-analysed coal pillar strengths from failed cases. It was also strongly suggested that the overburden GRC may commonly approximate to that shown in **Figure 4**, hence there was no significant disconnect between back-analysed and actual coal pillar strengths.

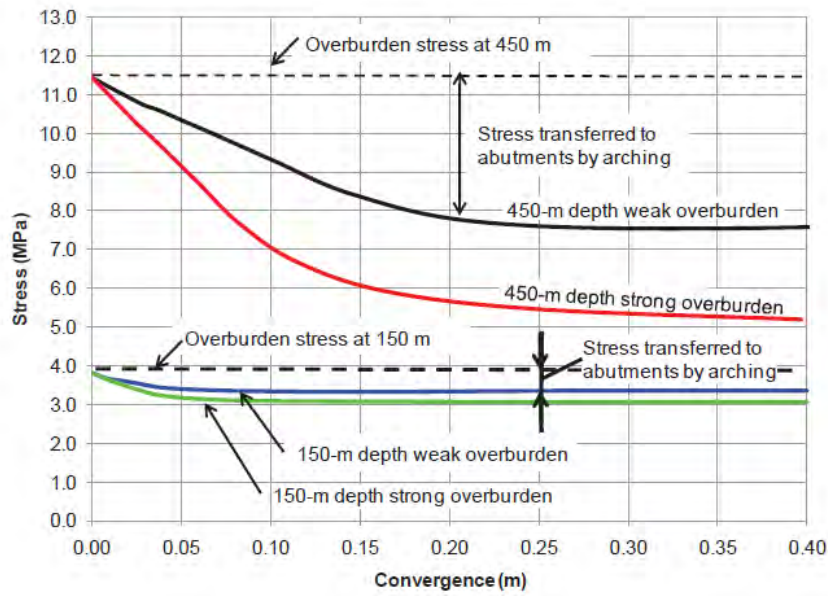


Figure 6. Ground Response Curves at the Centre of a 300 m wide Panel in Weak and Strong Overburden Strata at 150 m and 450 m Depth of Cover (Esterhuizen *et al* 2010)

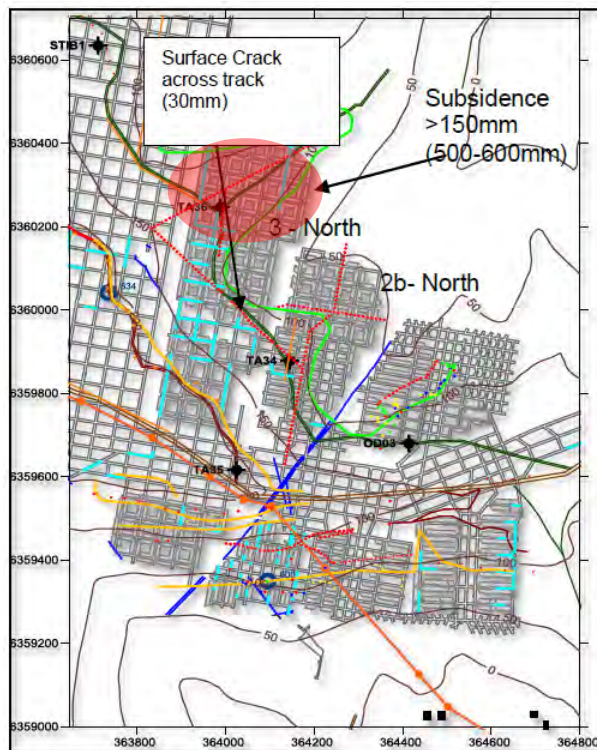


Figure 7. Modified Duncan Panels (2b-North, 3 North & 4 South) to West of Transition Zone and Cover Contours (Ditton and Sutherland 2013) – shaded area added by authors

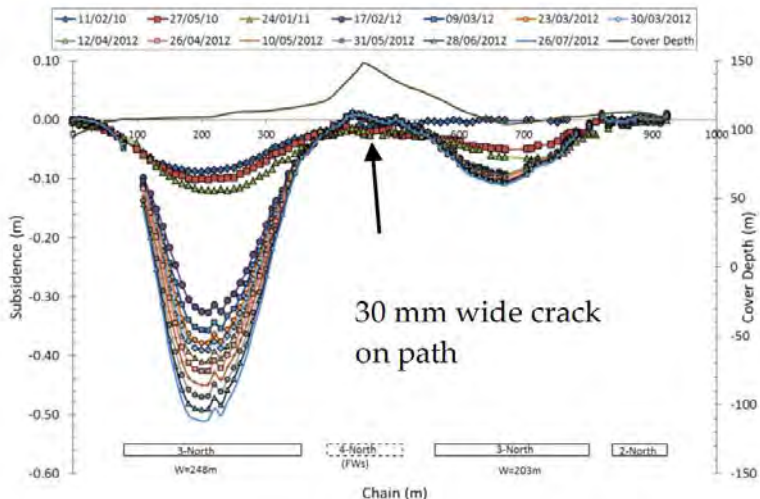


Figure 8. Delayed Subsidence above 3 North in Level 1 Area (Ditton and Sutherland 2013)

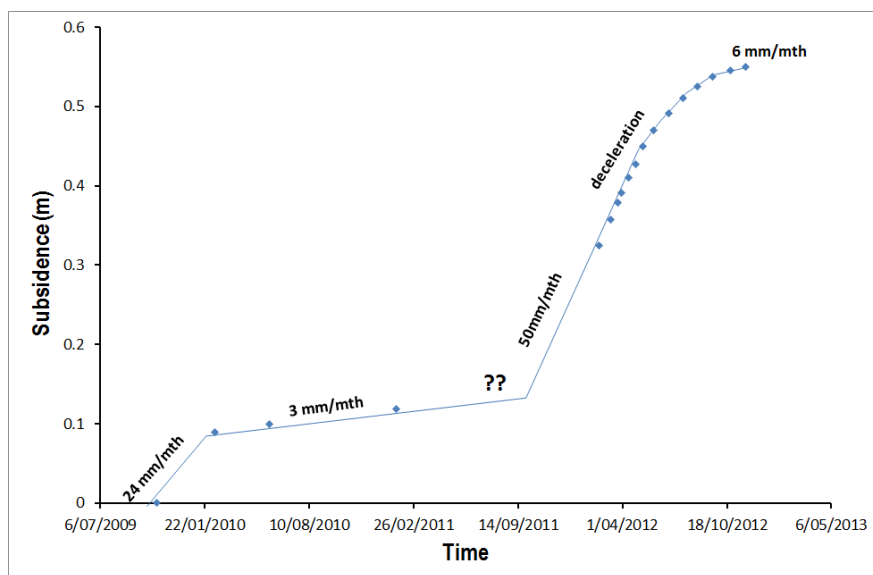


Figure 9. Time Dependent Variation in S_{\max} Within 3 North Subsidence Exceedance Area

These statements are hypothetically correct and even the fundamental work of **Esterhuizen et al 2010** provides only limited assistance in addressing them as the study was undertaken without field data validating the numerically produced GRC's (see **Figure 6**), the statement being made that "*it is difficult to measure the ground response curve in actual underground excavations because of the significant loads that would have to be applied to balance the original ground pressure*". This again is correct, but it doesn't alter the need for field data to validate GRCs if their value in the design of underground mines using coal pillars is to be maximised.

A literature search has been undertaken to identify surface subsidence data from above coal pillar systems that have allowed overburden collapses. Fortunately, such subsidence data exists from the Lake Macquarie area of NSW in Australia relating to partial extraction layouts, and despite pillar system failure relating to floor rather than pillar failure, as it is the GRC of the overburden that is of specific interest, this makes no material difference.

Ditton and Sutherland 2013 describe a significant unexpected subsidence exceedance related to completed Duncan Method partial extraction workings in the Fassifern Seam with a soft claystone

floor at the Tasman Mine. The exceedance was within the 3 North Panel and was limited to an area whereby the standard 5 heading development layout was extended to 6 headings over a panel length of four pillars (i.e. approximately 180 m) – see **Figure 7**.

Figure 8 shows the variation in vertical subsidence across the exceedance area of 6 headings and the adjacent area of 5 headings, **Figure 9** containing a time-dependent plot of S_{\max} above the 6 heading area as estimated from **Figure 8**. Based on these two figures and what is known about the Tasman geotechnical environment (including from **McTyer and Sutherland 2011**), the following comments are made:

- (i) Immediately post-mining, the development of S_{\max} follows a trend of a high rate that decelerates to a longer-term condition, in this case very slow creep at an average rate of 3 mm/month.
- (ii) Based on extrapolation, once S_{\max} reached 150 mm to 200 mm, an obvious change of state occurred via a substantial increase in settlement rate (to around 50 mm/month) followed by a deceleration back to a second longer-term condition with $S_{\max} > 450$ mm (NB questions-marks have been included in **Figure 9** as reading frequencies do not allow the exact nature of the transition to be reliably identified).
- (iii) The floor of the mine workings was soft and heaved following mining (**Figure 10**), coal pillars remaining relatively intact.
- (iv) The overburden included the Teralba Conglomerate in the order of 20 m thick.
- (v) The subsidence exceedance was restricted to the 6 headings area with an extraction width between solid coal of 248 m, as compared to the 5 heading area at a width of 203 m – see **Figure 8**.
- (vi) Both 5 and 6 heading areas were at a cover depth in the order of 130 m (see **Figure 8**) and so using the selection criterion used by Salamon and Munro as well as UNSW, both were under full tributary area loading to surface and presumably had identical pillar loadings.
- (vii) The increased subsidence did not extend into adjacent 5 heading areas, indicating that the “event” was controlled by the excavation geometry and overburden stability, rather than pillar stability.
- (viii) With a seam outcrop around three sides of the mine (see **Figure 11**), tectonic horizontal stress levels were low, as discussed by **McTyer and Sutherland 2011**.

The conclusion reached is that the increased subsidence in the 6 heading area was likely caused by the onset of “plug” type overburden instability within the Teralba Conglomerate once a critical or threshold level of overburden movement had been reached (around 150 mm) due to on-going overburden creep with time due to floor instability.



Figure 10. Moderate Floor Heave in 3-North Panel (outbye)

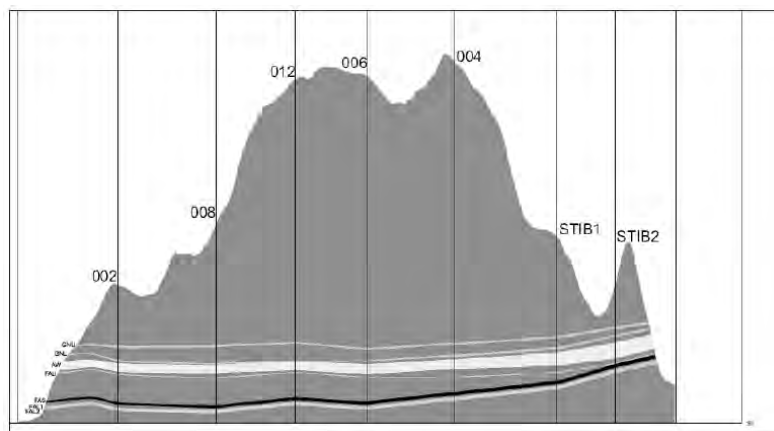


Figure 11. North-South Section Across the Tasman Mine Lease Showing the Fassifern Seam Outcrop around the Sugarloaf Range (H:V = 20:1) - Fassifern Seam is shown in black (McTyer and Sutherland 2011)

Four similar examples to that described for the 3 North Panel at Tasman Mine have been found in the published literature.

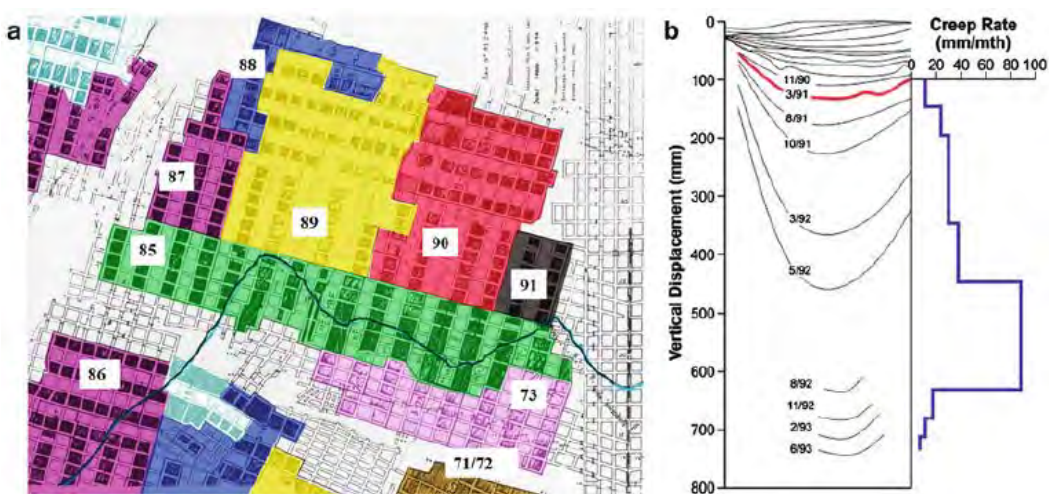


Figure 12. An Example of the Rate of Development and Magnitude of Vertical Surface Displacement Due to Bearing Capacity Failure of the Floor In Partial Extraction Workings at a Depth of 160 m (Galvin 2016)

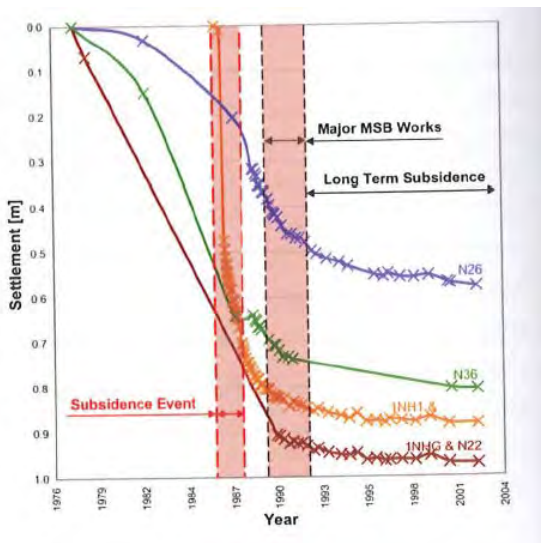


Figure 13. Surface Settlements from Newvale Colliery (Shirley and Fagg 2017)

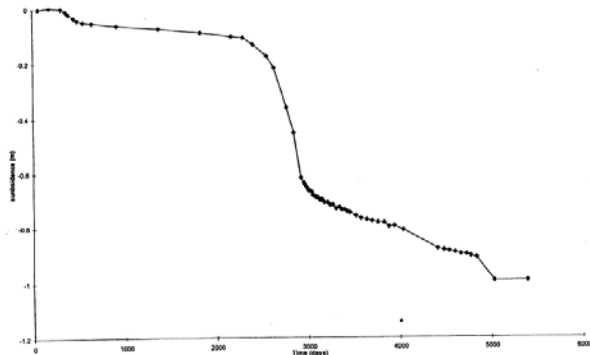


Figure 14. Subsidence vs Time Plot for 5NE Panel, Newvale 2 Colliery (Vasundhara et al 1998)

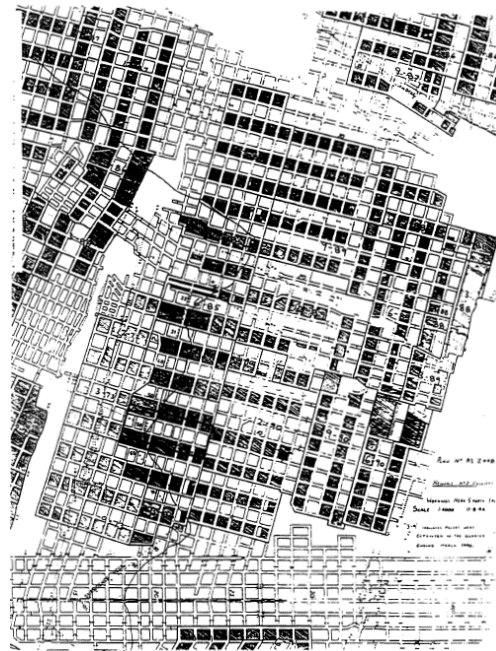


Figure 15. Remnant Mine Layout, NE Panels, Newvale 2 Colliery (Vasundhara et al 1998)

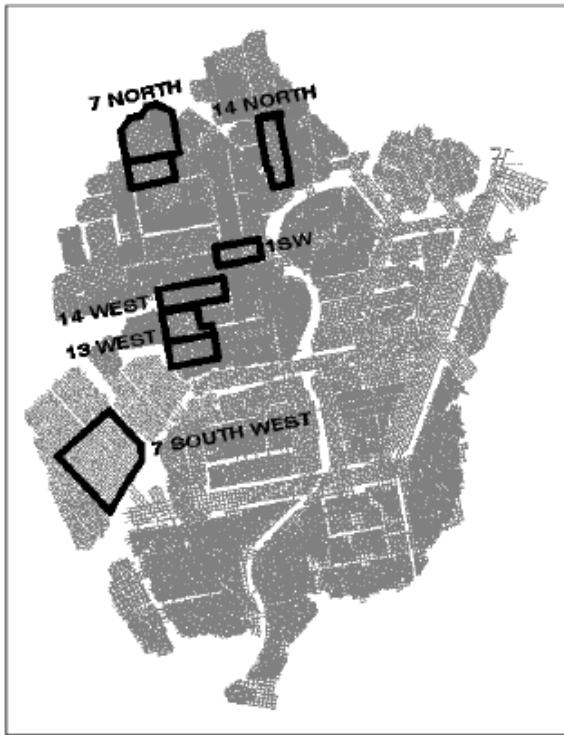


Figure 16. Some of the Known Rapid Floor Heave and Subsidence Events in the Great Northern Seam at Awaba Colliery (Seedsman 2008)

Figure 12 is taken from **Galvin 2016** and **Figure 13** from **Shirley and Fagg 2017** relating to the section of the Newvale Mine associated with the well-publicised lowering of the lake foreshore in Chain Valley Bay in the late 1980's/early 1990's. **Figure 14** contains measured surface settlements vs time above the 5NE Panel at Newvale 2 Colliery (**Vasundhara et al 1998**) with **Figure 15** showing the remnant mining layout in the NE Panels. **Figure 16** is taken from **Seedsman 2008** whereby he back-analysed what were described as “*rapid floor heave and subsidence events*” at Awaba Colliery, noting that some of these events occurred at depths as low as 60 m with coal pillars on 20 m centres having pillar Factor of Safety (FoS) values in excess of 3.

All of the listed case histories have a number of common characteristics that are of particular relevance herein:

- (i) The partially extracted areas are all super-critical in that W/H values are $\gg 1$. The partial extraction areas shown in **Figures 12** and **15** are in the order of 600 m x 600 m with cover depths in the order of 160 m to 180 m, resulting in W/H values in the order of 3 to 4.
- (ii) Following the completion of partial extraction, initial subsidence levels were low with longer-term trends consisting of very low rates of creep with time (where sufficient measurements were taken to allow time-dependent trends to be reliably identified).
- (iii) At subsidence values of 150 mm and greater, the rate of subsidence with time rapidly increases with longer-term subsidence levels approaching 1 m.
- (iv) Longer-term settlement rates commonly return to low values with no evidence of further sudden increases, even several years later.

- (v) As Great Northern Seam workings, the presence of thick, massive conglomerate units in the overburden as well as soft tuffaceous floor material, can be reliably inferred.

Figure 17 (Mills and Edwards 1997) succinctly summarise some 29 remnant pillar case histories incorporating soft floor measures in the Lake Macquarie area, whereby measured surface subsidence magnitudes clearly polarise into two distinctly different categories, namely “pillars intact” for $S_{\max}/T < 0.075$ and “pillars failed” with S_{\max}/T varying as a direct function of pillar w/h. A gradual transition between the two conditions via increasing surface subsidence over time is also identified in 4 of the case histories. With the stated seam thickness involved being 2.2m to 2.5 m, provides for an upper S_{\max} value for “pillars intact” (or overburden stable in more general terms) in the order of 165 mm to 187.5 mm.

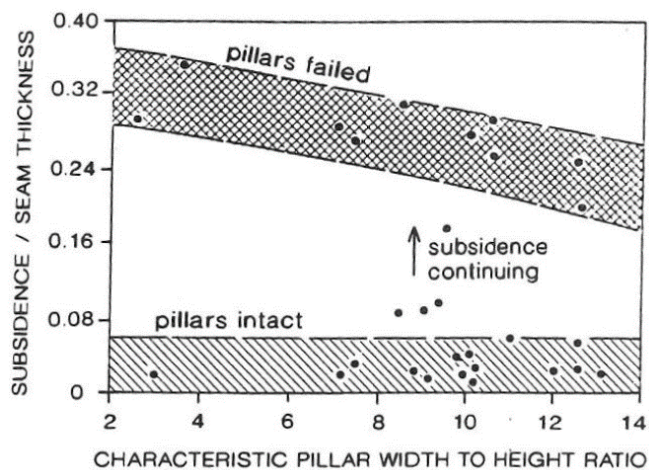


Figure 17. Subsidence as Function of Pillar Width to Height Ratio for Soft Floor Failures (Mills and Edwards 1997)

Using these specific case histories and relevant geotechnical characteristics, a technical discussion on mechanistic causation can be developed.

The majority of the investigative work that accompanied these delayed and unexpected surface settlement events above partial extraction areas, focused on the failure and compression of soft floor material beneath remnant coal pillars. This is fully understandable given the nature of the floor material and commonly observed floor heave in the workings.

The technical issue that received almost no attention was determining the cause of the rapid increase in the rate of subsidence months after the completion of mining, this being a common feature of the case histories.

Seedsman 2008 makes the statement that “massive conglomerates may span and delay evidence of imminent over-loading of pillars – temporarily stiff loading system”. However when the mined-out areas have widths and lengths in the order of 600 m at cover depths < 200 m, conventional subsidence thinking would inevitably eliminate the possibility that even thick massive conglomerates could span across such areas, this being consistent with the periodic weighting classification for longwalls (**Frith and McKavanagh 2000**) whereby a 30 m thick conglomerate can only span across an extraction width of 200 m (see **Figure 18**), certainly not 600 m. Clearly there is a major problem or disconnect using overburden caving behaviour from total extraction panels such as longwalls, to estimate overburden spanning ability when substantial coal pillars are left in place.

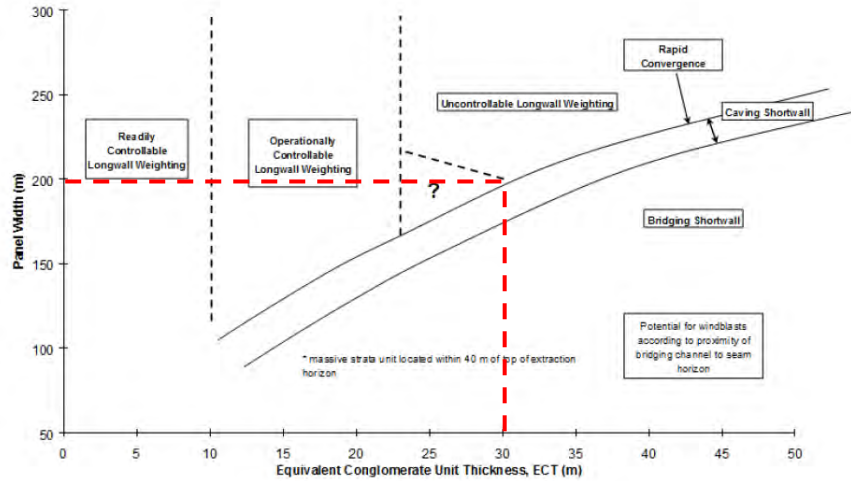


Figure 18. Near-Seam, Massive Strata Weighting Classification (Frith and McKavanagh 2000)

The suggested solution to this conundrum, which is as per as that stated by **Van de Merwe 2006** and addressed in **Frith and Reed 2017** in relation to the non-collapsed area at Coalbrook, is found in two aspects of bord and pillar workings and/or partial pillar extraction that are absent from longwall extraction once full caving has been established, namely:

- (i) the contribution of the remnant coal pillars to overburden stability, and
- (ii) the stabilising influence of horizontal stress within the overburden.

In other words, the GRC for the overburden must be being altered by remnant coal pillars, this being consistent with the idea that coal pillars “reinforce” rather than “suspend” the overburden, as was discussed in **Frith and Reed 2017**.

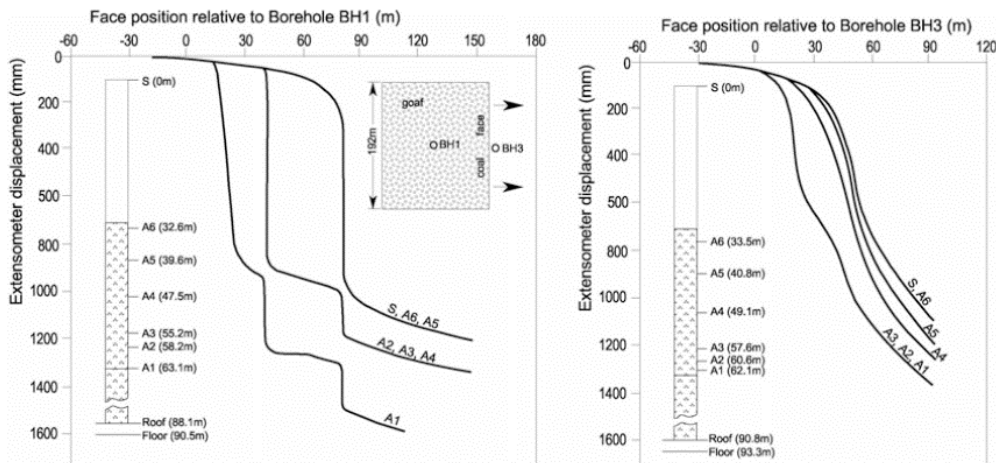


Figure 19. Graphs Showing Progressive Step-Failure of a Dolerite Sill as Recorded using Surface to Seam Borehole Extensometers (reproduced from Galvin 2016)

As illustrated in **Figure 5**, it is postulated that the onset of super-critical overburden conditions to surface is dictated by the overburden exceeding a critical level of subsidence, which based on data published by **Mills and O’Grady 1998** and **Ditton and Frith 2003** was suggested as being in the order of 200 mm by **Frith and Reed 2017**. Surface extensometry data published by **Salamon et al 1972** further indicates the onset of rapid subsidence for values exceeding 150 mm to 200 mm (see **Figure**

19). The close correlation with measured subsidence magnitudes at the onset of rapid subsidence in the previously described partial extraction cases from the Lake Macquarie area of NSW, is also noted.

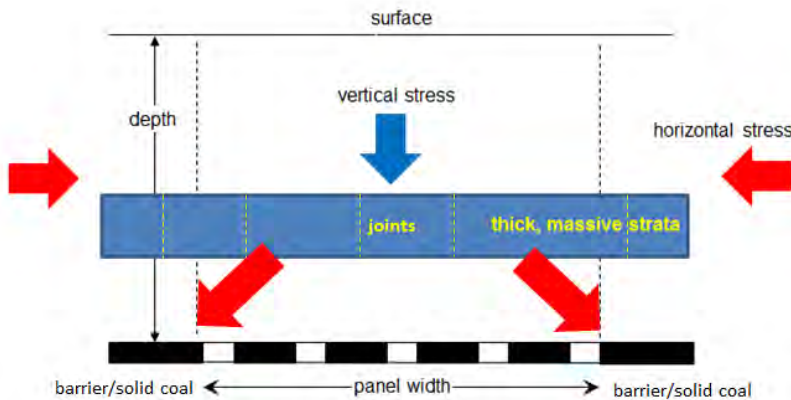


Figure 20. Schematic Illustration of a Reinforcing Problem Representation for Coal Pillar Design Including Super-incumbent Load Transfer to Solid Coal or Barrier Pillars

Re-defining the role of coal pillars as reinforcing rather than suspending the overburden, was discussed in length by **Frith and Reed 2017**, a general arrangement for the pillar design problem including a more detailed overburden representation containing thick massive strata units, vertical joints and *in situ* horizontal stresses, being shown in **Figure 20**. It is noted and accepted in this representation, that the *in situ* vertical stresses acting on the production pillars cannot be re-distributed out to any flanking barrier pillars by the action of the overburden, as this would require said pillars to vertically expand or extend due to mining. Therefore, it is only the *in situ* vertical stress that is released by the formation of mining excavations that can be re-distributed, either in full or more likely, in part.

The controlling influence of overburden horizontal stress on surface subsidence was recognised by **Mills 2012**, who concluded that “sag” subsidence increases in the presence of high horizontal stress, based on subsidence data from the Newcastle Coalfield in NSW. The explanation for this phenomenon is beyond the scope of this paper, but inevitably leads into the significance of high horizontal stress in roadway roof control as being the driver for uncontrolled buckling of the roof strata, the control and limiting of which is a reinforcing rather than suspension roof support design problem.

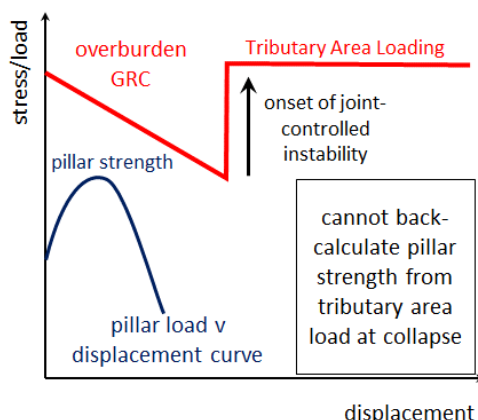


Figure 21. Schematic GRC Showing the Displacement Mismatch Between Pillar Strength Being Generated and the Onset of Overburden Instability to Surface

If overburden instability to surface (i.e. the “vertical shear slip” line within the GRC in **Figure 5**) occurs as a distinct change due to vertical joints becoming unstable at subsidence values of 150 mm and greater, then as discussed in **Frith and Reed 2017** any coal pillars that subsequently collapse as a direct consequence will have inevitably exceeded their peak strength well prior to this occurring. This is illustrated schematically in **Figure 21** and is consistent with the quotation from **Galvin 2006**, the question then being whether the magnitude and design significance of coal pillar strength over-estimates can be quantified or not?

HOW SIGNIFICANT CAN COAL PILLAR STRENGTH OVER-ESTIMATES ACTUALLY BE?

A general equation for the reinforcement of a mine roadway roof was provided in **UNSW 2010** and has been slightly modified as follows:

$$\text{FoS} = f(P_{\text{roof}}, P_{\text{support}})/\text{applied load} \quad [1]$$

where:

FoS = a measure of stability

P_{roof} = contribution to stability from the roof strata itself (e.g. Coal Mine Roof Rating)

P_{support} = contribution to stability from installed roof support (e.g. PRSUP)

applied load = horizontal stress in the case of roadway roof reinforcement

This basic equation manifests in the statistically significant empirical relationships published by **Colwell and Frith 2009 and 2012** relating to primary roof support design in normal width and wider coal mine roadways respectively. It is also the foundation of the AMCRR Method as published by **Colwell and Frith 2010**.

Equation 1 can be modified for coal pillar design as follows:

$$\text{FoS} = f(P_{\text{overburden}}, P_{\text{pillar}})/\text{applied load} \quad [2]$$

where:

FoS = a measure of stability

$P_{\text{overburden}}$ = stability contribution from the overburden (linked to both the structural competence of the overburden and horizontal stresses acting as outlined previously)

P_{pillar} = stability contribution from coal pillars left in place

applied load = either horizontal stress or vertical stress based on the problem being reinforcement of suspension respectively (NB $P_{\text{overburden}} = \text{zero}$ represents the special case of full-tributary area loading to surface with the overburden being critically unstable)

If the model for overburden and coal pillar stability (**Figure 20**) is accepted along with both the generic GRC concept (**Figure 5**) and Equation 2, it logically follows that the accuracy of back-analysed coal pillar strengths from failed cases must improve as the stabilising influence of horizontal stress and/or massive strata within the overburden decreases, the overburden GRC then tending towards that shown in **Figure 4** with no stabilising contribution from the overburden from the outset.

Two obvious scenarios whereby the stabilising influence of horizontal stress is likely to be minimised or reduced are:

- highwall mining (HWM) from an open cut highwall, this entire issue being at the centre of a recently published pillar strength equation specifically for Australian HWM pillars (**Mo et al 2017**), and
- decreasing cover depth more generally whereby surface topography effects, the depth of weathering and reducing strata stiffness should increasingly act to reduce horizontal stress magnitudes in the overburden.

The significant mismatch between underground mining failed cases and those from HWM, in Australia at least, is obvious in **Figure 22** (Hill 2005). This representation of failed pillar cases resulted in a strong response (Galvin 2006) arguing that as pillar w/h was included in both axes, it was mechanistically incorrect or “ill-advisable” to represent failed cases in this manner. Unfortunately, the more obvious question went either unnoticed or unaddressed at that time, namely why is the stability of HWM pillars so different to those from the underground mining environment?

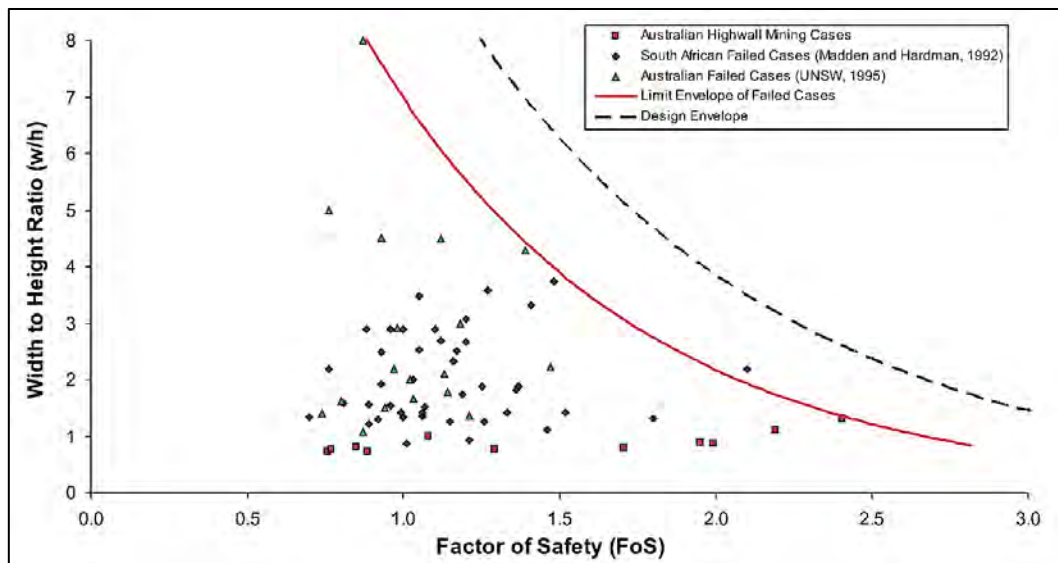


Figure 22. Database of Pillar Collapses – Width to Height Ratio vs. FoS (Hill 2005)

Various arguments have been made by others concerning the weakening influence of minor geological structures on the strength of low w/h ratio pillars due to the absence of pillar confinement, but this would surely equally apply to both HWM and underground coal pillars. **Figure 22** does not support such a hypothesis, particularly given that the number of underground failed cases is greater than those from HWM, such that the effect should be more, rather than less, obvious in the underground failed cases if it were present in low w/h ratio pillars. Nonetheless, UNSW undertook a back-analysis of the HWM failed cases shown in **Figure 22** and developed a HWM-specific strength equation (Equation 3 from **Canbulat et al 2016**) with the equation itself included in **Mo et al 2017**:

$$\sigma_p = 4.66 (0.56 + 0.44 w/h) \text{ or } 2.61 + 2.05 w/h \quad [3]$$

However Equation 3 for HWM pillars results in the illogical situation whereby the strength of a long strip pillar (as given by Equation 3) is less than for a square pillar of the same width and height as given by the **Salamon and Munro 1967** equation for w/h < 5 as an example (Equation 4).

$$\sigma_p = 7.176 (w^{0.46}/h^{0.66}) \quad [4]$$

However, it is intriguing to consider that Equation 3 is very similar in magnitude to the **Bieniawski 1968** equation that was derived from the *in situ* testing of coal pillars in South Africa as given by Equation 5.

$$\sigma_p = 2.76 + 1.52 w/h \quad [5]$$

The suggestion that coal pillar design in underground mining is a reinforcing problem whereby the stabilising contribution of the overburden needs to be given due consideration, is seemingly strengthened by the fact that Australian HWM coal pillars, where the stabilising influence of overburden horizontal stress is inevitably lower than in underground mining, return lower inferred pillar strengths as compared to pillars in underground mining.

In terms of the stabilising influence of horizontal stress being reduced by ever-decreasing cover depth, it is judged that both the US and Australian collapsed pillar databases are too small to provide any meaningful insights. However, the South African collapsed pillar database in its entirety (i.e. including as many failed cases as the authors have been able to identify) is sufficiently large and does show intriguing trends as will now be detailed.

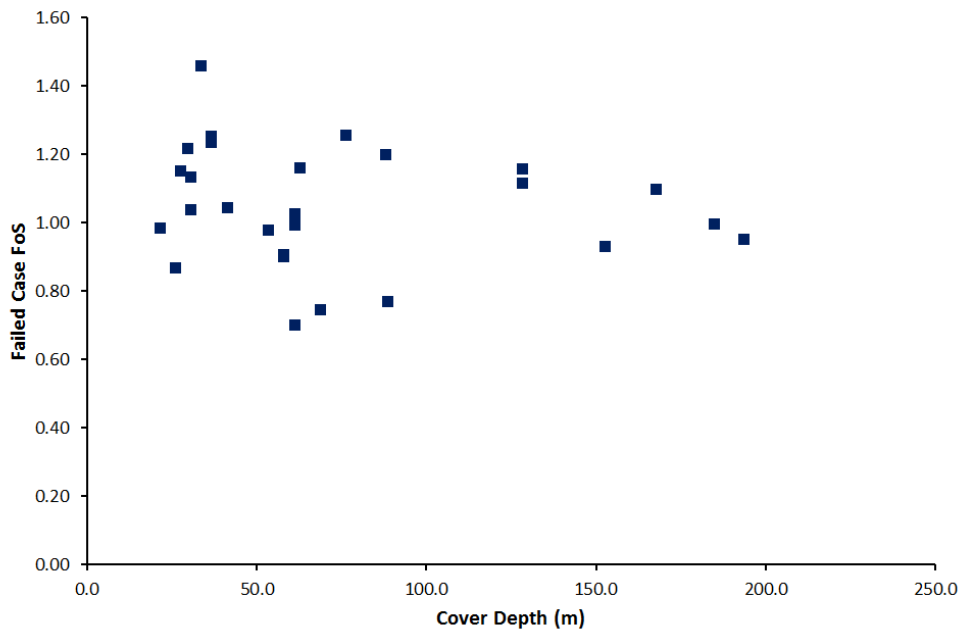


Figure 23. FoS v Depth For Cases Used by Salamon and Munro 1967

Figure 23 shows the 27 collapsed cases that were used by **Salamon and Munro 1967** whereby the FoS using the **Salamon and Munro 1967** strength equation (Equation 4) is plotted against cover depth. The collapsed cases centre around an FoS in the order of 1 with no obvious significant trend of increasing FoS with reducing cover depth.

Figure 24 contains those collapsed cases used by **Salamon and Munro 1967** and the additional 17 cases considered by Bernard Madden between 1967 and 1988 (**Madden 1991**). Again the cases centre around 1, but there is a hint of increasing SF with decreasing cover depth at less than 50 m.

Figure 25 includes all of the known collapsed cases from South Africa, with both the Salamon and Munro and Madden data points being differentiated from the other cases. The clear and obvious trend for maximum FoS value to incrementally increase with decreasing cover depth below 100 m being obvious. This is not dissimilar to that shown in **Figure 22** for Australian HWM cases, the point being

that the South African cases in **Figure 25** are all from underground mines. Therefore, perhaps it is not HWM that is the driver for reduced coal pillar strength in HWM, but something far more fundamental?

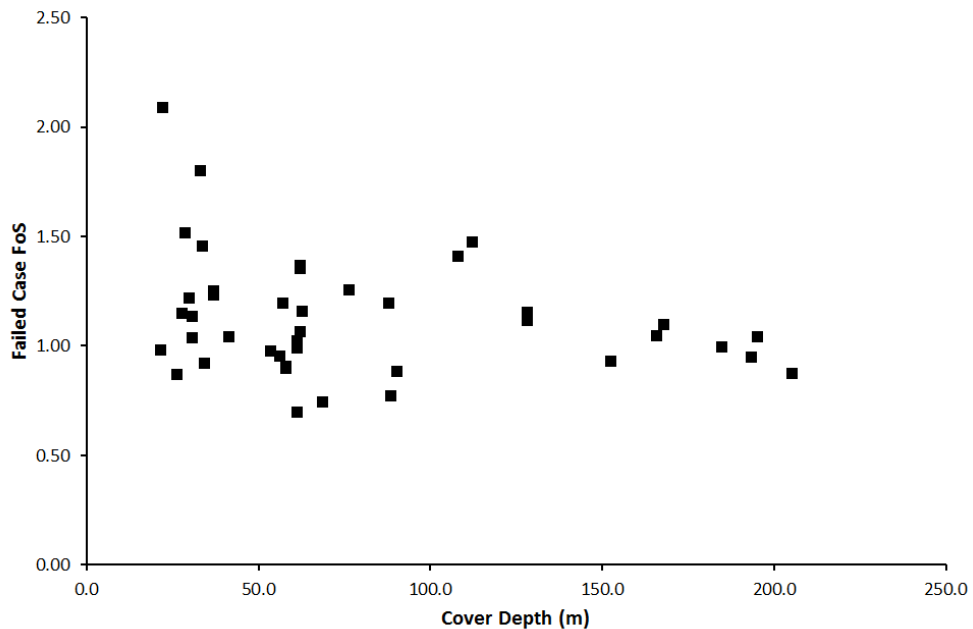


Figure 24. FoS v Depth for Failed Cases Used by Salamon and Munro 1967 and Madden 1991

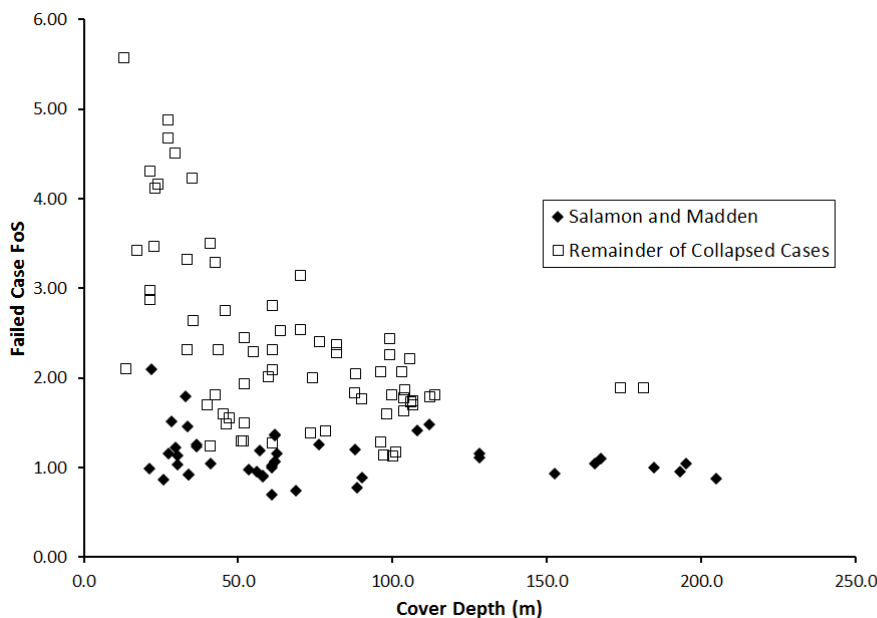


Figure 25. FoS v Depth for Failed Cases Used by Salamon and Munro 1967 and Madden 1991 Along with Other South African Failed Cases

An explanation for the apparent conundrum of these very high FoS collapsed cases from South Africa was linked to the time-dependent spalling or scaling of pillars, such that pillar collapse must have eventually collapsed when the FoS reduced to a suitably low level as compared to the as-formed pillars. **Van der Merwe 1993** examined this issue for Vaal Basin collapsed cases and determined that the rate of pillar scaling was a direct function of mining height. **Salamon et al 1998** developed the idea that pillar scaling was driven by the swelling of montmorillonite clays within the coal seam, this basic

model then being utilised by **Canbulat 2010** in his treatment of the time to failure problem (**Figure 26**).

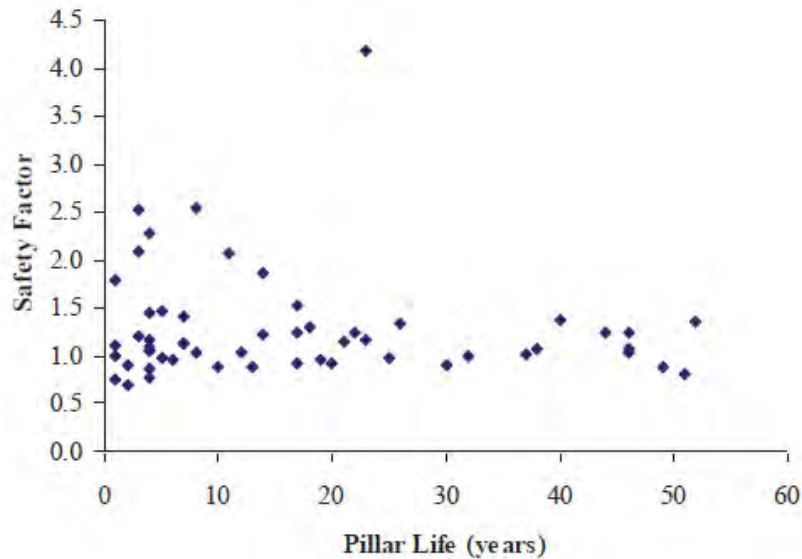


Figure 26. Design Safety Factor vs Time Interval (Canbulat 2010)

Unfortunately the originators of this hypothesis only ever put forward the idea of swelling clays driving pillar scaling as a possible mechanism to explain high SF collapsed cases, making the following clarification:

"No direct evidence appears to exist to substantiate the proposed model of pillar scaling. Thus, it is not possible to prove convincingly the validity or otherwise of the approach" (Salamon et al 1998).

They also state that

"It is important that the cause of abnormal collapses be investigated and explained as soon as possible. Such study is likely to find that anomalous behaviour is due to more than one cause. Van der Merwe's observations imply that pillar scaling could be a reason for some of the premature failures. This deduction and the promising performance of the model proposed here provide a powerful basis for recommending that further study should be initiated to clarify the role of scaling or spalling in pillar mechanics".

In other words, the work of **Salamon et al 1998** was no more than an initial attempt at explaining failed cases with anomalously high FoS values.

One possibility that was not considered, but would be well supported by the overburden reinforcing model for coal pillars outlined herein, is that the high FoS values of failed cases were erroneous in the first instance due to the strength equation that was used substantially overestimating actual coal pillar strength due to the fundamental assumptions used as part of its derivation. When this possibility is combined with the stabilising contribution of the overburden decreasing with decreasing cover depth, the occurrence of pillar scaling over time makes good sense, such scaling being related to under-designed coal pillars that are being compressed over time above yield and towards their ultimate strength, until overburden instability and inevitably pillar collapse eventually occurs.

The suggestion that pillar scaling over time could be due to coal pillars being under-designed to start with is hardly controversial. However, if high pillar FoS values were accepted as correct due to reliance being placed on the coal pillar strength equation that was used in their derivation, then searching for an alternate explanation that was independent of coal pillar strength would be a logical path to follow.

OVERALL SUMMARY

A set of technical arguments backed-up with various field data have been presented to support the hypothesis that bord and pillar-type coal pillar design in underground coal mining is generally one of the coal pillars reinforcing the overburden, such that they combine with the overburden to stabilise the mine workings. The reinforcing representation put forward is comparable with that which is well established in coal mine roadway roof control and contains the same basic input parameters, including the significant influence of horizontal stress magnitudes.

If it is assumed (for the sake of illustration only) that the full-tributary area loading model is correct and is applied within a GRC representation (as shown in **Figure 27**), then for collapsed pillar cases one must conclude that the actual peak pillar strength is inevitably less than full-tributary area pillar loading, otherwise the two curves would have intersected and system stability would have been returned. In other words, the assumption of full-tributary area loading when back-analysing collapsed pillar cases must result in pillar strength equations that over-estimate the true strength of the pillars by some amount, even in those situations whereby there is no contribution to system stability from the overburden. The pertinent question therefore is the potential magnitude and significance of over-estimated or optimistic coal pillar strengths being returned due to this irresolvable and undefined error, this being the main subject of on-going work.

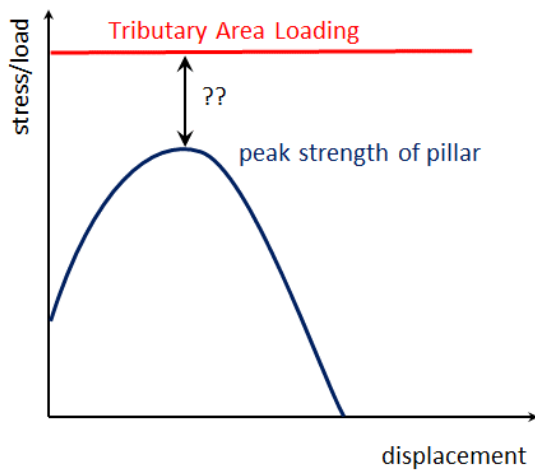


FIGURE 27. Schematic Illustration of Pillar Strength Over-Estimate Even if Full-Tributary Area Loading is Appropriate in a Collapsed Case

The reinforcing model logically suggests that pillar strength equations derived from the back-analysis of failed pillar cases under the assumption of full-tributary area loading, in reality more likely provide a measure of the combined stabilising influence of both coal pillars and the overburden. The result of this is that under specific conditions whereby the stabilising influence of horizontal stress within the overburden is either low or indeed absent, highly optimistic mine layouts can inadvertently and unknowingly be developed and implemented if those same pillar strength equations are applied without this realisation.

The design risks associated with determining pillar strengths from back-analysed case histories, particularly from single or only a small number of cases, are potentially substantial if one accepts this conclusion, the worst-case consequence of which is perhaps best summarised in the following statement in relation to the Crandall Canyon disaster:

"In a December 3, 2007 submission to MSHA, a consultant explained that the "coal strength was calibrated from three mining stages in the south panel of Section 36. The coal strength was incrementally increased from 900 psi to 1640 psi until modelling results were consistent with actual conditions. The average cover depth in this calibration panel was about 1,700 ft. We were told that all the pillars during retreat mining were stable and only limited yielding occurred at some pillar ribs." – taken from **US Senate 2008**

Therefore, perhaps it might be prudent for coal pillar strength equations that are determined from case histories to never be given units (such as MPa or psi), even if the associated statistical correlations are compelling. Treating them as “index” parameters that are linked to a particular design method, or re-naming them as an *“estimate of the combined stabilising influence of coal pillars and the overburden”* for example, may assist in ensuring that such equations are not used out of context.

Based on the content and conclusions of this paper, the quotation from **Esterhuizen 2014** in regards to only using empirically design methods within the limits of their supporting database, has great substance, but leaves one further key question unanswered – *what are those limits and how are they defined?* Given the critical importance of this to the mine designer, the developers of the various bord and pillar-type coal pillar design methods may wish to consider this question in more detail according to the known specific characteristics of the supporting case histories.

REFERENCES

- Bieniawski Z T. The Effect of Specimen Size on Compressive Strength of Coal. International Journal of Rock Mechanics and Mining Sciences & Geomechanical Abstracts 1968;5(4), pp. 325–335.
- Canbulat, I. (2010). Life of Coal Pillars and Design Considerations. Proc. 2nd Ground Control Conference, Sydney, pp 57-66.
- Canbulat, I. Mo, S. Zhang, C. Hagan, P. Oh, J (2016). Coal Pillar Design for Highwall Mining and Geotechnical Considerations in Backfilling. Sydney, The University of New South Wales.
- Colwell, M. Frith, R. (2009). ALTS 2009 – A 10 Year Journey. Proceedings of the 9th Underground Coal Operator’s Conference, Wollongong NSW, pp. 37-53.
- Colwell, M. Frith, R. (2010). AMCMRR – An Analytical Model for Coal Mine Roof Reinforcement. Proceedings of The Coal Operators Conference, University of Wollongong, pp 73-83.
- Colwell, M. Frith, R. (2012). Analysis and Design of Faceroad Roof Support (ADFRS). Final Report to ACARP, Project C19008.
- Ditton, S. and Frith, R. (2003). Influence of Overburden Lithology on Subsidence and Sub-Surface Fracturing on Groundwater. Final Project Report. Brisbane, Queensland: ACARP Project C10023.
- Ditton, S. Sutherland, T. (2013). Management of Subsidence at the Tasman and Abel Mines - Issues and Outcomes. Proceedings of COAL 2013, University of Wollongong.
- Esterhuizen, G.S. Mark, C. Murphy, M. (2010). The Ground Response Curve and Its Impact on Pillar Loading in Coal Mines. Proceedings 3rd International Workshop on Coal Pillar Mechanics and Design. Morgantown, West Virginia. pp. 123-131.

Esterhuizen, G.S. (2014). Extending Empirical Evidence through Numerical Modelling in Rock Engineering Design. *The Journal of The Southern African Institute of Mining and Metallurgy*, Vol. 114, October.

Frith, R C. McKavanagh, B. (2000). Optimisation of Longwall Mining Layouts under Massive Strata Conditions and Management of the Associated Safety and Ground Control Problems. End of Grant Report, ACARP Project C7019.

Frith, R. Reed, G. (2017). Coal Pillar Design When Considered a Reinforcement Problem Rather Than a Suspension Problem. Proceedings of 36th ICGCM, Morgantown, West Virginia, pp. 89-99.

Galvin, J.M. (2006). Considerations Associated with the Application of the UNSW and Other Pillar Design Formulae. Proceedings of the 41st US Symposium on Rock Mechanics, Golden, Colorado.

Galvin, J. (2016). *Ground Engineering: Principles and Practices for Underground Coal Mining*. Switzerland: Springer International Publishing, pp. 684.

Hill, D. (2005). "Coal Pillar Design Criteria for Surface Protection." In: *Proceedings of the Coal Operators' Conference*. Brisbane, Queensland: University of Wollongong.

Madden, B. (1991). A Re-assessment of Coal-Pillar Design. *J. S. Afr. Inst. Min. Metall.*, Vol. 91, No. 1. January. pp. 27 - 37.

McTyer, K. Sutherland, T. (2011). The Duncan Method of Partial Pillar Extraction at Tasman Mine. Proc. 30th Int. Conference on Ground Control in Mining, West Virginia.

Mills, K. Edwards, J. (1997). Review of Pillar Stability in Claystone Floor Strata. *Symposium on Safety in Mines, The Role of Geology*, Sydney, NSW, pp. 161-168.

Mills, K. and O'Grady, P. (1998). Impact of Longwall Width on Overburden Behaviour. In: *Proceedings of the Coal Operators' Conference*. Brisbane, Queensland: University of Wollongong.

Mills, K. (2012). Observations of Ground Movements Within the Overburden Strata Above longwall Panels and Implications for Groundwater Impacts. 38th Symposium on the Advances in the Study of the Sydney Basin, Coalfields Geology Council of New South Wales.

Mo, S. Canbulat, I. Zhang, C. Oh, J. Shen, B. Hagan, P. Numerical Investigation into the Effect of Backfilling on Coal Pillar Strength in Highwall Mining. *International Journal of Mining Science and Technology*, 2017.

Salamon, M. D. G and Munro, A. H. (1967). A Study of the Strength of Coal Pillars." *Journal of the Southern African Institute of Mining and Metallurgy* 68: 56–67.

Salamon, M. D. G. Oravecz, K.I. Hardman, D. (1972). Rock Mechanics Problems Associated with Longwall Trials in South Africa. Research Report No. 6/72 (pp. 35). Chamber of Mines of South Africa Research Organisation.

Salamon. M. Ozbay, M. and Madden, B. (1998). Life and Design of Bord and Pillar Workings Affected by Pillar Spalling. *Journal of Southern African Mining and Metallurgy*. 98:135-145.

Seedsman, R. (2008). Awaba – Understanding Soft Floors And Massive Conglomerates. Presentation to Mine Managers Association, May 2008.

Shirley, A. Fagg, S. (2017). Subsidence Events, Investigation and Litigation: The Need for a Forensic Approach. Proceedings 10th Triennial Conference on Mine Subsidence.

UNSW (2010). Strata Control Graduate Diploma Course Notes.

US Senate (2008). Report on the August 6, 2007 Disaster At Crandall Canyon Mine.

Van Der Merwe, J. N. (1993). Revised Strength Factor for Coal in the Vaal Basin. J S African Inst. Min. Metal. March.

Van Der Merwe, J. N. (2006). "Beyond Coalbrook: Critical Review of Coal Strata Control Developments in South Africa." In: Proceedings of the 25th International Conference on Ground Control in Mining. Morgantown, WV: West Virginia University, pp. 335–346.

Vasundhara, Galvin, J, Hebblewhite, B. (1998). Geomechanical Behaviour of Soft Floor Strata in Underground Coal mines. ACARP Report, Project C4026.





Project Office

7/8 Clarence House
9 Clarence Street
Moss Vale NSW 2577
Ph: +61 2 4869 8200
E: info@humecoal.com.au

Mailing Address

Hume Coal Pty Limited
PO Box 1226
Moss Vale NSW 2577